UNIVERSIDADE DE SÃO PAULO
PROGRAMA DE PÓS-GRADUAÇÃO EM ENERGIA
EP-FEA-IEE-IF

GIORGIO SPAGARINO

LOW AND MEDIUM TEMPERATURE FUEL CELLS: EXPERIMENTAL TESTS AND ECONOMIC ASSESSMENT

SÃO PAULO
2012

GIORGIO SPAGARINO

LOW AND MEDIUM TEMPERATURE FUEL CELLS: EXPERIMENTAL TESTS AND ECONOMIC ASSESSMENT

Dissertação apresentada ao Programa de Pós-Gradução em Energia da Universidade de São Paulo (Escola Politécnica / Faculdade de Economia e Administração / Instituto de Eletrotécnica e Energia / Instituto de Física) para a obtenção do título de Mestre em Ciências.

Orientador: Prof. Dr. Roberto Zilles

Versão Corrigida

(versão original disponível na Biblioteca da Unidade qua aloja o Programa e na Biblioteca Digital de Teses e Dissertações da USP)

SÃO PAULO

2012

FICHA CATALOGRÁFICA

Spagarino, Giorgio

Low and medium temperature fuel cells: experimental tests and economic assessment/ Giorgio Spagarino; orientador Roberto Zilles – São Paulo, 2012.

121 f..: il.; 30 cm

Dissertação (Mestrado) – Programa de Pôs-Gradução em Energia – EP / FEA / IEE / IF da Universidade de Sàao Paulo.

1. Fuel cell 2. Hydrogen 3. Inverter 4. Public grid 5. Phosphoric acid fuel cell 6. Co- generation 7. Natural Gas

I. Título

UNIVERSIDADE DE SÃO PAULO

PROGRAMA DE PÓS-GRADUAÇÃO EM ENERGIA

EP – FEA – IEE - IF

GIORGIO SPAGARINO

"Low and medium temperature fuel cells: experimental tests and economic assessment"

Dissertação defendida e aprovada pela Comissão Julgadora:

Prof. Dr. Roberto Zilles – PPGE/USP

Orientador e Presidente da Comissão Julgadora

Prof. Dr. Ildo Luis Sauer – PPGE/USP

Dr. Edgar Ferrari da Cunha - IPEN

AGRADECIMENTOS

Ao meu orientador, Prof. Dr. Zilles, pelo conhecimentos e experiências repassadas na fase experimental da minha dissertação.

Ao Doutor Edgar Ferrari do IPEN, por ter permitido o desenvolvimento experimental do trabalho e para todo o apoio durante o realização deste trabalho.

Ao Mestre Marcelo Pinho Almeida, por a sua fundamental ajuda durante as ultimas etapas experimentais do trabalho.

Ao Prof. Dr. Ildo Luís Sauer, por ter acompanhado a realização do paper que constituiu a segunda parte do trabalho e para todo o conhecimento repassado durante esta etapa.

Aos amigos que fiz durante o curso, que o tornaram uma experiência única, com muitos momentos agradáveis e que contribuíram à realização deste trabalho por meio de inúmeras conversas e troca de informações.

Aos professores do programa, cujos ensinamentos abriram luz para muitas reflexões e aprendizagem durante o curso.

Ao apoio concedido pelo IBP– Instituto Brasileiro de Petróleo, Gás e Biocombustíveis para a realização desta pesquisa.

E por ultimo e mais importante, aos meus pais, Maria Ausilia e Pier Sandro, que, mesmo distantes, me dispensaram muito amor e incentivo.

RESUMO

Spagarino, Giorgio. **Células de combustível de baixa e média temperatura: testes experimentais e avaliação econômica**. 2012. Dissertação (Mestrado em Ciências) – Programa de Pós-Graduação em Energia da Universidade de São Paulo, São Paulo, 2012

A presente pesquisa foi desenvolvida para avaliar as potencialidades das células de combustível como tecnologia em si, inclusive os beneficios econômicos que se podem ter por meio do suprimento de energia elétrica se comparada com o aproveitamento da mesma por meio da rede pública.

Além de uma parte descritiva do estado de arte da tecnologia, a presente dissertação foi focada em duas partes: a primeira trata de um estudo experimental onde uma célula, a membrana polimérica, foi conectada a um inversor, permitindo assim de fornecer energia elétrica na rede pública.

Na segunda parte foi realizada uma avaliação engenhero-econômica com uma Célula de Combustível de Ácido Fosfórico para o aproveitamento da energia elétrica com cogeração de calor para as condições de mercado brasileiro.

O primeiro estudo mostrou como seja possível abastecer uma célula (neste caso alimentada por hidrogênio) para fornecer continuamente energia elétrica na rede, onde necessário ou onde seja impossível para o usuário se conectar a rede pública.

O segundo estudo, por sua vez, mostrou que atualmente a células de combustível de média temperatura de Ácido Fosfórico (PAFC) não é uma tecnologia ainda madura e que é viável economicamente somente em aplicações de nicho, por exemplo setores indústriais eletro-intensivos e com necessidade de energia termica também. Todavia, projeções futuras baseadas em curvas de aprendizados e a queda do preço do gás natural mostram como a expansão da tecnologia e a possibilidade de acessar um combustível barato podem abrir futuro para a PAFC mundialmente.

Palavras-chave: Células de combustível, Hydrogênio, Inversor, Rede pública, Células de Combustível de Ácido Fosfórico, Cogeração, Gás Natural

ABSTRACT

Spagarino, Giorgio. **Low and medium temperature fuel cells: experimental tests and economic assessment**. 2012. Master's Dissertation – Graduate Program on Energy, Universidade de São Paulo, São Paulo, 2012

This Master's dissertation aims to study technical potentialities of Fuel Cell technology, including the economical benefits that can provide compared with public grid as well.

Thus, the dissertation has been focused in two main parts: the first concerns in an experimental approach to supply electrical power to the public grid using a Polymer Electrolyte Membrane Fuel Cell (PEMFC), while the second one presents a global (from an engineering and economic point-of-view) assessment of a Phosphoric Acid Fuel Cell (PAFC) for the co-generation of heat with electrical energy in Brazil.

The first study has been accomplished connecting a PEMFC with a power inverter to the public grid. It has been proved experimentally that Fuel Cell is an alternative device that, as long as fuel is fed, may provide electrical energy continuously and more efficiently than traditional devices.

The second study has been focused in the so-called Phosphoric Acid Fuel Cell (PAFC) that, being a Medium Temperature Fuel Cell, beyond to supply electrical energy, may be used for co-generation of thermal energy. Through this study it has been showed that, at the current state-of-art, PAFC is is not already a mature technology and it becomes economically viable only for niche market applications, represented by the industrial sectors with high base load power and continuous thermal energy demand. However, accumulated knowledge expressed by learning curve and natural gas shock price caused by possible LNG supplying and shale gas recovery are the two main factors that may turn investment in PAFC profitable worldwide.

Keywords: Fuel cell, Hydrogen, Inverter, Public grid, Phosphoric acid fuel cell, Co-generation, Natural Gas

Summary

List of figures

List of tables

Dissertation proposals: main aim

Technical and economical assessment of two different classes of Fuel Cells (FCs): a Polymeric Membrane Fuel Cell (PEMFC) and a Phosphoric Acid Fuel Cell (PAFC), low and medium temperature fuel cells, respectively.

Dissertation proposals: secondary aims

Show the procedures to build a plant for power production using a PEMFC fed with Hydrogen.

Demonstrate the economical feasibility of a commercial PAFC for Brazilian market conditions.

1. Introduction

In order to achieve such goal, the research has been pointed out on three main investigation lines: state-of-art of current technology, experimental tests and economic assessment in agreement with Brazilian market conditions.

In the first part, fuel cell technology has been investigated. After an introductory part (Chapters 1-3) where it has been presented how FC work and the major differences between those and heat engines, fuel cell categories (low and high temperature FCs) and the types of fuels exploitable in these devices have been studied in deep (Chapters 4-5).

In the second part (Chapters 6-7), experimental tests with a proton-exchange membrane FC has been carried out. This experimental study was accomplished at IPEN (Instituto de Pesquisas Energéticas e Nucleares) and aimed to build a system that could provide (using pure hydrogen as feedstock) electrical energy to public grid with higher efficiency than traditional thermal power plants (roughly 33-38% for simple cycle power plant).

In the third part, a global assessment for a commercial FC class (Phosphoric Acid Fuel Cell PAFC) has been achieved (Chapter 8). In this section, firstly material and energy balance and secondly a financial assessment were achieved.

To conclude, in chapter 9, all the results obtained were summarized and deeply commented.

1.1 What is a fuel cell?[1]

Fuel cells are electrochemical devices that convert the chemical energy of a fuel (typically hydrogen) combined with an oxidant (oxygen for small application, air for large stationary plant) directly into power, without the use of a thermal fluid, as occurs in the most common power plants. Furthermore, they produce heat and water as by-product, permitting to accomplish co-generation of thermal energy. A schematic representation of a fuel cell device is represented in Figure 1.

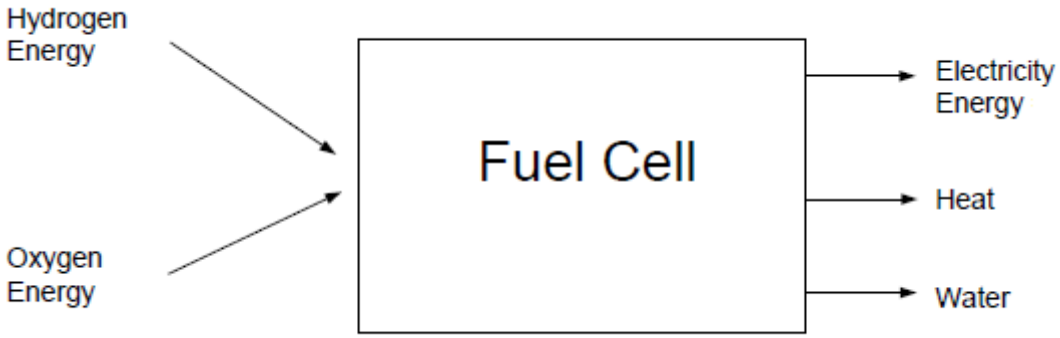

Figure 1. Fuel Cell device

Fuel cell works very simply: according to Larminie et al. (2003, p.), the first demonstration of a fuel cell was carried out by William Grove in 1839, using the experiment shown in Figures 2a and 2b. Firstly, Grove split water into hydrogen and oxygen using an electrical current (Electrolyses process, figure 2a). Subsequently, the electrolysis was reversed and, combining the same reagents, he saw that with such process, electrical current and power may be produced (Figure 2b).

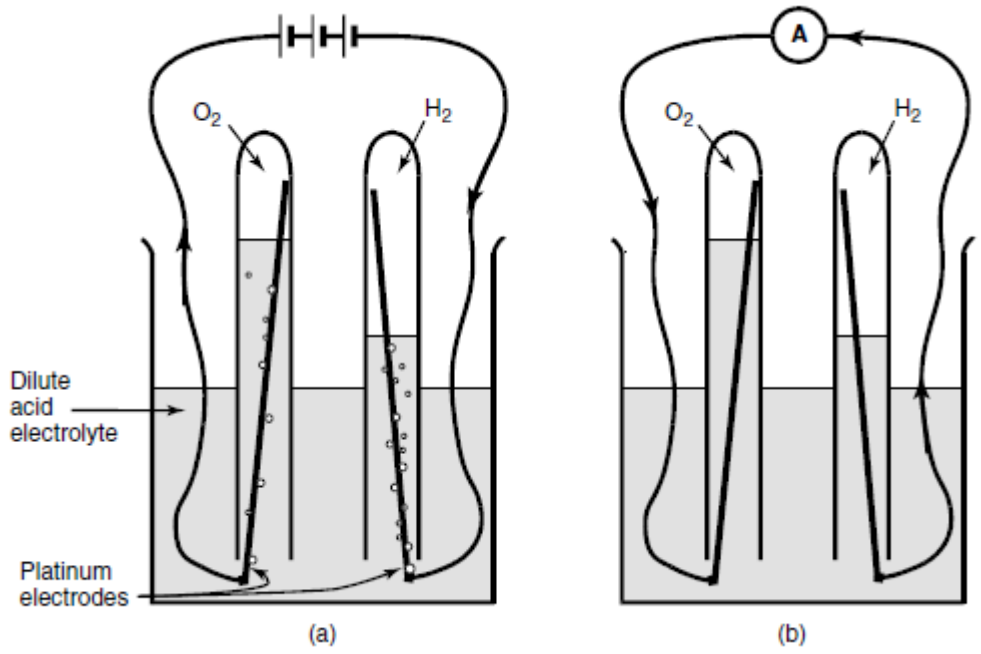

Figure 2. Grove's experiment[1]

At the anode (negative terminal), the hydrogen is split into an electron (e^-) and a proton (H^+):

$$H_2 \rightarrow 2H^+ + 2e^- \qquad \text{Eq. 1}$$

At the cathode (positive terminal), oxygen reacts with electrons taken from the electrode, and H+ ions from the electrolyte, to form water.

$$\tfrac{1}{2}\, O_2 + 2e^- + 2H^+ \rightarrow H_2O \qquad \text{Eq. 2}$$

So, the overall reaction is, as follows:

$$H_2 + \tfrac{1}{2}\, O_2 \rightarrow H_2O \qquad \text{Eq. 3}$$

Clearly, in order that these reactions could proceed continuously, the electrons formed at the anode must reach the cathode, passing through an electrical circuit. In addition to electrical power generated, the “protagonists” of the process (electron, proton and oxygen) combine together to generate water as by-product. A better schematic representation of how FC works is showed in Figure 3.

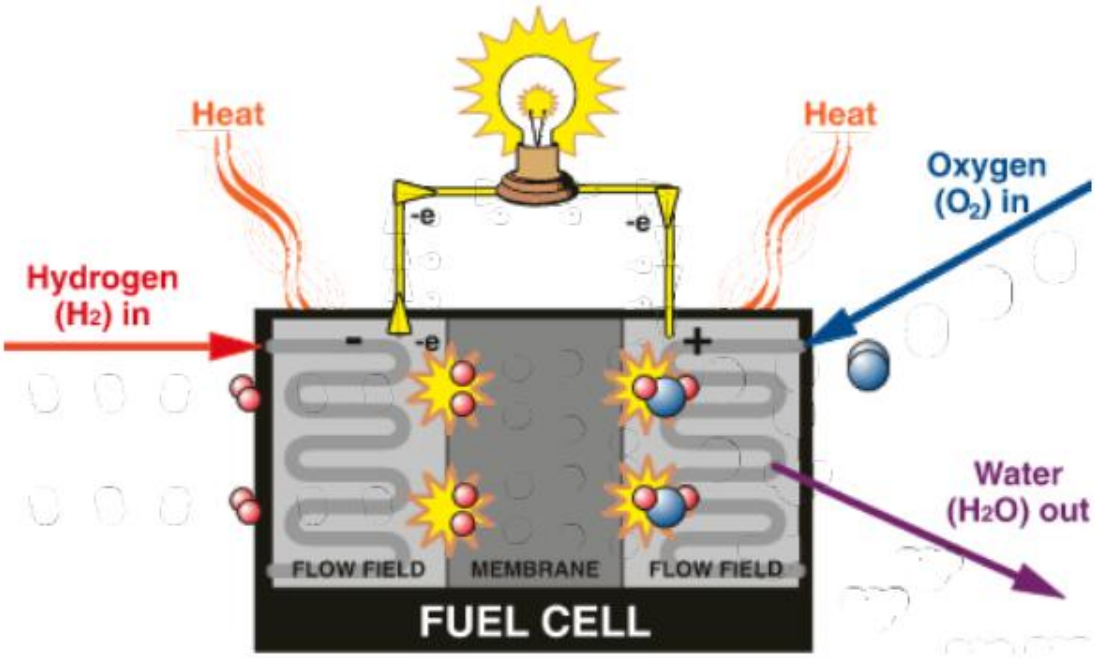

Figure 3. Basic Fuel Cell operation

Besides that, problems arise when simple FC is constructed. In fact, FCs have a very small area of contact between the three main components: electrolyte (the membrane), electrode (anode and cathode) and gas fuel. This condition, in addition to the high resistance through the electrolyte (due to the distance between the electrodes) cause in a very small current produced.

To overcome these problems, flat electrodes are usually made and a thin layer of electrolyte is used. Moreover, the electrode is porous permitting the simultaneous penetration of both the electrolyte and the gas. This design permits to maximise the area of contact between electrodes, electrolyte and gas, increasing the performances (in term of current and efficiency) of the FC.

1.2 What limits the current?[2]

When the hydrogen reacts, it releases energy. Nevertheless, it does not mean that the reaction can progress at an unlimited rate. Indeed, as occurs in all the chemical reaction, at least the so-called "activation energy" must be supplied to overcome the "energy hill" (Figure 4).

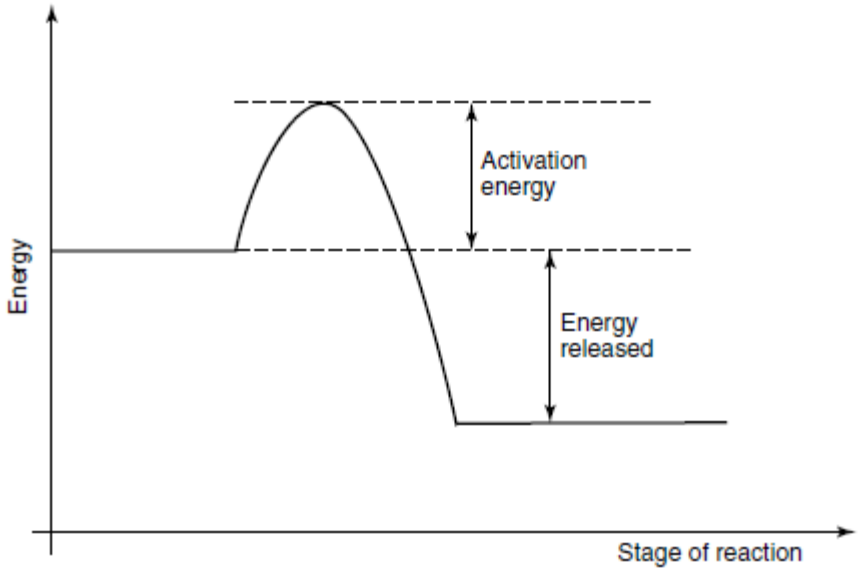

Figure 4. Classical energy diagram for a simple exothermic chemical reaction[2]

Basically, there are three methods of increasing reaction rates:

- using a catalysts,
- raising the temperature,
- increasing the electrode area.

The first two are common procedures for any chemical reaction. However, the third is a typical technique only for fuel cells applications. Clearly, the rate of the electrochemical reaction will be proportional to the area of the electrode. This concept states that the area is a vital issue and the performance of a FC is generally reported in terms of current per cm^2. However, this is not the only issue. As has been mentioned in the previous section, the electrode should be porous, permitting to increase the effective surface area. Modern FC

electrodes have a microstructure that gives them surface areas hundreds or even thousands times higher than their straightforward "length × width" (See Figure 5).

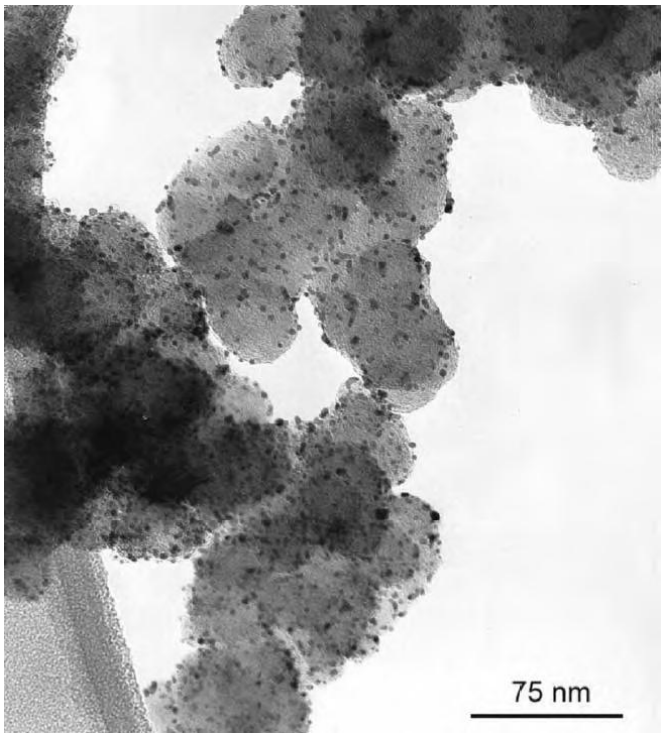

Figure 5. Fuel Cell catalyst[2]

2. Fuel Cell Vs Carnot Cycle: efficiency comparison

As it has been claimed in the chapter 1.1, a FC is classified as a direct energy conversion device: this means that the conversion of chemical energy into power is achieved without the intermediate step of transferring heat through a working fluid. According to Lutz et al. (2002, p. 1104)[3], for any process that use energy to produce work, the basic definition of thermal efficiency is the work output divided by heat input.

$$\eta = \frac{W_{out}}{Q_{in}} \qquad \text{Eq. 4}$$

In order to assess the above definition for a specific device, the work and heat terms must be evaluated using the first law of thermodynamics. The first law claims that the change of

internal energy is accomplished by heat transfer to the system and work done by the system. As follows,

$$dU = dQ - dW \quad \text{Eq. 5}$$

For a FC, the work can be splitted into flow work (pdV) and electrical work. Readjusting,

$$dU = dQ - pdV - dW_{elec} \quad \text{Eq. 6}$$

If you consider a constant-pressure process and you introduce the term enthalpy,

$$H \equiv U + pV \quad \text{Eq. 7}$$

Eq. 5 becomes, as follows:

$$dH = dQ - dW_{elec} \quad \text{Eq. 8}$$

Working with the ideal limit of reversible process, heat transfer is dQ=TdS. Thus, the left-hand side of Eq. 5 is the change in Gibbs energy (G≡H–TS) for a constant temperature process. So, the net work output is then:

$$W_{out} = -\Delta G_R, \quad \text{Eq. 9}$$

where:

$$\Delta G_R = \Delta G(T, \text{products}) - \Delta G(T, \text{reactants}) \quad \text{Eq. 10}$$

where the subscript R denote the change athwart the reaction.

In other hand, the maximum work available in a FC is equal to the change in the Gibbs energy for the reaction. The heat input is the heating value of the fuel, which corresponds to the change in enthalpy for the reaction,

$$Q_{in} = -\Delta H_R \quad \text{Eq. 11}$$

Replacing the net work and heat input into Eq. 4, the efficiency becomes simply the ratio of the changes in Gibbs energy and enthalpy.

$$\eta_{FC} = \frac{\Delta G_R}{\Delta H_R} \quad \text{Eq. 12}$$

Appleby and Foulkes[4] present values for the maximum efficiencies for several fuel cell reactions, including some where η is greater than 100%. To understand how such values may be achieved, free Gibbs energy has to split into:

$$\eta_{FC} = \frac{\Delta H_R - T\Delta S_R}{\Delta H_R} = 1 - \mathrm{T}\,\frac{\Delta S_R}{\Delta H_R} \qquad \text{Eq. 13}$$

The change in enthalpy for any exothermic reaction is negative. However, the entropy change, even if it is normally negative, can be positive. For example, if we look to the follow reaction:

$$\mathrm{C(s) + ½\ O_2\ (s) \rightarrow CO\ (g)}$$

the efficiency could seem greater than 1. Physically it indicates that the FC, besides to exploit completely the chemical energy of the reactants, absorbs thermal energy from the environment, converting both sources into electrical energy. In such case, the additional energy provided by the environment must be taken in account for the balance of Q_{in}. A more general definition of heat input includes a switch based on the sign of the entropy change.

$$Q_{in} = \begin{cases} -\Delta H_R & if\ \Delta S_R \leq 0 \\ -\Delta H_R + \Delta S_R & if\ \Delta S_R > 0 \end{cases}$$

Then, for $\Delta S_R > 0$, the thermal efficiency of fuel cell becomes:

$$\eta_{FC} = \frac{-\Delta G_R}{-\Delta H_R + T\Delta S_R} = \frac{-\Delta H_R + T\Delta S_R}{-\Delta H_R + T\Delta S_R} = 1$$

and the maximum efficiency corresponds to the unit for any fuel where $\Delta S_R > 0$. This is a much more satisfactory result, especially comparing fuel cell performances with heat engines.

2.1 Carnot cycle efficiency

The Carnot cycle establishes the maximum efficiency for any cycle that work transferring thermal energy between two temperature reservoirs. According to the model expressed by Carnot, the work done on and by the system is isentropic (reversible and adiabatic), while the heat transfer to and from the system is reversible and isothermal. As already defined in Eq. 4, the thermal efficiency is the work output divided by heat input. If we are examines a

continuous process, the internal energy cannot change. So, according to the first law of thermodynamics:

$$\oint dU = 0 = \oint dQ - \oint dW \qquad \text{Eq. 14}$$

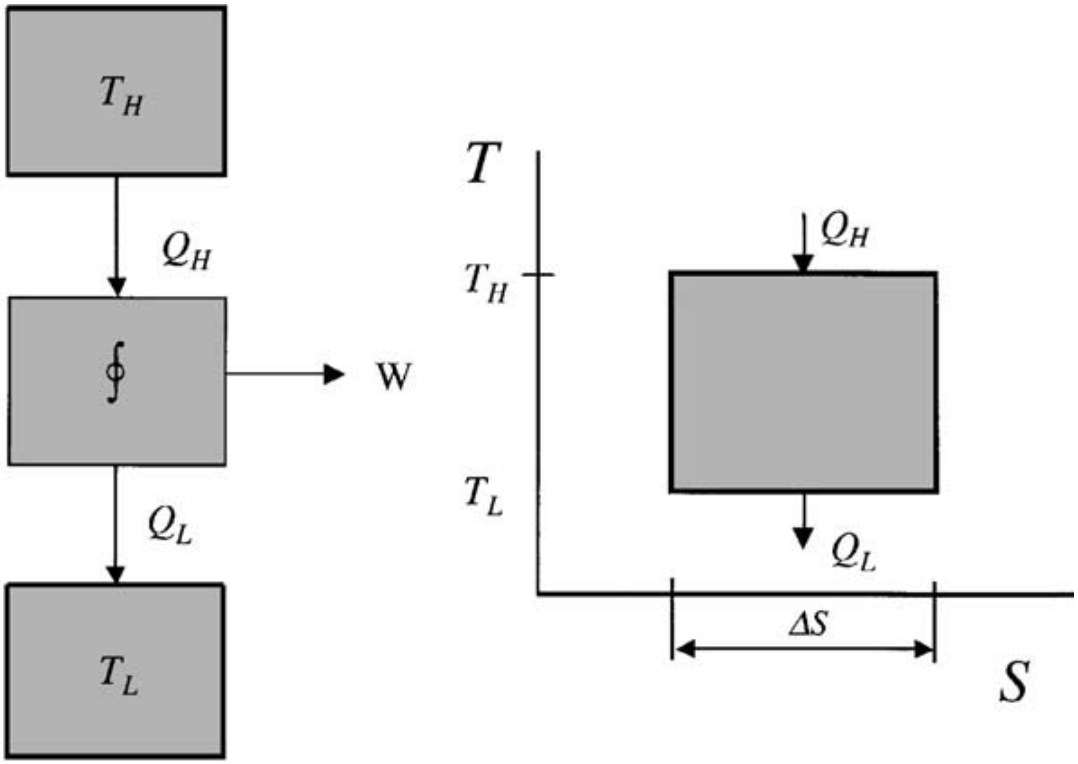

Figure 6. Carnot Cycle[3]

Resolving the integrals we have that net work output, $W_{out} = Q_H - Q_L$, where the subscripts H and L refer to heat transfer at the high and low temperatures. Moreover, according to the arrows represented in Fig. 6, Q_H and Q_L are positive. The thermal energy provided into the cycle is generated by Q_H, obtaining the following thermal efficiency:

$$\eta_{Carnot} = \frac{Q_H - Q_L}{Q_H} \qquad \text{Eq. 15}$$

For any reversible process, the heat transfer is $dQ = TdS$. Thus, at constant temperature, the heat supplied and rejected are $Q_H = T_H \Delta S$ and $Q_L = T_L \Delta S$, respectively. Therefore, Eq.15 turns:

$$\eta_{Carnot} = \frac{T_H - T_L}{T_H} = 1 - \frac{T_L}{T_H} \qquad \text{Eq. 16}$$

Since T_L is usually set by surrounding conditions, the Carnot expression shows that to increase the efficiency of a heat engine, we must increase as hot as possible the temperature of the the working fluid. Nevertheless, the limit

$$T_H \to \infty$$

means:

$$\text{Carnot} \to 1.$$

Nevertheless, practically this limit does not make sense, because to reach the unity, the temperature should be infinite; however, it is important in establishing the equivalence of the two processes. In fact, although we analyze a fuel cell and a Carnot cycle starting from the same basic definition (Eq. 4), the resulting expressions for efficiency look different (Eq. 13 versus Eq. 16). To conclude, the Carnot efficiency is a ratio of temperatures, while the fuel cell efficiency is a ratio of energy changes for a reaction.

2.2 Fuel Cell efficiency

If we want to compare the two models (Carnot Cycle and Fuel Cell), we should start admitting that the high temperature reservoir should be generated by the release of chemical energy. In order to obtain the maximum Carnot efficiency, the highest temperature possible is needed. This temperature is achieved when the change in Gibbs free energy is zero.

$$\Delta G_R = 0 = \Delta H_R - T\Delta S_R \qquad \text{Eq. 17}$$

This defines the combustion temperature, T_C as follow:

$$T_C = \frac{\Delta H_R}{\Delta S_R} \qquad \text{Eq. 18}$$

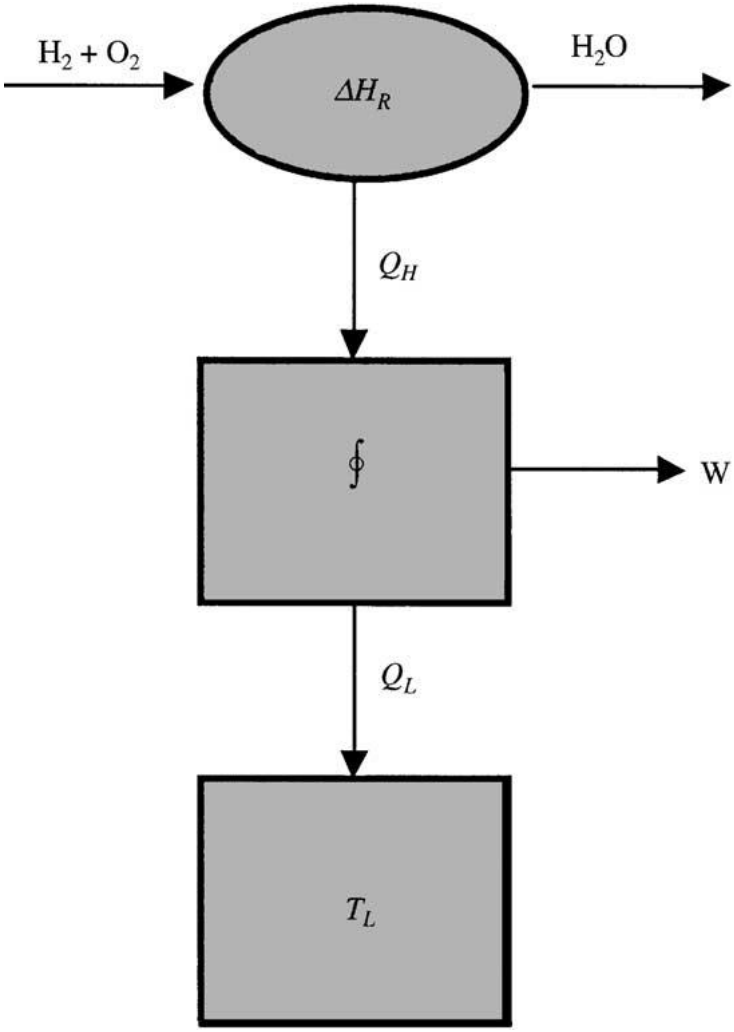

Figure 7. Carnot cycle running with Fuel Cell as High Temperature reservoir[3]

Since the chemical reactor itself does not accomplishes work, other than flow work (pdV), the first law energy balance is simply:

$$Q_H = -\Delta H_R(T_C) \qquad \text{Eq. 19}$$

Considering a reversible heat transfer, the thermal energy rejected by the heat engine is $Q_L = -T_L \Delta S_W$, where W denotes the working fluid and the entropy change is negative (going from right-to-left on the T–S diagram). In a Carnot cycle, the entropy changes for the working fluid at the low and high temperatures must be equal and opposite, $\Delta S_W(T_L) = -\Delta S_W(T_H)$. So, the heat loss becomes:

$$Q_L = -T_L \Delta S_W(T_L) = T_L \Delta S_W(T_H) \qquad \text{Eq. 20}$$

Overhauling the reactor and combining Eq. 18 and Eq. 19 we may write:

$$Q_H = -\Delta H_R(T_C) = -T_C \Delta S_R(T_C) \quad \text{Eq. 21}$$

The working fluid receives $Q_H = T_H \Delta S_W$ by reversible heat transfer, which requires the temperature difference between the reactor and working fluid to be infinitesimal, so $T_H = T_C$. Readjusting Eq.21:

$$Q_H = -T_C \Delta S_R(T_C) = T_C \Delta S_W(T_H) \quad \text{Eq. 22}$$

Or:

$$-\Delta S_R(T_C) = \Delta S_W(T_C) \quad \text{Eq. 23}$$

This shows that the change in entropy of the working fluid and the reactor are equal. Combining Eq.20 and Eq.23, the heat rejection term is:

$$Q_L = T_L \Delta S_W(T_H) = -T_L \Delta S_R(T_C) \quad \text{Eq. 24}$$

Substituting Eqs. 10 and 14 into Eq. 6, the thermal efficiency is:

$$\eta_{Carnot} = \frac{Q_H - Q_L}{Q_H} = \frac{\Delta H_R(T_C) - T_L \Delta S_R(T_C)}{\Delta H_R(T_C)} \quad \text{Eq. 25}$$

This equation represents the efficiency of a Carnot cycle where thermal energy is provided by an isothermal reactor operating at the maximum temperature sustainable. It is important to recognize that Eq.25 is equivalent to Eq.15 when the combustion temperature defined by Eq.18 is inserted for T_H. The final step in comparing the two models needs an approximation. Typically, the enthalpy and entropy of reaction are not strong functions of temperature. Thus,

$$\Delta H(T_L) \approx \Delta H(T_C)$$

and:

$$\Delta S(T_L) \approx \Delta S(T_C)$$

then Eq.22 can be written entirely at the low temperature, T_L. Then by definition,

$$\Delta G_R(T_L) = \Delta H_R(T_L) - T_L \Delta S_R(T_L) \quad \text{Eq. 26}$$

and the efficiency of the reactor driven by the Carnot cycle now looks the same as for the fuel cell (Eq.12).

$$\eta_{Carnot} \approx \left(\frac{\Delta G_R}{\Delta H_R}\right)_{T_L}$$

This process, well described by Lutz et al.(2002, p. 1104), shows that if a reversible heat engine could work under the maximum temperature limit allowed by a "perfect" combustion of a fuel/oxidant mixture, its performances (expressed in term of efficiency) would be the same of a reversible isothermal fuel cell using the identical fuel/oxidant mixture and operating at the same level of temperature. On the other hand, the maximum possible efficiency is the same for both fuel cells and heat engines[5]. Therefore, the common statement that fuel cell is not subjected to the Carnot efficiency, resulting in higher efficiency[6,7] is partly "correct" and partly "incorrect", depending on the angle of viewpoint. It is "correct" because fuel cells do not require two thermal source to work (thus no T_H e T_L are needed). Clearly, it is better to express the same concept reporting that Carnot efficiency does not apply to fuel cell.

Reporting that heat engines and fuel cells are subject to the same second law limitation, the reasons why fuel cells could achieve higher energy conversion efficiency that the corresponding heat engines are, as follows:

- the theoretical combustion temperature T_H is cannot be achieved in practice: indeed, for a perfect combustion, flame temperature should be well above 3000K. However, product dissociation occurs and incomplete combustion products are formed, such as CO, NO, C (particulates), OH, O, N, etc., leading to a lower temperature T_H' (generally 2200 K for hydrocarbon fuels).
- Due to a metallurgic point-of-view, T_H' has to be lowered in heat engines to permit metallic components have sufficient mechanical strength. For example, the maximum allowable temperature for gas turbines is about 1000K (with good cooling of turbine blades).
- The heat rejected to the lower temperature is not achieved in practice at the ambient atmospheric temperature T_L, but at a temperature T_L' which is higher. (e.g., $T_L' \cong$ 550K for gas turbine instead of about 300K).

Therefore, the actual maximum efficiency

$$\eta' = 1 - \frac{T_H'}{T_L'} \cong 1 - \frac{550}{1000} = 45\%$$

Which is only about half of the theoretical value,

$$\eta = 1 - \frac{T_H}{T_L} \cong 1 - \frac{300}{3000} = 90\%$$

Considering other related losses such as frictions, heat engines usually have lower than about 40% energy efficiency.

On the other hand, fuel cells can operate isothermally at a temperature sufficiently low to do not permit limitation imposed by materials and sufficiently close to the atmospheric temperature so that the degree of irreversibility arising from cooling requirement is much less than the corresponding heat engines. Even though, irreversibilities occur in fuel cells as well, but at lower degree, so that they achieve higher efficiency that the conventional heat engines. Moreover, in order to improve exergy efficiency, one of the chief investments in high-temperature fuel cells research are finalized even to reduce this working temperature. Figure 8 shows a comparison of the practical energy conversion efficiency for different power generation technologies as a function of scale[8], which clearly illustrated the superior performance of fuel cells over the conventional heat engines.

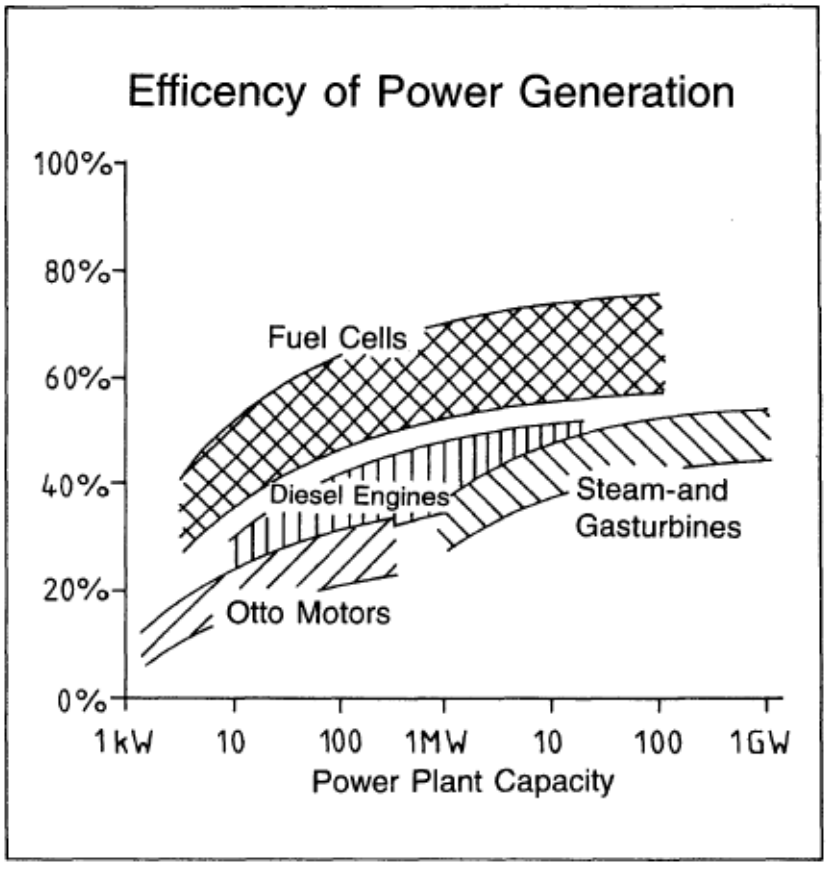

Figure 8. Efficiencies of Different Technologies as a Function of Scale[8]

2.3 Effect of temperature on thermodynamic efficiency[9]

If the entropy change of a reaction is negative, Eq. 13 shows that the thermodynamic efficiency would decrease with an increase of temperature (remember the negative sign of ΔH). Larminie et al. (2003, p. 45) affirm that an important difference between this result and the corresponding one for a common thermal engine should be pointed out. As much the temperature of the hot thermal fluid increases, the difference between the temperatures of the heat source (T1) and the heat sink (T2) also increases. Consequently the corresponding Carnot efficiency increases with temperature. However, it cannot simply be assumed that, as much T1 increase, T2 continues remaining fixed at ambient temperature. In fact, increasing T1 would automatically cause some increase in T2. In Figure 9, the variation of thermodynamic maximum efficiency of a hydrogen-oxygen fuel cell and of heat engines as a function of temperature is shown. Considering the changes in thermodynamic efficiency as a function of the temperature, the advantages of fuel cells performance are reduced if compared with conventional thermal engines. However, it should be pointed out that, at higher temperatures, there is no need for expensive electro catalysts (because the temperature itself increases the reaction rate), allowing cheaper FC construction cost.

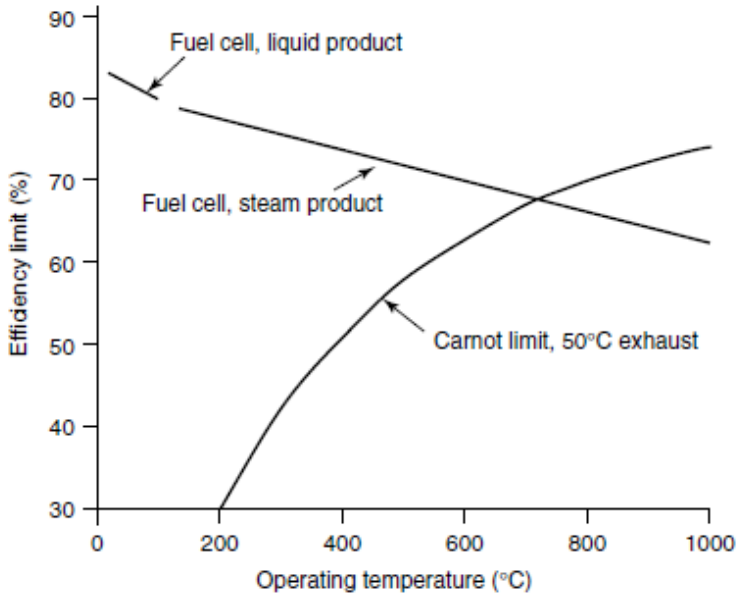

Figure 9. Comparison between the Carnot and the thermodynamic efficiency of a Fuel Cell[9]

2.4 Efficiency and Fuel Cell Voltage

According to electrochemical reaction of Eq. 3 (typical of a fuel cell fed with pure hydrogen and oxygen), each water molecule produced corresponds to two electrons passing through the external circuit and providing power. In order to express mathematically this concept, it has been stated that for one mole of hydrogen used, 2N electrons pass round the external circuit (where *N* is Avogadro's number). If *e* is the charge on one electron, then the charge that flows is:

$$-2\,Ne = -2F \quad [C] \qquad \text{Eq. 27}$$

F is the Faraday constant (the charge on one mole of electrons). If E is the voltage of the fuel cell, then the electrical work done is:

$$\text{Electrical work done} = \text{charge} \times \text{voltage} = -2FE \quad [J]$$

If the system is reversible (no losses), then this electrical work done will be equal to the Gibbs free energy released G_f. So,

$$G_f = -2FE \quad [J] \qquad \text{Eq. 28}$$

Thus:

$$E = -\frac{\Delta G_f}{2F} \quad [V] \qquad \text{Eq. 29}$$

This fundamental equation gives the electromotive force (EMF) or reversible open circuit voltage of the hydrogen FC. The EMF of a FC can also be very easily related to its efficiency. If all the energy derived from the enthalpy of formation hydrogen fuel is transformed into electrical energy, then the EMF would be given by:

$$E = -\frac{\Delta H_f}{2F} \quad [V] \qquad \text{Eq. 30}$$

However, in Eq. 30, two different values of ΔH_f may be used. For the 'burning' of hydrogen, if water produced is in form of steam:

$$H_2 + ½\ O_2 \rightarrow H_2O \text{ (steam)}$$

$$\Delta H_f = -241.83 \text{ kJ/mol}$$

Whereas, if the water is recovered in liquid form, the reaction is:

$$H_2 + ½\ O_2 \rightarrow H_2O \text{ (liquid)}$$

$$\Delta H_f = -285.84 \text{ kJ/mol}$$

The difference between these two values (ΔH_f=44.01 kJ/mol) is the molar enthalpy of vaporisation of water. Commonly, in the first scenario, enthalpy corresponds to the higher heating value (HHV), while in the second one, obviously, to the lower heating value (LHV). Usually, for a commercial fuel cell, efficiency should report if it relates to HHV or LHV. If this information misses, the LHV has probably been used, since it gives a higher efficiency value.

Thus, according to Eq. 30, EMF would be 1.25 V if water is gaseous or 1.48 if the product is in the liquid phase.

These above values are the voltages that would be obtained from a 100% efficient system, with reference to the HHV or LHV. So, the actual efficiency of the FC is calculated dividing the actual voltage by these values, or:

$$Cell\ Efficiency_{HHV} = \frac{V_c}{1.48} \times 100\% \qquad Eq.31$$

Based on HHV, or:

$$Cell\ Efficiency_{LHV} = \frac{V_c}{1.25} \times 100\% \qquad Eq.32$$

Based on LHV.

However, in practice, not all the amount of fuel that is fed can be used. As typically happens in all chemical reaction, a certain portion of fuel does not react. Because of this, Eq. 31 and Eq. 32 should be restructured, as follows:

$$Efficiency_{HHV} = u_f \times \frac{V_c}{1{,}48} \times 100\% \qquad Eq.33$$

$$Efficiency_{LHV} = u_f \times \frac{V_c}{1{,}25} \times 100\% \qquad Eq.34$$

Where u_f is the fuel utilization (typically 0.95).

Event the pressure and concentration of the reactants take part in the Gibbs free energy, and thus the voltage and the efficiency. The correlation is expressed by the Nernst equation. If the pressures of the reactants and products are given in bar and the water product is in the form of steam, then:

$$E = E_0 + \frac{RT}{2F} ln\left(\frac{p_{H_2} p_{O_2}^{1/2}}{p_{H_2O}}\right) \qquad Eq.35$$

where E_0 is the cell EMF at standard pressure.

3. Operational Fuel Cell Voltage

In practice, the previous described cell potential is not achieved in practice. In fact, several types of irreversible losses occur. Larminie et al. (2003, p. 48)[9] relate that the main causes of voltage losses are:

- Activation losses: in practice, a certain portion of the voltage generated into the fuel cell is lost by the slowness of transferring stage of the electrons to or from the electrode. This voltage drop is highly non-linear.
- Fuel crossover and internal currents: The electrolyte, in practice, should only transport ions through the cell, however, a certain amount of fuel and electron flow can occurs as well. Except in the case of direct methanol fuel cells, the fuel and current losses are small, and effects are negligible.
- Ohmic losses (or resistive losses): this voltage drop represents the resistance to the flow of electrons through the material of the electrodes and the various interconnections, as well as the resistance to the flow of ions through the electrolyte. This voltage loss is essentially proportional to current density and linear.
- Mass transport or concentration losses: these losses are mainly caused by the change in concentration of the reactants at the surface of the electrodes. This voltage drop occurs for a failure to transport of reactants to the electrode surface: because of this, this loss is also called “mass transport loss”.

These losses result in a cell voltage (V) for a fuel cell that is always less than its ideal potential E.

V = E - Losses

In Fig. 10 and Fig. 11, there are represented graphically the three areas corresponding to the three main losses (fuel crossover and internal currents are negligible). Thus, typical voltage/current density is shown:

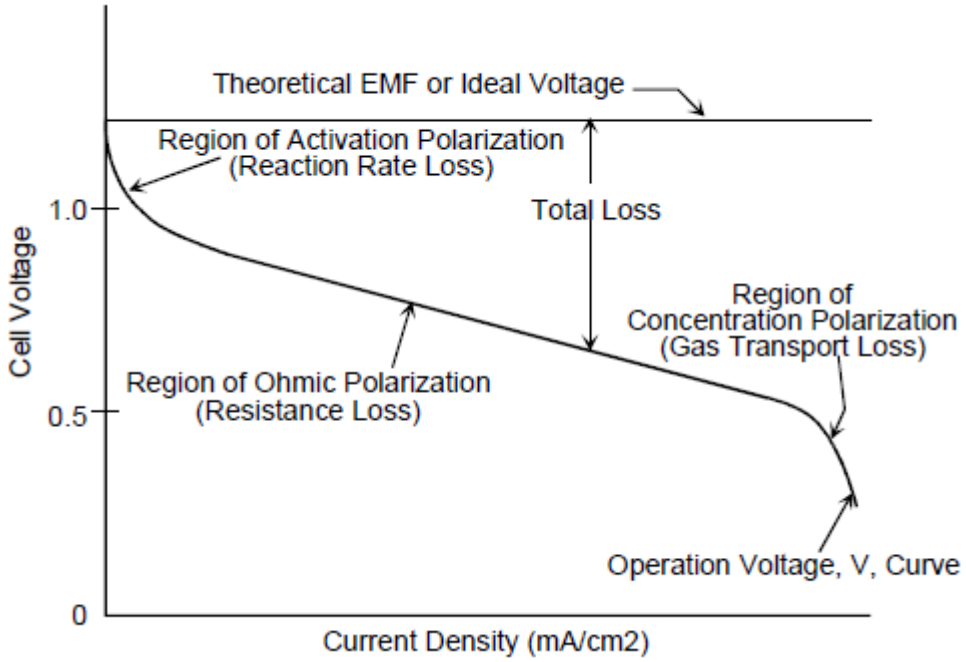

Figure 10. Graph showing the voltage for a typical low temperature fuel cell[9]

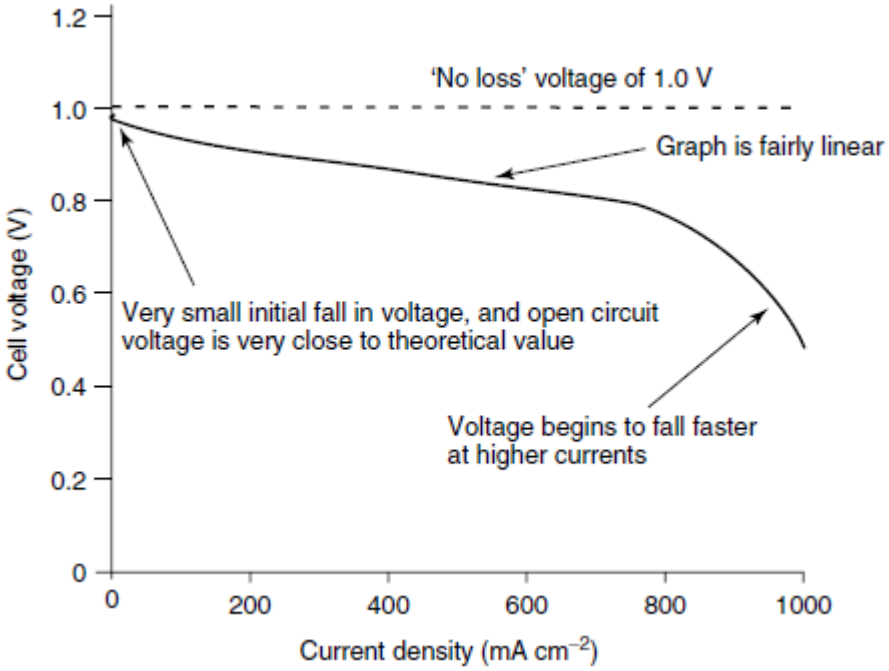

Figure 11. Graph showing the voltage of a typical high temperature fuel cell[9]

The two figures above represent voltage drops for low and high-temperature FCs. As Fig. 10 and Fig. 11 show, voltage losses of the two graphs are quite similar. The only difference is represented by activation losses that does not occur if high temperatures are used.

3.1 Connecting Cells in Series[10]

For the reasons explained in Section 3, the voltage of a fuel cell is quite small (about 0.7 V when useful current is carried out). This means that to produce a useful voltage, many cells have to be connected in series. Such a collection of FCs is called "stack" and the best way to made it is called "bipolar connection". In fact, such configuration serves as feeder for oxygen to the cathode and fuel gas to the anode (Figure 12).

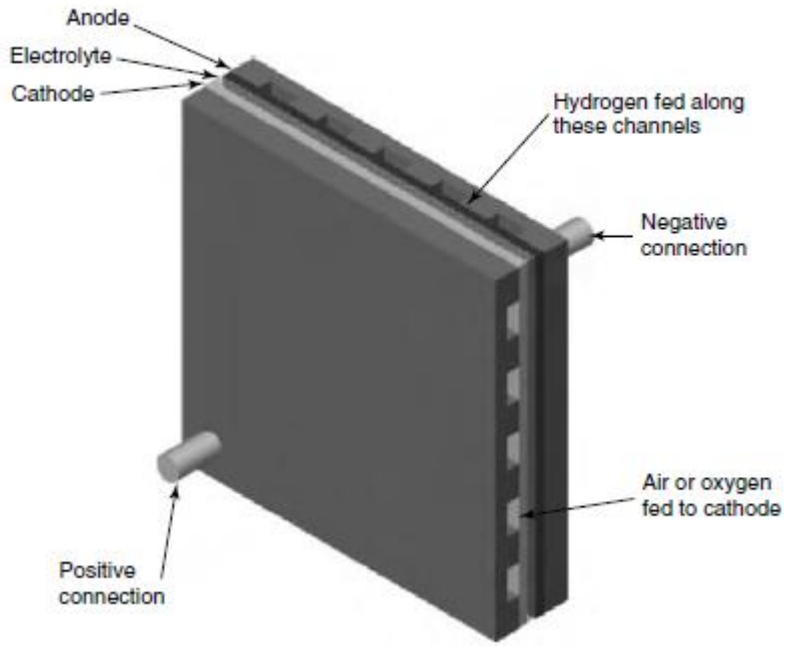

Figure 12. Single cell, with end plates for taking current from all over the face of the electrodes, and also supplying gas to the whole electrode[10]

Figure 12 represents a 'bipolar connection' for a stack formed by a single fuel cell. However, to connect several cells in series, 'bipolar plates' are made. These plates (or cell interconnects) present channels to permit to gases to flow over the face of the electrodes,

giving a solid block, called ‘stack’ (Figure 13). This ‘stack’ has vertical channels for feeding hydrogen over the anodes and horizontal channels for feeding oxygen (or air) over the cathodes.

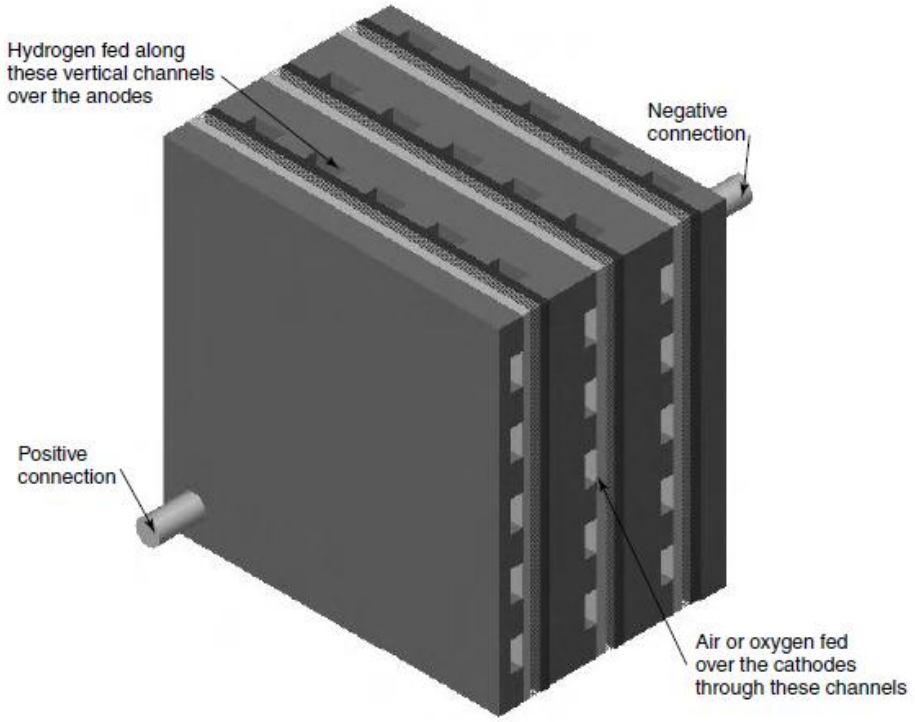

Figure 13. A three-cell stack showing how bipolar plates connect the anode of one cell to the cathode of its neighbour[10]

4. Fuel Cell types[11]

At the actual state-of-art, six classes of fuel cell have emerged as viable systems for the present and near future. These fuel cell are usually divided in three categories, depending by working temperature:

•Low-temperature cells, includes proton exchange membranes fuel cell (PEMFC) and alkaline fuel cells (AFC) which operate in the range 50-120°C.

•Medium-temperature cells, comprise the phosphoric acid fuel cells (PAFC) which operates around 190 - 220°C.

•High-temperature cells, which operate at higher temperatures are the molten carbonates fuel cell (MCFC) and the solid oxide fuel cells (SOFC) which operate in the range 600-700 and 700-1000°C, respectively.

4.1 Low-Temperature Fuel Cell

4.1.1 Proton Exchange Membrane Fuel Cell

The proton exchange membrane fuel cell (PEMFC), even called the solid polymer fuel cell (SPFC), was first developed by General Electric in the United States in 1960s for use by NASA on their space vehicles. Nowadays, PEMFCs are used for a wide range of applications, from stationary applications to automotive and portable applications. However, especially to this high interest in fuel cell vehicles, investment in PEMFC over the past decade easily surpasses all other types of fuel cells. The electrolyte in this fuel cell is good proton conductor membrane (fluorinated sulfonic acid polymer or other similar polymers). The only liquid in this fuel cell is water, thus corrosion problems are minimal. Instead, the water management in the membrane is crucial for efficiently performance. The by-product water should not evaporate faster than it is produced because the membrane must be continuously hydrated. Because of the limitation on the operating temperature (usually less than 120°C) imposed by the polymer, a H_2 rich gas with little or no CO (a poison at low temperature) is used and Pt catalysts is required in the anode and cathode.

4.1.1.1 Advantages

The PEMFCs operate at low temperature allowing rapid start-up and. Absence of corrosive cell constituents and the non use of sophisticated materials (usually required in high temperature fuel cells) represent other main vantages of PEMFC compared to other ones. The PEMFC is used particularly into situations where pure hydrogen can be used as a fuel.

4.1.1.2 Disadvantages

The low operating temperature range makes thermal management complicated and the use of the rejected heat for cogeneration is difficult as well. Water management is a significant challenge in PEMFC design: in fact, it should be balanced sufficient hydration of the electrolyte against flooding of the electrode. In addition, PEMFCs are quite sensitive to poisoning of CO, sulfur species, and ammonia. Some of these disadvantages can be counteracted by lowering operating current density and increasing electrode catalyst loading, but both increase cost of the system. If hydrocarbon fuels are used, the processing fuel system (generally reforming) causes negative impacts: plant size, complexity, efficiency and system cost. Finally, the use of hydrogen needs a specific and safety infrastructure that, nowadays, causes a barrier yet.

4.1.2 Alkaline Fuel Cell

Even if PEMFC was chosen for the first NASA spacecraft firstly, it was the alkaline fuel cell (AFC) the device that permit man to reach the moon with the Apollo missions. After this, the AFC has found considerable success in space applications. However, the strong sensitivity to CO_2 has not permitted its propagation even for terrestrial applications yet. The electrolyte is a porous matrix saturated with a concentrated (85wt%) KOH solution for AFC operating at high temperature (~250°C), or less concentrated (35 to 50wt% of KOH) for lower temperature (<120°C) operation. The electrolyte is kept in a matrix of asbestos and several electro-catalysts can be used (e.g., Ni, Ag, metal oxides, spinels, or noble metals). For what may concern contaminations, CO and CO_2 (even the small amount presented in the air) are poisons: the latter reacts with the KOH to form K_2CO_3 altering the electrolyte. Regarding fuel supply, hydrogen is considered the preferred fuel for AFC.

4.1.2.1 Advantages

AFC achieves excellent performance on H_2 and oxygen O_2 compared to other fuel cells. This is due to its active O_2 electrode kinetics and its flexibility to use a large range of electro-catalysts.

4.1.2.2 Disadvantages

Because of high sensitivity of the electrolyte to CO_2, highly pure H_2 has to be supplied. In case of use another hydrocarbon fuels, reforming process would need a highly effective CO and CO_2 removal system. Moreover, if ambient air is used as the oxidant, the CO_2 of the air must be removed: all of this problems have a significant impact on the size and cost of the system, not permitting a easily used for civil applications.

4.2 Medium and High-Temperature Fuel Cell[12]

Up to now, just fuel cells working in the range 60-120 °C were described. In addition to those, several classes of medium and high temperature work at temperature up to 1000°C . The main advantages are, as follows:

- The electrochemical reaction proceeds faster, and lower activation voltage losses does not occurred. Also, noble metal catalysts are often not needed.
- The high temperature of the cell and the exit gases temperature means that there is thermal energy available from the cell at temperatures high enough to facilitate the reforming process of a more available fuel, such as natural gas.
- Medium and high temperature fuel cells are excellent ‘combined heat and power systems’: the high-temperature of the cells give the possibility to co-generate the recovered thermal energy for buildings applications or used to drive a turbine for produce more electricity, thus increasing exergy efficiency.

4.2.1 Phosphoric Acid Fuel Cell

Among medium and high temperature, PAFC is the most well developed fuel cell device. Phosphoric Acid Fuel Cells were the first fuel cells to be commercialized[13]. Developed in the mid-1960s and field-tested since the 1970s, they have improved significantly in stability, performance, and cost. At the current state-of-art, these characteristics have made the PAFC the best candidate for stationary applications[14].

As electrolyte, the PAFC uses a phosphoric acid (H_3PO_4), that is the only common inorganic acid that has the thermal, chemical, and electrochemical stability and a low enough volatility (above approximately 150°C) to be considered as an electrolyte for fuel cells[15]. The operating temperatures and acid concentrations of PAFCs have increased to achieve higher levels of performance: at the present time, temperatures of approximately 200°C and acid concentrations of 100% H_3PO_4 are used[16]. This temperature is near the maximum feasible temperature because, at 210°C, phosphoric acid starts to decompose[17]. Because of this temperature range (150-200 °C), PAFCs are considered to be medium temperature fuel cells[18] that are well suited for the textile, food and beverage industries.

PAFCs are mostly developed for stationary applications. Both in the US and Japan, hundreds of PAFC systems were produced, sold and used in field tests and demonstrations. It is still one of the few fuel cell systems that are available for purchase.

4.2.1.1 Advantages

PAFCs are much less sensitive to CO than PEMFCs and AFCs[19]: PAFCs can tolerate about one percent of CO as a diluent. The working temperature also provides considerable design flexibility for thermal management. PAFCs have demonstrated system efficiencies of 37-42% (based on LHV of natural gas fuel), which is higher than most PEMFC systems could achieve (but lower than many of the SOFC and MCFC systems). In addition, the waste heat generated by PAFC can be easily used in most commercial and industrial cogeneration applications, as well as in bottoming cycle.

4.1.2.2 Disadvantages

The oxygen reduction in PAFC is slower than in AFC. Thus, platinum catalyst is needed. PAFC temperatures are not adequate for a direct reforming fuel. Thus, although less complex than for PEMFC, reforming process is needed. Moreover, to achieve good performance, a water gas shift reactor is typically installed as well. Finally, the highly corrosive nature of phosphoric acid, oblige the use of expensive materials in the stack (especially the graphite separator plates).

4.2.2 Molten Carbonate Fuel Cell

For what concerns the structure of MCFC, the electrolyte is usually a compound of alkali carbonates, kept in a ceramic matrix of LiAlO2. The fuel cell operates at 600 to 700 °C permitting to the alkali carbonates to form a good conductive molten salt. At this high operating temperatures in MCFCs, Ni (anode) and nickel oxide (cathode) are adequate to promote reaction, not requiring noble metals. In addition, because of the high temperature, many hydrocarbon and renewable fuels can be reformed internally. The focus of MCFC development has been for larger stationary and marine applications, where the relatively large size and weight of MCFC and slow start-up time are not the main issue. MCFC-like technology is also considered for Direct Carbon Fuel Cell (DCFC)[20]. Even though less developers and investment are working on MCFC, scientists state that MCFC can be considered as a second generation fuel cell because it is expected to reach commercialization after PAFCs

4.2.2.1 Advantages

The high operating temperature of the MCFC (roughly 650 °C) make the electro-catalysts use not necessary with the possibility to use directly both CO and hydrocarbons as fuels. This results in a simplified plant and higher performances. In addition, the high temperature waste

heat allows the use of a bottoming cycle or co-generation process to achieve larger first-law efficiencies.

4.2.2.2 Disadvantages

The main challenge for MCFC developers regards the high corrosive and mobile electrolyte, which requires use of nickel and high-grade stainless steel for cell hardware. Obviously, the high temperatures affect mechanical stability and stack life. Also, an additional plant component is needed: in fact, a source of CO_2 has to be supplied at the cathode (usually recycled from anode exhaust) to form the carbonate ion.

4.2.3 Solid Oxide Fuel Cell

The SOFC has started to be developed several years before the AFC and is probably the fuel cell with the longest continuous development period. The cell operates in the band 600-1000°C where ionic conduction by oxygen ions takes place. For what concern the structure, the electrolyte is a solid, nonporous metal oxide (usually Y_2O_3 stabilized ZrO_2), while the anode is Co-ZrO_2 or Ni-ZrO_2 cermet, and the cathode is Sr-doped $LaMnO_3$.

4.2.3.1 Advantages

Because the electrolyte is solid, the cell can be made into flexible shapes, such as tubular, planar, or monolithic (Figure 14).

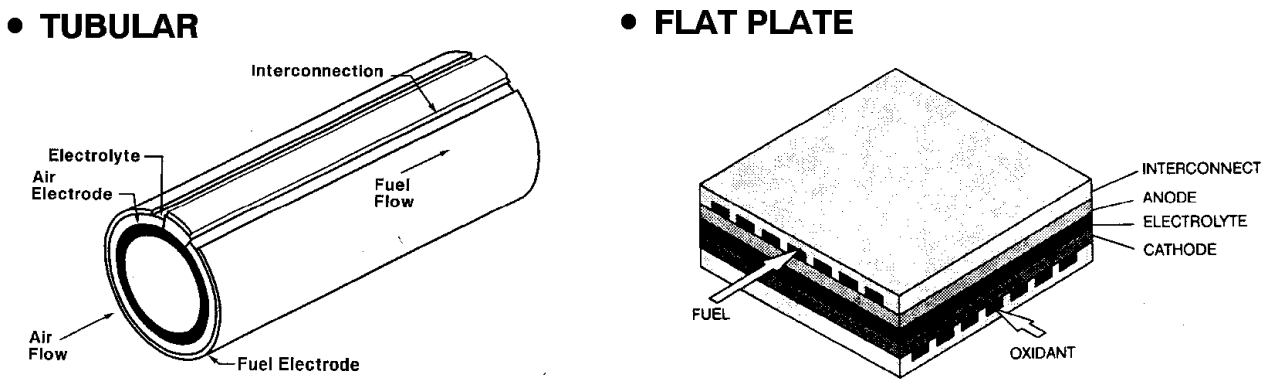

Figure 14. SOFC designs at the cathode[12]

Unlike MCFC, the solid ceramic of SOFC is not affected by any corrosion problem. The absence of liquid (as in MCFC) also eliminates the problem of electrolyte movement or flooding in the electrodes. As in the MCFC case, the kinetic of the cell is fast, CO is a directly useable fuel (while there is no requirement for CO_2 at the cathode) and at the working temperature (~1000°C), fuel can be readily reformed within the cell. Some scientists are studying to push SOFC operating temperatures even at lower temperature (to avoid any material problems and increasing stack life). As a consequence of the performance improvements, SOFCs are now considered for a wide range of applications, including stationary power generation, mobile power, auxiliary power for vehicles, and specialty applications (e.g. DCFC[20]).

4.2.3.2 Disadvantages

The high temperature of the SOFC is a problematic issue as well. Thermal expansion of materials are common problems. The high operating temperature forces to severe constraints on materials selection causing difficult fabrication processes.

5. Fuel Consumption

On earth, hydrogen is found combined with other elements. The easily example may be the water that is a combination between hydrogen and oxygen. For what concern fossil fuels (such as petroleum, natural gas or coal), hydrogen is combined with carbon[21]. All the fuel cell types run with hydrogen as the preferred fuel (high reactivity and production of an environmental friendly compound, as water is). Unfortunately, hydrogen is not available naturally as a gaseous fuel, and so for practical fuel cell systems it usually has to be generated from fuel sources more available[22].

For example, the hydrogen used to fed a fuel cell can be produced from natural gas, liquid hydrocarbon fuels including biomass fuels, landfill gases, water and electricity (via the process of electrolysis), biological processes including those involving algae, and from gasification of biomass, wastes, and coal[23].

The fuel for the FC system varies also depending from applications. In transportation, it may be methanol, gasoline, or diesel. In stationary systems, the main fuel used it natural gas, but even propane works. In certain niche markets, the fuel could be ethanol, butane, or biomass-derived materials. In any case, all these fuels are hydrocarbons or oxygenates that need to be reformed[24].

Table 1[25] shows the chemical and physical data on hydrogen and some of these other fuels that might be considered for fuel cells feeding.

	Hydrogen	Methane	Ammonia	Methanol	Ethanol	Gasoline
Molecular Weight [g/mol]	2,016	16,04	17,03	32,04	46,07	114,2
Freezing Point [°C]	-259,2	-182,5	-77,7	-98,8	-114,1	-56,8
Boiling Point [°C]	-252,77	-161,5	-33,4	64,7	78,3	125,7
Net Enthalpy of Combustion at 25 °C [kJ/mol]	241,8	802,5	316,3	638,5	1275,9	5512
Heat of Vaporization [kJ/kg]	445,6	510	1371	1129	839,3	368,1
Liquid Density [kg/m^3]	77	425	674	786	789	702
Specific Heat at STP [J/molK]	28,8	34,1	36,4	76,6	112,4	188,9
Flammability limits in air [%]	4-77	4-16	15-28	6-36	4-19	1-6
Auto ignition temperature in air [°C]	571	632	651	464	423	220

Table 1. Properties of hydrogen and other fuels considered for fuel cell systems

Although hydrogen is characterized by one of the highest specific energies (energy per kilogram) that enable its use mainly for space missions, due to a very low density, it has one of the lowest energy densities (energy per cubic metre). Thus, high pressures have to use to compact this large volume. Due to the leak rate faster than other gases, the problem of storing hydrogen is not so simple. Moreover, it is very difficult to liquefy. It cannot be simply compressed in the way that LPG or butane can. It has to be cooled down approximately at 22 K, and even in liquid form its density is quite low at 71 kg/m^3. In addition, hydrogen is a highly volatile and flammable gas and it can detonate. Even considering all of this, it should

be made clear that, hydrogen is no more hazardous than other commonly commercial fuels such as Methane and Propane (Table 2)[26]. In particular application, it is more convenient and efficient to store the hydrogen fuel. It is the case where it needed to store electrical energy from renewable sources as wind driven generators, photovoltaic and hydroelectric power stations, whose production might well be higher than peak consumption.

	Hydrogen	Methane	Propane
Density at STP [kg/m^3]	0,084	0,65	2,01
Ignition limits in air at NTP [volume%]	4 - 77	4,4 - 16,5	1,7 - 10,9
Ignition temperature [°C]	560	540	487
Min. ignition energy in air [MJ]	0,02	0,3	0,26
Max. combustion rate in air [m/s]	3,46	0,43	0,47
Detonation limits in air [v/v%]	18 - 59	6,3 - 14	1,1 - 1,3
Stoichiometric ratio in air	29,5	9,5	4

Table 2. Properties relevant to safety for hydrogen and two other commonly used gaseous fuels

Table 2 reports that the major problem with hydrogen is the minimum ignition energy, indicating a risk of fire very easily. However, all these energies are lower than those encountered in most practical cases and a spark can ignite any of these fuels. Moreover, propane is heavier than air: it sinks at low points (such as in basements, in drains, and in the hulls of boats), where it can explode with devastating effects. Conversely, hydrogen is so light that it quickly disperses up.

5.1 The storage of hydrogen as a compressed gas[27]

Storing hydrogen gas in pressurised cylinders (about 200bar) is the most common technique and in practice it is largely used for small amounts of gas. The main advantages of storing hydrogen as compressed gas are, as follows:

- Simplicity
- Indefinite storage time
- No purity limits on the hydrogen.

Typically, it is used in places where the demand for hydrogen is variable and not so high.

5.2 Storage of hydrogen as a liquid[28]

The storage of hydrogen in cryogenic liquid form (commonly called LH_2), at approximately 22 K, is the only largely used technique of storing large quantities of such a fuel.

5.3 Hydrocarbon fuels processing[29]

Since H_2 is not available in nature in pure form, it is common practice (especially for stationary system) to fed FC with hydrocarbon fuels (for example, natural gas). Not any fuel works correctly for each type of fuel cells: FCs stack has in fact particular feeding requirements. For example, the fuel used for a PEM fuel cell needs to be essentially CO free (less than 50ppm), while both the MCFC and the SOFC may run with CO through the water-gas shift reaction that occurs within the cell.

5.3.1 Desulphurized stage

Natural gas and petroleum liquids contain organic sulphur compounds that normally have to be removed before any reforming process. Sulfur cause catalysts poisoning[30,31]. Even if sulphur levels in fuels are below 0.2 ppm, some deactivation of steam reforming catalysts can occurs.

In the case of natural gas, the desulfurizer system removes practically all the sulfur that is used as odorant in natural gas, as well as small amounts of oxygen in the gas[32].

In this stage, the sulphuring compounds are converted (over a supported nickel-molybdenum oxide or cobalt-molybdenum oxide catalyst), into hydrogen sulphide through a hydrogenolysis reactions:

$$(C_2H_5)_2S + 2H_2 \rightarrow 2C_2H_6 + H_2S$$

The hydrogenolysis operating temperatures is in the range of 300 to 400 °C, and in the presence of excess hydrogen, the reaction is normally complete. The H_2S that is formed by such reactions is subsequently absorbed onto a bed of zinc oxide, forming zinc sulphide:

$$H_2S + ZnO \rightarrow ZnS + H_2O$$

Other developers have opted for removing sulphur from the feed gases using an absorbent. In this case, activated carbon is especially suitable and can be impregnated with metallic promoters to enhance the absorption of specific materials such as hydrogen sulphide. However, the absorption capacity of this carbon material is quite low, and it needs a fixed bed of absorbent that has to be replaced at regular intervals. This may cause serious economic disadvantage for large systems.

5.3.2 Steam Reforming SR[24]

Currently, the main mature process used industrially to carry out conversion of fuel in H_2 is the steam reforming. SR reaction for any fuel is, as follows:

$$Fuel(C_nH_mO_p) + steam \leftrightarrow carbon\ oxides + H_2$$

In this process, steam reacts with the fuel in the presence of a catalyst to produce hydrogen, carbon monoxide and dioxide. As reaction above is strongly endothermic, high temperatures are needed.

The SR process yields the highest hydrogen conversion. However, two other processes may be carried out for H_2 production: partial oxidation and auto thermal reforming. Unlike SR, the two reactions are exothermic. Thus, they can be more attractive for several applications more focalized in energy-efficient.

5.3.3 The integrated low-temperature shift converter (ILS)

The integrated low-temperature shift converter produces hydrogen through a water-gas reaction in which CO and water are converted to hydrogen and CO_2. The reduced CO content minimizes the adverse effect of the gas on fuel cell stack performance, as follows:

$$CO + H_2O \rightarrow CO_2 + H_2 \quad [\Delta H = -41{,}17\ kJ/mol]$$

The combination SR and ILS means that the overall product gas is a mixture of CO, CO_2 and H_2, together with unconverted methane and steam[33]. The water-gas-shift reaction plays an important role, in fact the thermal energy rejected by the electrochemical oxidation of CO and H_2 at high temperatures can be used for the endothermic SR process directly.

5.4 Reforming of Natural Gas

When NG is processed, the reaction is carried out in the steam reformer that operates approximately at 600-700 °C[34,35]. The steam-reforming reaction for natural gas (assuming pure methane) is the following:

$$CH_4 + H_2O \leftrightarrow CO + 3H_2 \quad [\Delta H = 205{,}80\ kJ/mol]$$

Traditional methane steam reforming catalyst are based on nickel/nickel oxide or cobalt composition on refractory alumina or support such as magnesium alumina spinel, precious metals (Rh, Ru, Pt, Pd, Re) on alumina, or on rare case oxides, particularly ceria[30,36,37]. At atmospheric pressure, 99% conversion of methane can be achieved with H_2O:CH_4 molar ratios of 3:1 at about 750 °C. As the pressure increases, the temperature requirement for 99% conversion increases dramatically, approaching 1000 °C for 15 bar pressure[38]. In order to minimize CO formation, an integrated low-temperature shift converter is provided (See: Section 5.3.3)

5.5 Reforming of Propane

Hydrogen production from Propane was studied by several scientists[30,39,40]. The reaction carried out in a SR reactor is, as follows:

$$C_3H_8 + 3H_2O \leftrightarrow 3CO + 7H_2 \quad [\Delta H = 498{,}53 \text{ kJ/mol}]$$

As with natural gas, SR of propane is followed by water gas shift reaction:

$$CO + H_2O \leftrightarrow CO_2 + H_2 \quad [\Delta H = -41{,}17 \text{ kJ/mol}]$$

Resini et al.[41] has proved experimentally that reaction over $Ni/NiAl_2O_4$ catalyst was more selective that reaction over $Pd–Cu/\gamma\text{-}Al_2O_3$ catalyst. The former gave the highest H_2 production (90%) at 750°C, while the with the latter, the highest selectivity of H_2 (nearly 45%) was obtained at 1000°C.

5.6 Reforming of ethanol

In the reforming of ethanol, hydrogen can be obtained according the follow reaction:

$$C_2H_5OH + 3H_2O \leftrightarrow 2CO_2 + 6H_2$$

These reforming reactions have been deeply studied in various metal-metal oxide catalysts, including Co, Ni, Cu, Ru, Rh, Pd, Pt and Ir supported on the metal oxides of Al_2O_3, CeO_2,

SiO_2, ZrO_2, TiO_2, MgO, La_2O_3, and Y_2O_3 [42-44]. Deluga et al.[45] have reported promising result of Rh/CeO_2 reformer, in which ethanol-water mixture can be converted to hydrogen with the selectivity about 100% and the conversion efficiency over 95%. Iulianelli et al.[46] developed a catalytic Pd–Ag membrane reactor packed with a $Co–Al_2O_3$ catalyst. They uphold operating at 400°C and 3 absolute bar, 100% ethanol conversion and 95% CO-free hydrogen recovery have been obtained.

Moreover, some exemplars of Direct Ethanol Fuel Cell (DEFC) have been investigated. Although the use of ethanol is attractive for the possibility to fed the cell with a renewable fuel, this technology, at the current state-of-art, is only a reality based on prototypes[47].

5.7 Reforming of methanol[48]

Hydrocarbons such as natural gas and propane are not the only fuels suitable for steam reforming. Nowadays, portable applications are met with fuel cell fed with methanol. Reforming of methanol is typically carries out in the presence of Cu–ZnO supported by Al_2O_3 at temperature ranging from 200°C to 300°C. The chemical reaction taking place during the reforming process is:

$$CH_3OH + H_2O \leftrightarrow CO_2 + 3H_2 \quad [\Delta H = 49{,}24 \text{ kJ/mol}]$$

That is the overall reaction of methanol decomposition:

$$CH_3OH \leftrightarrow CO + 2H_2 \quad [\Delta H = 90{,}41 \text{ kJ/mol}]$$

And water-gas-shift reaction:

$$CO + H_2O \leftrightarrow CO_2 + H_2 \quad [\Delta H = -41{,}17 \text{ kJ/mol}]$$

Due to the low enthalpy of reaction, steam reforming of methanol is weakly endothermic. This property is brownie point that make process of methanol energetically favourable. In fact, methanol reforming reaction generally occurs at comparatively lower temperature (200-300°C) as compared to the high temperature for natural gas (600-700 °C) and gasoline (800-900°C) reforming.

These alternative energy devices, invented at the Caltech/NASA Jet Propulsion Laboratory in collaboration with the University of Southern California, can be used to power a wide range of portable and mobile electronics. They operate silently, at relatively low temperatures and offer much longer operating time than today's batteries. Unlike DEFCs, DMFCs are a more advanced technology with already market applications. Direct Methanol Fuel cell Corporation, a subsidiary of Viaspace, developed disposable methanol fuel cartridges that provide the energy source for fuel cell powered notebook computers, mobile phones, military equipment and other applications being developed by electronics companies, such as Samsung and Toshiba[49].

5.8 Production of H_2 from coal gas[50]

Since MCFC and SOFC operate at a very high temperature (1000 °C), it is feasible to think in use hydrogen produced by coal gasification. Although coal is a non-renewable resource, it is very abundant and has well known properties. In coal gasification, coal is burned and then the reactant gases are combined with steam, which is produced by the burning coal. This mixture of coal and steam react to produce hydrogen and carbon dioxide. The overall reaction is:

$$C + H_2O \leftrightarrow CO + H_2 \quad [\Delta H = 131{,}28 \text{ kJ/mol}]$$

And it is strongly endothermic. In order to have a sufficient rate of reaction, this process requires a very high temperature. Therefore, MCFC and SOFC are perfect device for such applications.

The basic types of reformers used are: fixed bed, fluidized bed, fast fluidization and molten bat. Regarding the process used to produce the hydrogen, the most significant problem to be overtaken is desulphurisation (Section 5.3.1). In fact, coal often have high sulphur and ash content that make coal gasification stage difficult and expensive[51].

5.9 Hydrogen production from Bio Fuels[52]

There are several developing processes for the use of biomass aimed at hydrogen production. The two major processes are anaerobic digesters and pyrolysis gasifier: the former is useful in the kW range whereas the latter is useful at the MW range[53]. An anaerobic digester is a process that converts complex animal matter (manure) into simpler gasses (methane): this stage requires a fuel with a high nitrogen concentration. Pyrolysis gasifier is a process of thermal decomposition that aims to produce gases (methane). This technique is only efficient in large-scale production.

6. Conceptual design and modelling of a PEM Fuel Cell[54]

In this section, a design of a PEMFC was achieved. For simplify the modelling, it was assumed that the fuel cell operates directly with pure H_2 (Eq. 3).

Before to estimate the parameters of the system (H_2 and O_2 flow rate), it is important to claim that the two reagents are often supplied at greater than the stoichiometric rate (to avoid mass transport loss). This occurs preferably with oxygen, especially if it is supplied with ambient air (for obvious economical reasons). Thus, this stoichiometry ratio (indicated by the symbol λ) is a variable. If molar flow rate is $\dot{n}$ (moles per second), then the rate of supply will be $\lambda\dot{n}$ moles per second. Before to begin any modelling two parameters are needed:

- electrical power of the whole fuel cell stack P_e
- the average voltage of each cell V_c

The electrical power (total installed capacity) should be known, as it is the most basic and important information of a fuel cell system. For what concerns Vc, a polarization curves could be obtained thought experimentally tests. If this data is not known or given, it can be assumed a value between 0.6 and 0.7 V (most fuel cells operate in this region).

6.1 Oxygen and Air usage

According to the electrochemical reaction in Section 1.1 (Eq. 3), four electrons are transferred for each mole of oxygen. So:

$$Charge = 4F \times amount\ of\ O_2$$

Dividing by time, and rearranging:

$$O_2 usage = \frac{I}{4F} \quad \left[\frac{moles}{s}\right] \qquad Eq.36$$

This is for a single cell. For a stack of *n* cells,

$$O_2 usage = \frac{In}{4F} \quad \left[\frac{moles}{s}\right] \qquad Eq.37$$

However, it is more useful to express the formula in kg/s, to neglect the number of cells, and in terms of power, rather than current. If the voltage of each cell in the stack is V_c, then the electric Power P_e is calculated with the following equation:

$$P_e = V_c\, I\, n \quad [Watts] \qquad Eq.38$$

So,

$$I = \frac{\mathrm{P_e}}{\mathrm{V_c}\, n} \quad [Ampere] \qquad Eq.39$$

Substituting this into Eq. 37 gives:

$$O_2 usage = \frac{\mathrm{P_e}}{4\ \mathrm{V_c}\ F} \quad \left[\frac{moles}{s}\right] \qquad Eq.40$$

Changing from moles/s to kg/s:

$$O_2\ usage = \frac{32 \times 10^{-3}\ P_e}{4\ V_c\ F} \quad \left[\frac{kg}{s}\right] \qquad Eq.41$$

$$O_2\ usage = 8{,}29 \times 10^{-8}\ \frac{P_e}{V_c} \quad \left[\frac{kg}{s}\right] \qquad Eq.42$$

This formula allows to evaluate the O_2 usage for any fuel cell system for a power known. As already stated, V_c should be obtained from experimental polarization curve. If voltage is not known, the value of 0.65V can be used for a good approximation. However, if O_2 is taken from air, we need to readjust Eq. 40 to air usage. The molar proportion of oxygen in the air is 0.21, and the molar mass of air is 28.97×10^{-3} kg/mole. So, Eq. 40 becomes:

$$Air\ usage = \frac{28{,}97\ \times\ 10^{-3}\ P_e}{0{,}21 \times 4\ V_c F} \quad \left[\frac{kg}{s}\right] \qquad Eq.43$$

Eq. 43 expresses air flow rate at stoichiometric value, but as it was claimed in the beginning of this chapter, in practice the airflow is well above stoichiometry (typically twice as much). Remembering the physical meaning of λ (stoichiometric ratio), air flow rate becomes:

$$Air\ usage = 3{,}57 \times 10^{-7} \times \lambda \times \frac{P_e}{V_c} \quad \left[\frac{kg}{s}\right] \qquad Eq.44$$

However, it not common practice to express air flow rate in kilogram per second. Volume flow rate is a more typical measurement unit. So, the mass flow rate of Eq. 44 should be multiplied by:

- 3050 to give flow rate in m^3/h
- 5.1×10^4 to give flow rate in L/min
- 847 to give flow rate in L/s

6.1.1 Air Exit Flow Rate

For the design of a PEM, thermal management is a critical issue. In fact, in addition to cooling process, moisture of the reagents has to be assessed as well. Therefore, as air contains water, it is important to distinguish between the inlet flow rate of the air (Eq. 44) and the outlet flow rate. The difference is given by the consumption of oxygen (Eq. 42).

Exit air flow rate = Air inlet flow rate − oxygen usage

$$Exit\ air\ flow\ rate = 3{,}57 \times 10^{-7} \times \lambda \times \frac{P_e}{V_c} - 8{,}29 \times 10^{-8}\ \frac{P_e}{V_c}$$

$$= (3{,}57 \times 10^{-7} \times \lambda - 8{,}29 \times 10^{-8}) \times \frac{P_e}{V_c} \quad \left[\frac{kg}{s}\right] \qquad Eq.45$$

6.2 Hydrogen usage

As it has been assessed oxygen flow rate, hydrogen is calculated (except that two electrons are generated from each mole of hydrogen). So, equations 37 and 39 become

$$H_2 usage = \frac{In}{2F} \quad \left[\frac{moles}{s}\right] \qquad Eq.46$$

and:

$$H_2 usage = \frac{\mathrm{P_e}}{2\ \mathrm{V_c}\ F} \quad \left[\frac{moles}{s}\right] \qquad Eq.47$$

The molar mass of hydrogen is 2.02×10^{-3} kg/mole, thus Eq. 47 becomes:

$$H_2 usage = \frac{2{,}02\times10^{-3}\ \mathrm{P_e}}{2\ \mathrm{V_c}\ F} \quad \left[\frac{kg}{s}\right] \qquad Eq.48$$

$$= 1{,}05 \times 10^{-8} \times \frac{P_e}{V_c} \quad \left[\frac{kg}{s}\right] \qquad Eq.49$$

at stoichiometric operation.

6.3 Water production

In a hydrogen-fed fuel cell, water is produced at the rate of one mole for every two electrons. So, water moles flow rate is:

$$H_2O\ production = \frac{\mathrm{P_e}}{2\ \mathrm{V_c}\ F} \quad \left[\frac{moles}{s}\right] \qquad Eq.50$$

The molecular mass of water is 18.02×10^{-3} kg/mole, so this becomes:

$$H_2O\ production = 9{,}34 \times 10^{-8} \times \frac{\mathrm{P_e}}{\mathrm{V_c}} \quad \left[\frac{kg}{s}\right] \qquad Eq.51$$

Unlike oxygen (or hydrogen in such a cases), the rate of water production has to be approximately stoichiometric to avoid flooding problems. However, exceptions exist: if the fuel is a mixture of CO with H_2, CO_2 will be generated reducing the water production. If FC is fed with a hydrocarbon fuel internally reformed (for MCFC or SOFC applications), it must be considered that some of the product water would be used in the reformation process.

6.4 Heat Produced

Besides power, any fuel cell generate thermal energy. If all the enthalpy of reaction of a hydrogen fuel cell would be converted into electrical energy, according to Section 2.4, the output voltage would be

- 1.48V if the water product was in liquid form, or
- 1.25V if the water product was in vapour form.

For a stack of *n* cells at current *I* , the heat generated (considering the water exiting fuel cell in vapour form) is:

$$Heating\ Rate = n \times I \times (1{,}25 - V_c) \quad [W] \qquad Eq.52$$

Expressing the heating rate, function of net power, Eq. 52 becomes:

$$Heating\ Rate = P_e \times \left(\frac{1{,}25}{V_c} - 1\right) \quad [W] \qquad Eq.53$$

6.4.1 Cooling using air supply[55]

Several cooling strategies are used for fuel cell applications, depending mainly by its size. Fuel cells with a capacity below 100W are cooled with air convection, without recourse to any fan. However, in case of large amount of heat produced (it is the case of large stationary

fuel cells), small fans should be used. The common way of cooling cells in the range between 100 and 1000W is to create extra channels in the bipolar plates through which cooling air can be blown (Figure 15).

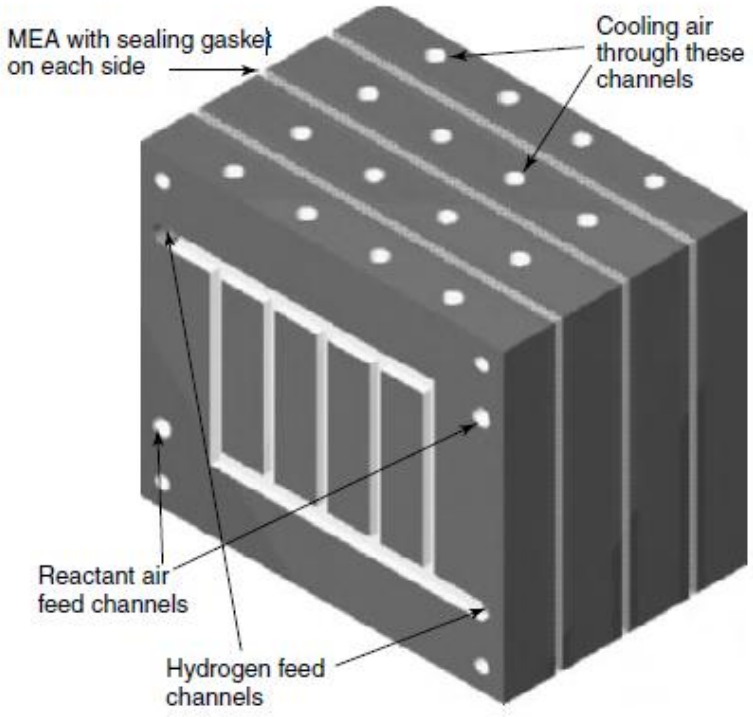

Figure 15. Three cells from a stack, with the bipolar plate modified for air cooling using separate[55]

For larger application (< 1 kW), cooling water is preferable.

6.4.1.1 Fan and Blower for FC cooling[56]

Depending on the cooling demand, fans and blowers are readily available in the market and in a wide range of size. Typical axial fan is an excellent device for air cooling, but only against very small pressures (p<0,07 barg).

For greater pressure (p<2,7 barg), the centrifugal are used.

Equation design for a fan or a blower is, as follows:

$$W = \dot{m}\, c_p\, \Delta T \quad [W] \qquad Eq.54$$

Where:

- W is the power of fan or blower [W];
- $\dot{m}$ is mass flow rate of air [kg/s];
- c_p is the specific heat of air [1,005 kJ/kgK] [57]
- ΔT is the raise in temperature [°C]

6.4.2 Water cooling of PEM fuel cells[58]

Alike that typical engines (for example, internal combustion engines), one of the main issues for fuel cell developers is when to change from air cooling to water cooling. Essentially, air cooling is simpler, but in large system, it is hard to guarantee a homogeneous cooling for the whole fuel cell. In fact, remembering heat transfer properties:

	W/m^2K
Water (heating or cooling)	300-20000
Air (heating or cooling)	1-50

Table 3. Magnitude of heat transfer coefficient[59]

Heat transfer coefficient of water is several orders of magnitudes larger than heat transfer coefficient of air. Thus, according to the following equation:

$$Q = U\, A\, \Delta T \qquad Eq.55$$

Where:

- Q is the amount of heat that should be removed [W];
- U is the overall heat transfer coefficient [W/m^2K]
- A is the heat transfer surface area [m^2]

It is clear that cooling with air needs larger areas compared with water cooling. Moreover, it is well known that water has a density several order of magnitude larger than air (1 kg of water can be pumped through a much smaller channel than 1 kg of air). Thus, PEM fuel cells cooled with air should be well larger than PEM cooled with water. In practice, in order to not prejudice efficiency cooling and avoiding disproportionate stack cost, PEM above 5 kW are cooled with water, whereas below 2kW air cooled is preferred. The method of cooling a fuel cell with water is essentially the same as for air (Figure 15), except that water is pumped through the cooling channels.

6.5 Humidity of PEMFC air[58]

To permit proton conductivity, the polymeric membrane of PEM should be wet continuously. At the same time, electrolyte flooding has to be avoided as well. This two concepts point out that the humidity of the air in a PEMFC must be carefully controlled: air must be dry enough to evaporate the product water, but not in excess, because it is essential that the electrolyte membrane retains a high water content. To estimate the humidity of exit air, partial pressure of a gas is used. Partial pressure is proportional to the molar fraction of that gas in the mixture. If we consider the exit gas of a fuel cell, then we can write:

$$\frac{P_w}{P_{exit}} = \frac{number\ of\ water\ molecules}{totale\ number\ of\ molecules}$$

$$\frac{P_w}{P_{exit}} = \frac{\dot{n_w}}{\dot{n_w} + \dot{n_{O_2}} + \dot{n_{rest}}} \qquad Eq.56$$

Where:

- $\dot{n_w}$ is the number of moles of water leaving the cell per second,
- $\dot{n_{O_2}}$ is the number of moles of oxygen leaving the cell per second,
- $\dot{n_{rest}}$ is the number of moles of the 'non-oxygen' component of air per second,
- P_{W} is the vapour pressure of the water, and
- P_{exit} is the total air pressure at the fuel cell exit.

Assuming that all the product water is removed by the air supply, using Eq. 50:

$$\dot{n}_w = \frac{\mathrm{P_e}}{2\,\mathrm{V_c}\,n} \qquad \text{Eq. 57}$$

Using Eq. 40, which gives the oxygen flow rate consumed in the cell, oxygen flow rate that leave the PEMFC:

$$\dot{n}_{O_2} = rate\ of\ supply\ of\ O_2 - \ rate\ of\ use\ of\ O_2$$

So,

$$\dot{n}_{O_2} = (\lambda - 1)\frac{\mathrm{P_e}}{4\,\mathrm{V_c}\,n} \qquad \text{Eq. 58}$$

If the fuel cell is fed with air, there is an amount of 79% of "non-oxygen" components that just pass through the cell, but that they do not participate to the electrochemical reaction. This component flow rate is greater than the oxygen molar flow rate by the ratio 0.79/0.21 = 3.76. So,

$$\dot{n}_{rest} = 3{,}76 \times \lambda \times \frac{\mathrm{P_e}}{4\,\mathrm{V_c}\,n} \qquad \text{Eq. 59}$$

Substituting these three equations into Eq. 56 gives:

$$\frac{P_w}{P_{exit}} = \frac{\frac{\mathrm{P_e}}{2\,\mathrm{V_c}\,n}}{\frac{\mathrm{P_e}}{2\,\mathrm{V_c}\,n} + (\lambda - 1)\frac{\mathrm{P_e}}{4\,\mathrm{V_c}\,n} + 3{,}76\,\lambda\frac{\mathrm{P_e}}{4\,\mathrm{V_c}\,n}} = \frac{2}{1 + 4{,}76\lambda} \qquad Eq.60$$

$$P_w = \frac{0{,}420\,P_{exit}}{\lambda + 0{,}210} \qquad Eq.61$$

Eq. 61 shows well that water vapour pressure in the exit of the cell is function of the air stoichiometry (λ) and the air pressure at the exit (P_{exit}). This derivation ignores any water vapour in the inlet air. Thus Eq. 61 gives us the 'worst case' situation, with dry inlet air.

Typically, extra humidification of reagents (usually air, but in certain cases H_2 as well) is achieved. This procedure claims that it is not possible to neglect the water content of the inlet air. Readjusting Eq. 61, it can be shown that the outlet water vapour pressure is given by:

$$P_w = \frac{(0{,}420 + \psi\lambda)P_{exit}}{(1+\psi)\lambda + 0{,}210} \qquad Eq.62$$

Where ψ is a coefficient whose value is given by the simple equation:

$$\psi = \frac{P_{W_{in}}}{P_{in} - P_{W_{in}}} \qquad Eq.63$$

Where P_{in} is the total inlet air pressure, P_{exit} the total outlet air pressure (that it is usually lower than P_{in}) and P_{Win} is the water vapour pressure at the inlet of the PEMFC. At the current state of knowledge, Equations 61 and 62 are the two chief correlations used to assess accurately how to run a PEM fuel cell so that the air is not too wet or too dry.

7. Experimental test

The design achieved in Section 6 was used to carry out experimental tests that aim to use the chemical energy of H_2 combustion to provide electrical energy to the public grid.
The Fuel Cell used for the tests was a Low-Temperature Polymer Electrolyte Membrane Fuel Cell stack of a maximum electric net power of 1 kW, composed by 20 cells of 144cm^2 each. Fuel Cell module was composed by the PEM stack, a fan for cooling and two water tanks for humidification of H_2 and O_2. Moreover, the module was provided by a controlling station (Figure 16).

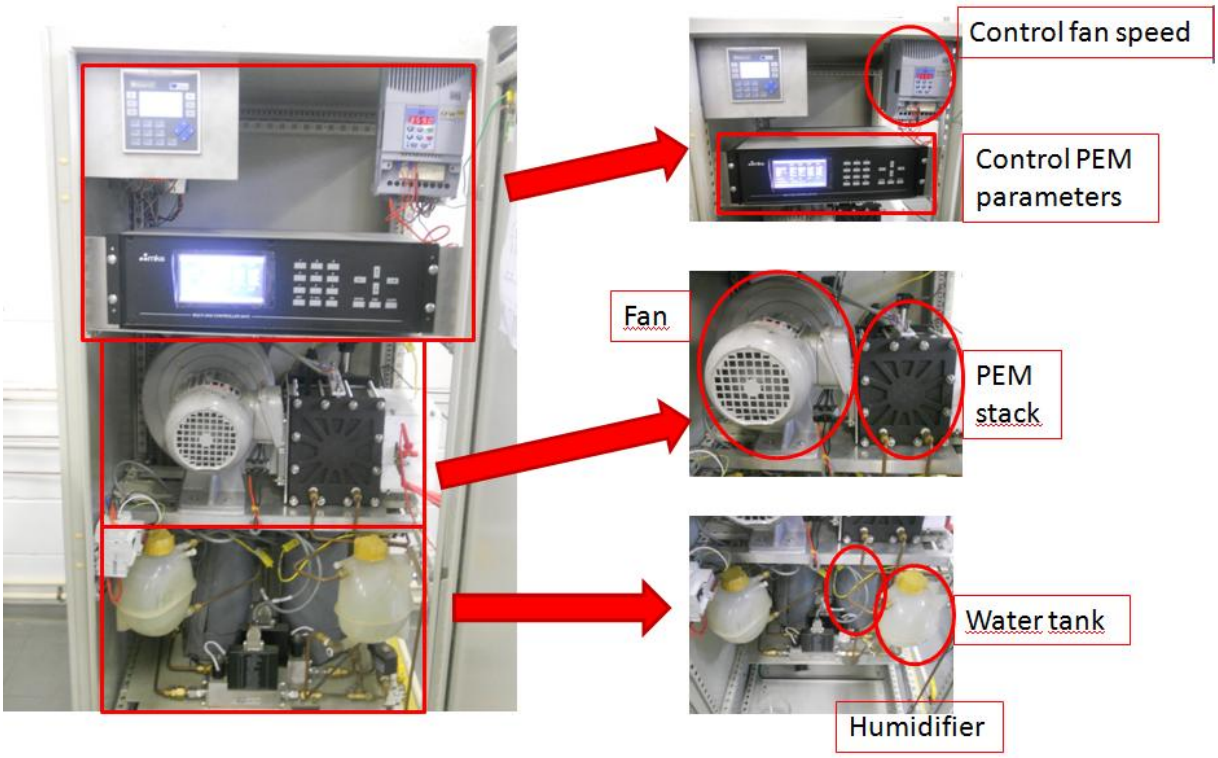

Figure 16. PEMFC module

Moreover, as FCs produce direct current (DC) power, in order to provide electrical power to the public grid, an inverter was needed.

The inverter used was the Hydro Boy-1124 from SMA Solar Technology.

Figure 17. Hydro Boy-1124

Technical data of Hydro Boy are showed in Table 4.

Input (DC)	
DC nominal power	1200 W
Max DC voltage	60 V
Nominal input voltage	24 V
Operating voltage range	20 V - 55 V
Max input current	56 A
Output (AC)	
Continuous AC output	1100 W
Max AC power	1200 W
Nominal output current	4,8 A
Nominal AC voltage	220 V – 240 V
Nominal AC voltage range	180 V – 260 V
AC grid frequency	50 Hz, 60 Hz
AC grid frequency range	± 4,5 Hz
Power factor (cosφ)	1
Efficiency	
Max Efficiency	>0,91
General data	
Weight	29 kg
Operating temperature range	-25°C … +60°C
Internal consumption: operation (standby)	< 5 W
Internal consumption: off	< 0,1 W
Cooling concept	Natural convection

Table 4. Technical data of Hydro Boy-1124

A schematic graph of the plant used is represented in Figure 18.

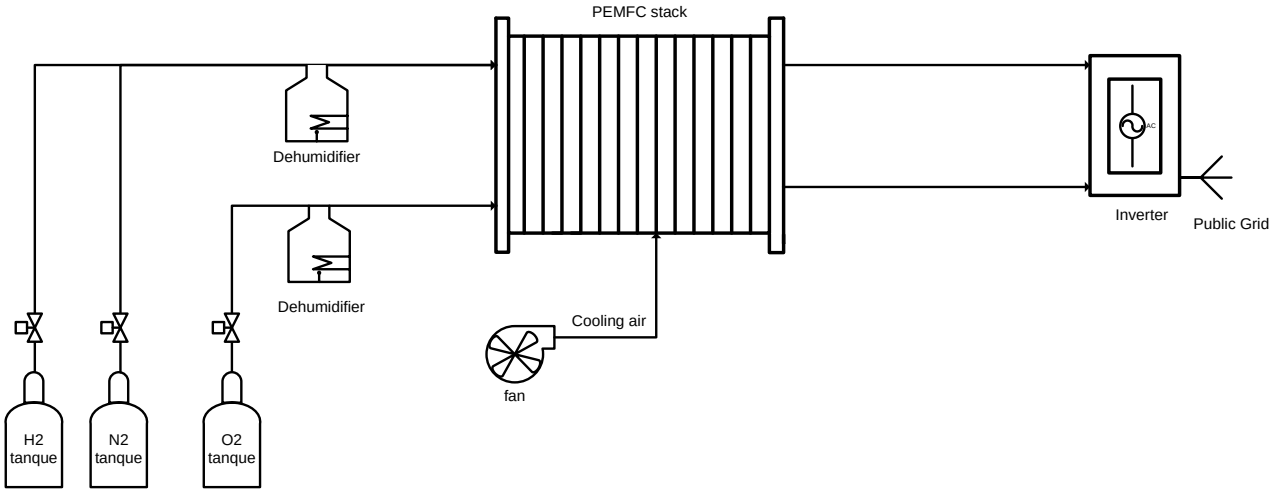

Figure 18. Plant based on PEMFC stack and inverter device

In the schematic plant represented in Fig. 18, the three pressurized tanks contain:

- Hydrogen stored at 160 bar
- Oxygen stored at 200 bar
- Nitrogen stored at 200 bar

Even if N_2 does not take part on electrochemical reaction that occurs in the FC, is usually used to warm and humidify the FC saving H_2.

Before the PEMFC starts to operate, the membrane has to be wet and it must reaches temperature of 65°C. Thus, at time 0, resistance of each humidifier turns on. When temperature of water is approximately 70°C, N_2 and O_2 started to flow. In order to save fuel, in this stage, N_2 is fluxed instead of H_2. When temperature of water is approximately 98-99°C, N_2 valve is closed and H_2 valve opens. From this moment only hydrogen and oxygen are fluxed and the electrochemical reaction occurs in the fuel cell.

The PEMFC provides 1kW, thus Eq. 40 and Eq. 47 are used to assess flow rate for the two reagents involved in the electrochemical reaction (H_2 and O_2).

In order to calculate volume flow rate, value of density for H_2 and O_2 are needed.

The density of gases varies with temperature. According to Perry's Chemical Engineers' Handbook[60], for H_2 at 1 bar, we have the follow graph:

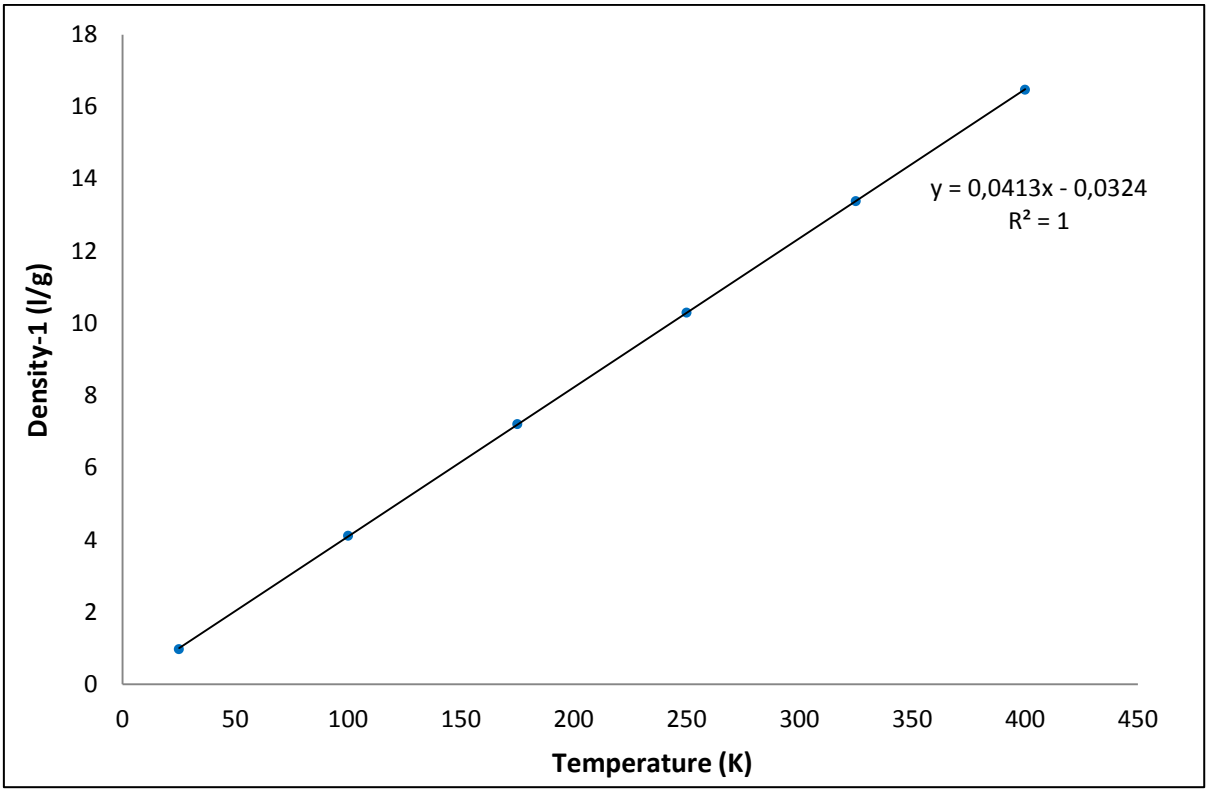

Figure 19. Density of H_2 function of temperature

The correlation obtained from the graph allows to calculate density for H_2 for temperature in the range 25K - 400K. As PEMFC works at 65°C, density of H_2 was assessed at that temperature.

Thus, ρ_{H2} (T=65°C) = 0.0718 g/l

Through Eqs. 47-48 and density assessment, volume flow rate of H_2 has been calculated.

Hydrogen – Molar flow rate	0.00797	mol/s
Hydrogen – Mass flow rate	0.01594	g/s
Hydrogen – Volume flow rate	13.33	L/min

Table 5. Hydrogen flow rate

The same study has been carried out with O_2.

Correlation of density as function of temperature is shown in Figure 20.

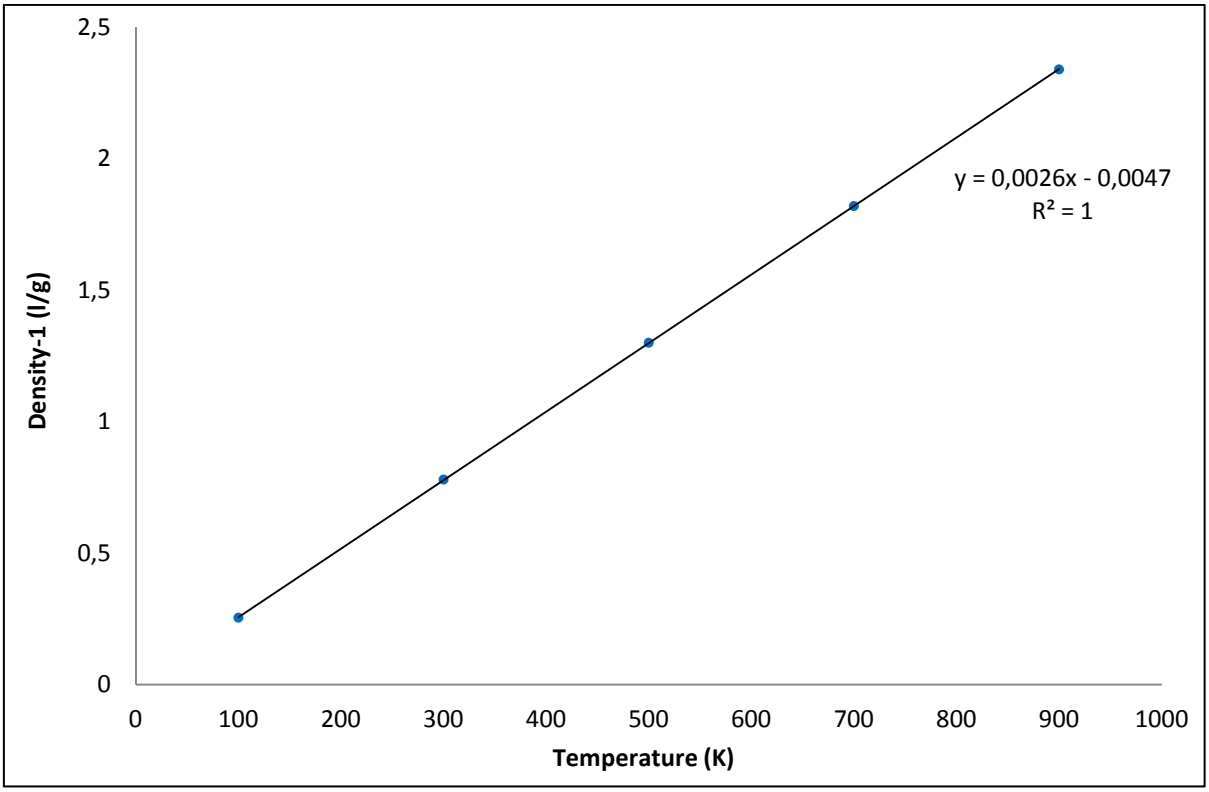

Figure 20. Density of O_2 function of temperature

With the correlation of Figure 20, density of O_2 at 65°C has been calculated.

Thus, ρ_{O2} (T=65°C) = 1.1435 g/l

With the same approach, volume flow rate of O_2 has been calculated.

Oxygen – Molar flow rate	0.00399	mol/s
Oxygen – Mass flow rate	0.12754	g/s
Oxygen – Volume flow rate	6.69	L/min

Table 6. Oxygen flow rate

According to tables 5 and 6, volume flow rate of 14 L/min and 7 L/min has been chosen for H_2 and O_2, respectively.

In order to test performances of the PEMFC, Agilent N3300 DC Electric Load for used for FC test.

Figure 21. Electric Load-Agilent N3300 DC Electric Load

Electronic load run at constant current (CC) allowing to step through currents incrementally and measuring the voltage output of the FC under test. This test allows to draw polarization and power curves for the PEMFC.

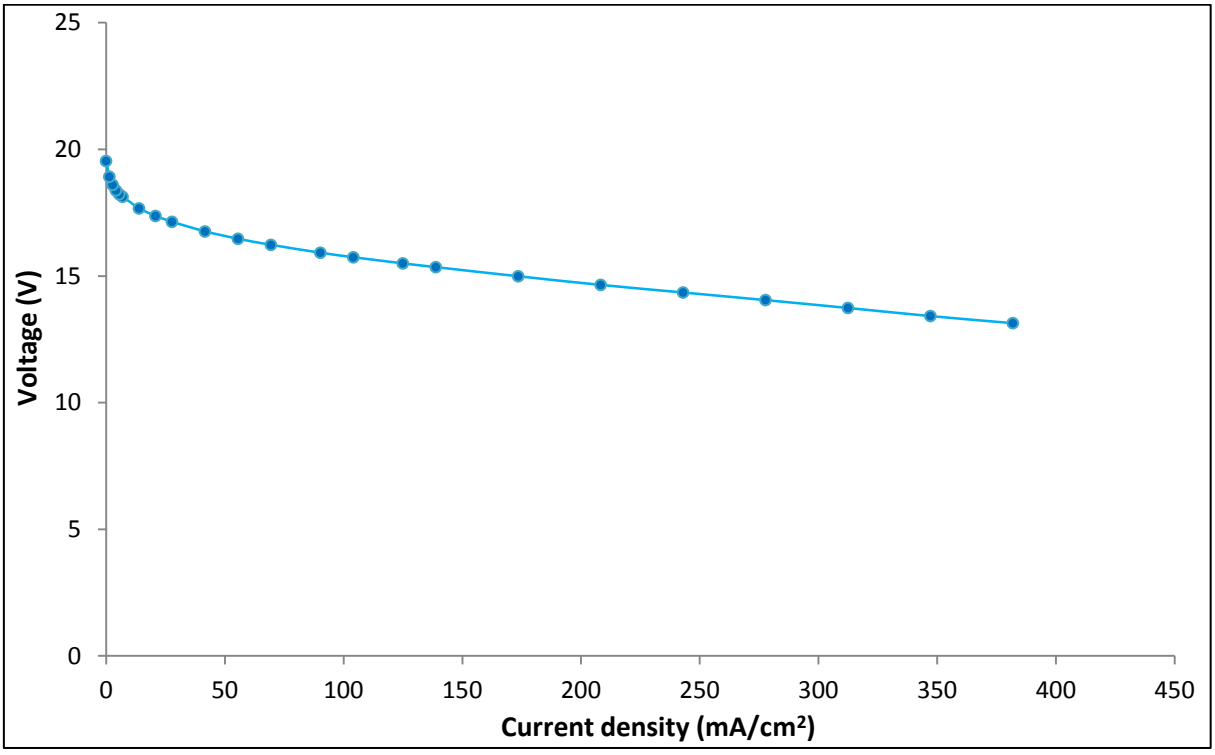

Figure 22. Polarization curve of PEMFC

From the shape of the voltage/current density graphs, it is possible to see the two causes of voltage drops during experimental tests. In fact, in the first part (approximately between 0 and 50 mA/cm^2) activation losses has been occurred, while in the second linear curve are affected by ohmic losses. Since the maximum input current for the inverter is 56 A, experimental tests were stopped when the dynamic load was at 55 A. From Fig. 22, concentration losses have

not been noticed. The reason is that at 55 A, power of stack is about 720-730W (Fig. 23) and volume flow rates of reagents have been calculated taken in account 1kW of net power. Thus, with the range of power used, H_2 and O_2 are in a large excess and mass transport losses do not occur.

Besides the polarization curve, with the experimental values of voltage and current, it is possible to draw the power curve as well.

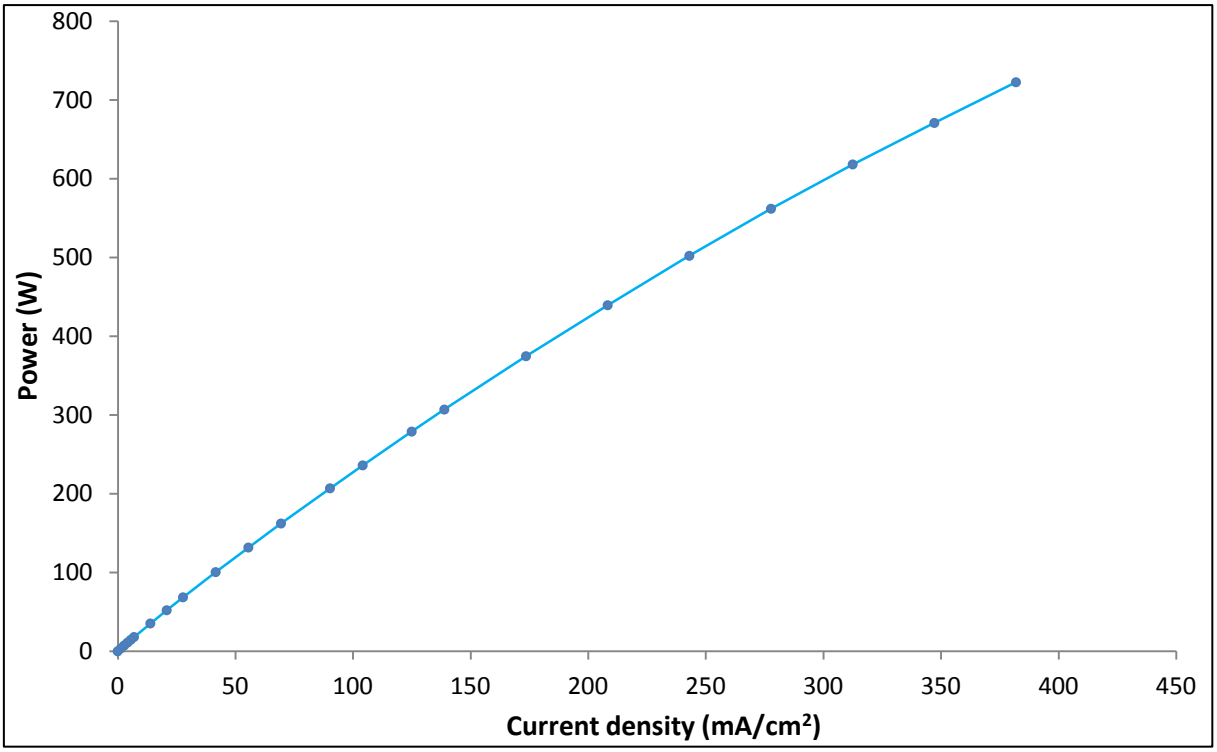

Figure 23. Power curve of PEMFC

The graph above gave a better overview of PEMFC performances: in fact, it is possible to notice that maximum power provided by the module is roughly 720-730W. The 1kW of net power was not accomplished because of cooling problem. In fact, PEMFC uses an air blower for cooling. According to Section 6.4.2, heat transfer using air convection is not an effective cooling system and to utilize all net FC power, a water cooling system would be preferred.

PEMFC stack is composed by 20 cells; thus, knowing voltage of single cells and power of the stack, it was possible to draw a graph that could show the influence of current in the stack over Power and FC efficiency.

As the product (water) is in liquid phase, from Section 2.4 the maximum voltage has been considered equal to 1.48V.

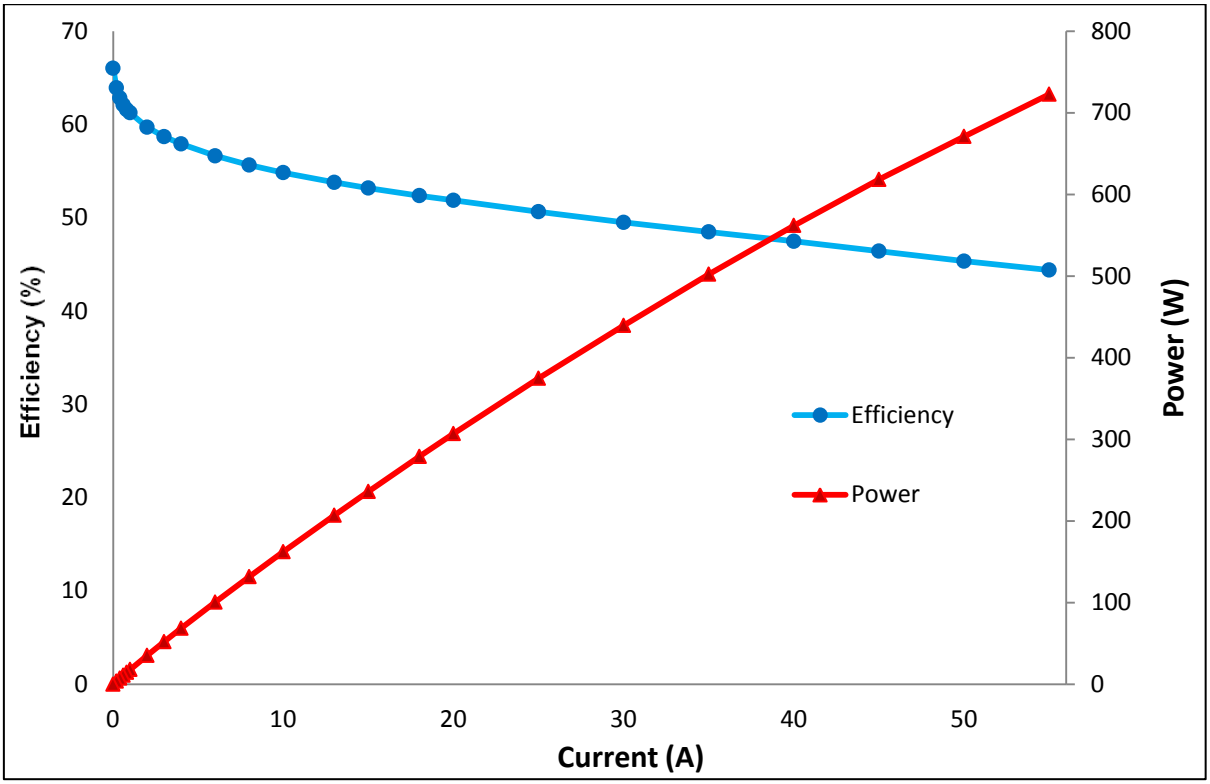

Figure 24. Power and efficiency of PEMFC

From Figure 24, it has been shown that increasing current, power increases too. Conversely, as much as current increases, efficiency of the stack decreases gradually from 0.66 to 0.45.

7.1 Connection with Voltage Source VS

The PEMFC may provide an electrical power in the range 19.5 – 13 Volts. This value is not large enough: in fact, according Table 4, a nominal voltage of 24V is needed for the Hydro Boy input (DC side). Thus, the voltage source TCA 10-200 DA1A has been connected in series to the Fuel Cell. The plant became:

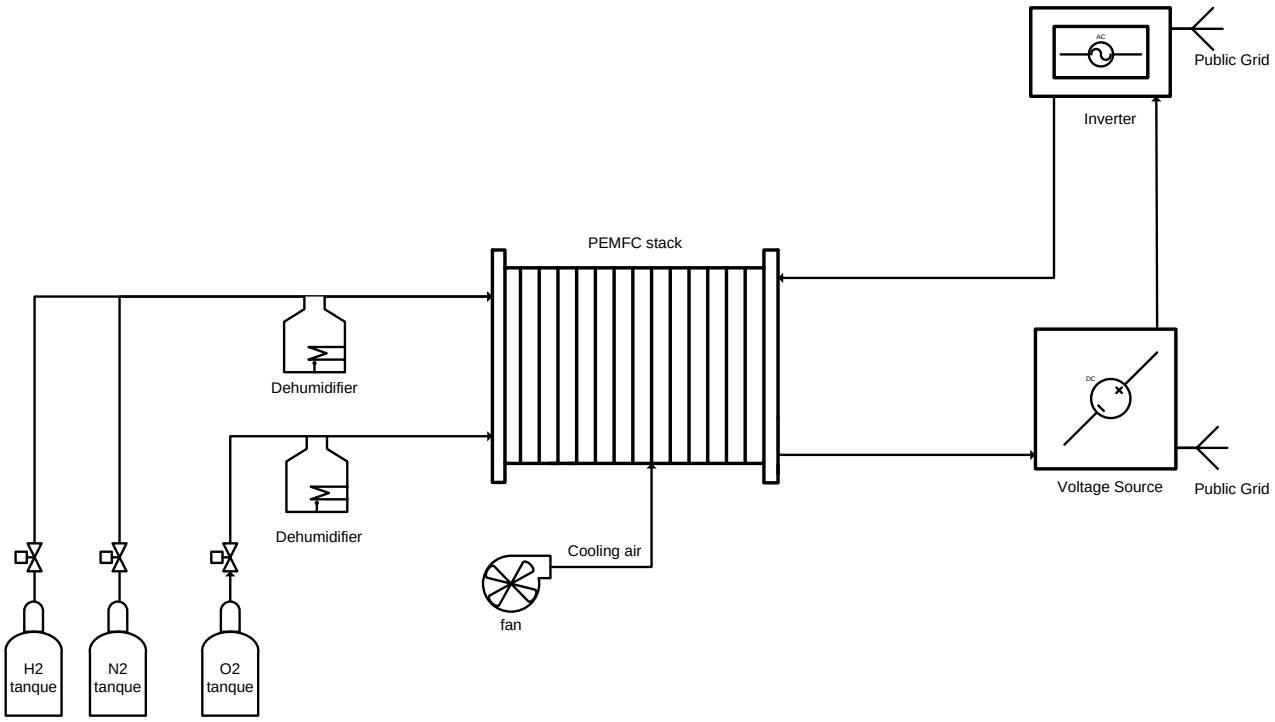

Figure 25. Plant based on PEMFC stack and inverter device with the voltage source

A voltage source is a device that permits to increase voltage of the system, keeping constant the current.

The point that has been claimed is that the voltage source needs public grid as power source.

In order to study performances of TCA 10-200 DA1A, a test with the Electric Load has been carried out.

Through experimental data, polarization curve has been drawn.

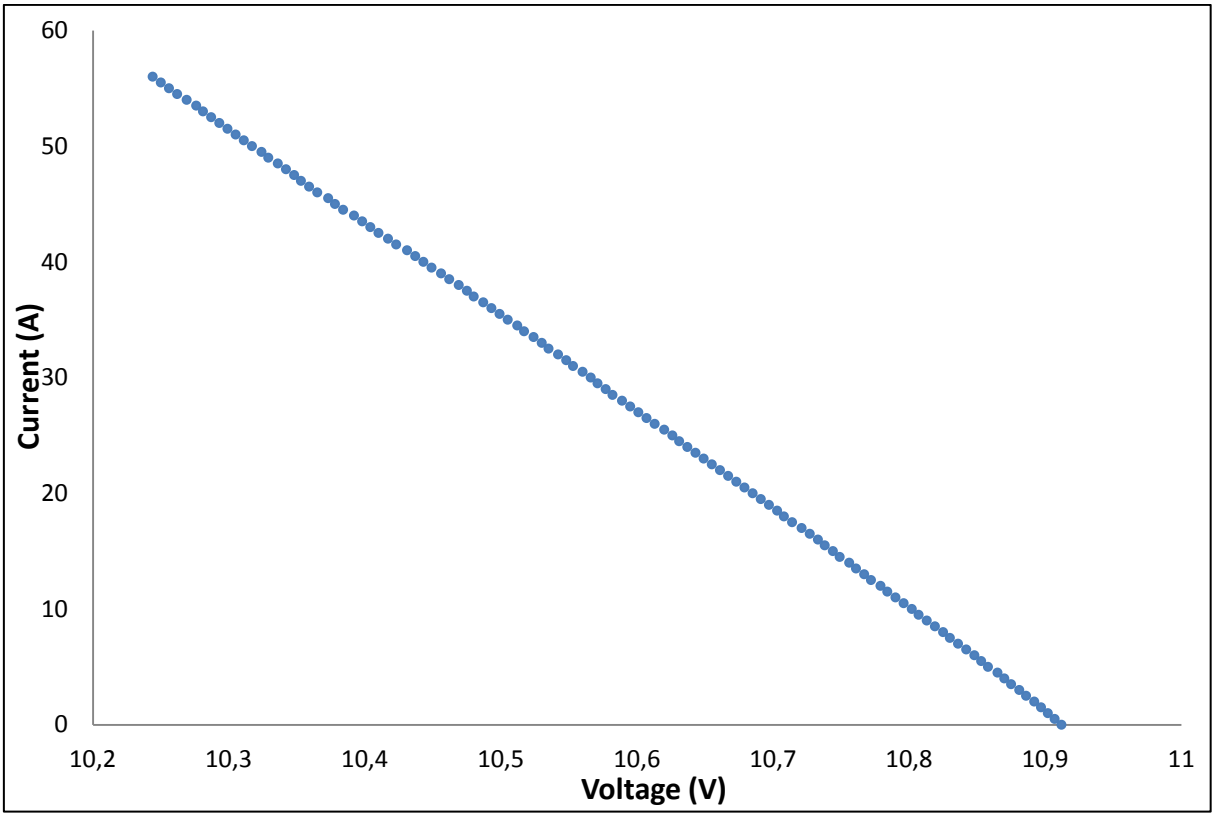

Figure 26. Polarization curve for the voltage source

The graph above shows that for any current value, voltage kept roughly constant. In fact, increasing value of current from 0 to 56A, only a slight voltage drop has been noticed (≅0.65V).

This test proved that, thought TCA 10-200 DA1A is possible to add approximately 10V to the system.

To verify the overall system voltage, PEMFC and voltage source were connected in series, obtaining a system that could provide electrical power in DC with a voltage value larger enough to connect the Hydro-Boy.

With the use of experimental data, polarization of the overall system (PEMFC+VS) has been drawn in Figure 27.

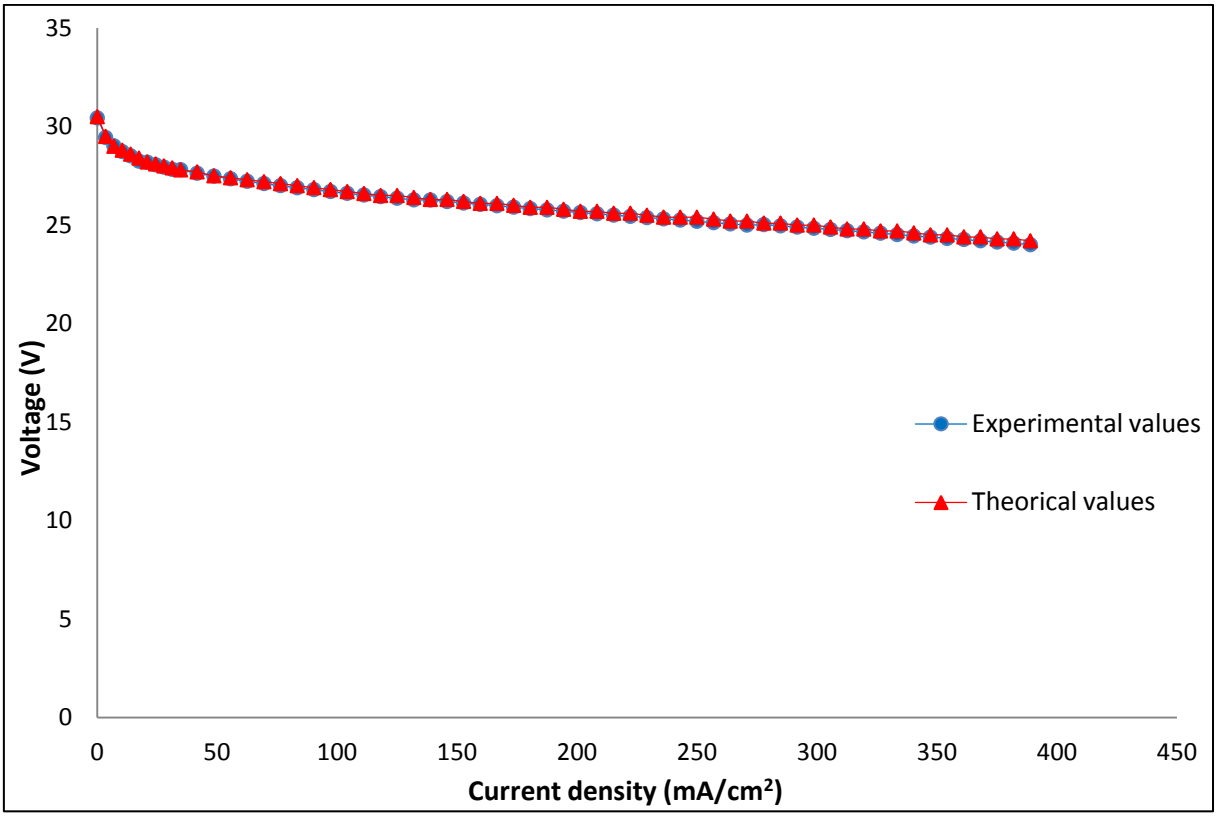

Figure 27. Polarization curve of PEMFC and VS connected in series

Figure 27 shows that the system created may supply between 30V and 24V of electrical power to the Input of the Hydro Boy. Thus, at the actual state-of-art, voltage is enough larger to allow the inverter be connected to the system. Fig. 27 has shown that experimental and theoretical values of the system PEMFC+VS are roughly equal: a little difference was detected when the current crossing the two devices had been increased (due to ohmic losses that affect electrical wiring).

With the same experimental data of Figure 26, a power curve has been drawn in figure 28.

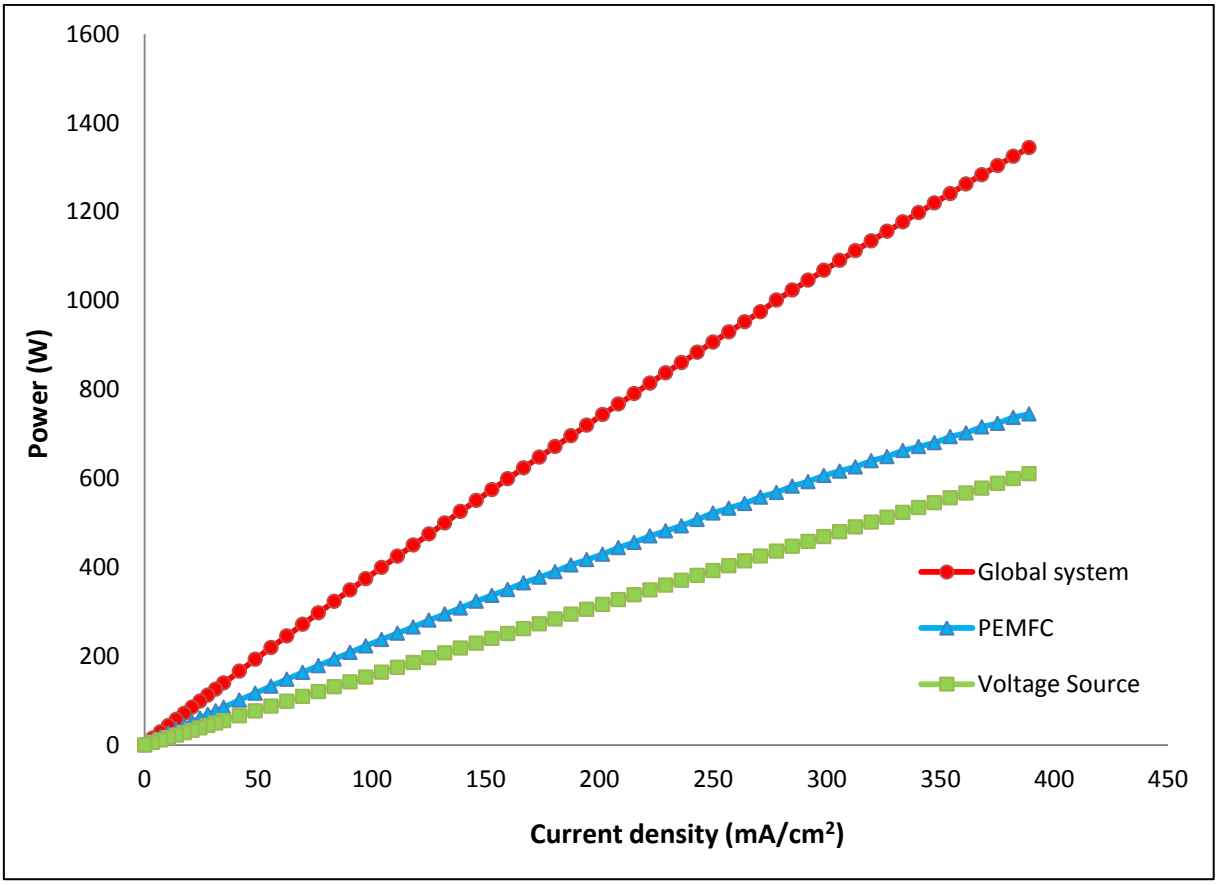

Figure 28. Power curve of PEMFC and voltage source connected in series

In figure 28, the blue curve represents the power of the global system. The red curve was the power provided by PEMFC and the blue one corresponds to voltage source's power.

Thus, the overall system created provides roughly 1350W (roughly 720-730W supplied by PEMFC and the remaining amount by voltage source). According table 4, nominal input power for Hydro Boy (DC side) is 1200W. Thus, for the connection with the inverter, we must be careful to choose the more suitable power to operate correctly, limiting the current of the Fuel Cell. In the designed system, it should flow a maximum current of 49A (approximately 340mA/cm^2).

7.1 Connection with Inverter

In order to fully assess our plant, the inverter HB 1124 was connected to the Electric Load (Xantrex, model: XDC 60-100) that work according to a fixed voltage and a current increasing rate of 50 mA/s. Moreover, the output power was assessed with a Power Quality Analyzer (model: Fluke 43B).

As the operational range of the PEM is between 22 and 28 V, seven tests has been achieved varying the voltage input of one unit for each test accomplished.

Collecting this data, it was possible to calculate the inverter efficiency (Eq. 64) function of its loading (Eq. 65).

$$\eta_{inveter} = \frac{\mathrm{P_{output(AC\ side)}}}{\mathrm{P_{input(DC\ side)}}} \qquad \text{Eq. 64}$$

$$Loading = \frac{\mathrm{P_{output(AC\ side)}}}{\mathrm{P_{nominal(AC\ side=1100W)}}} \qquad \text{Eq. 65}$$

Results are, as follows:

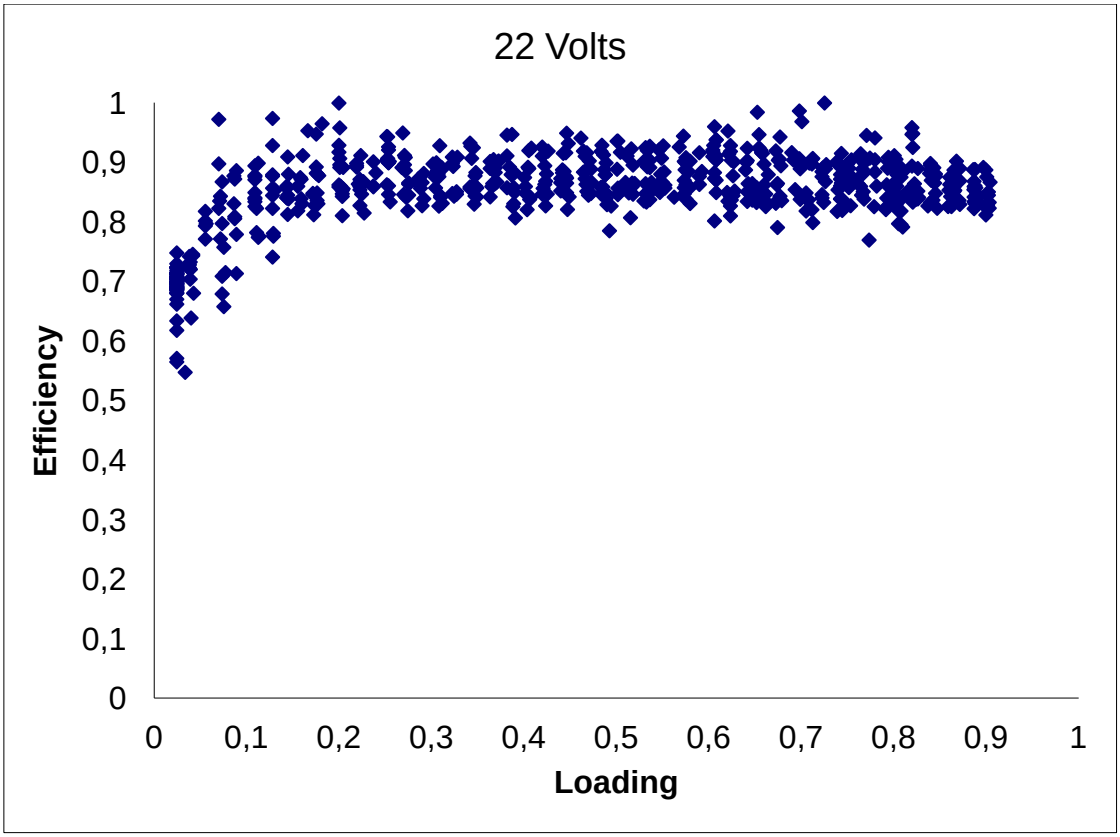

Figure 29. Inverter efficiency (at 22 Volts) function of its loading

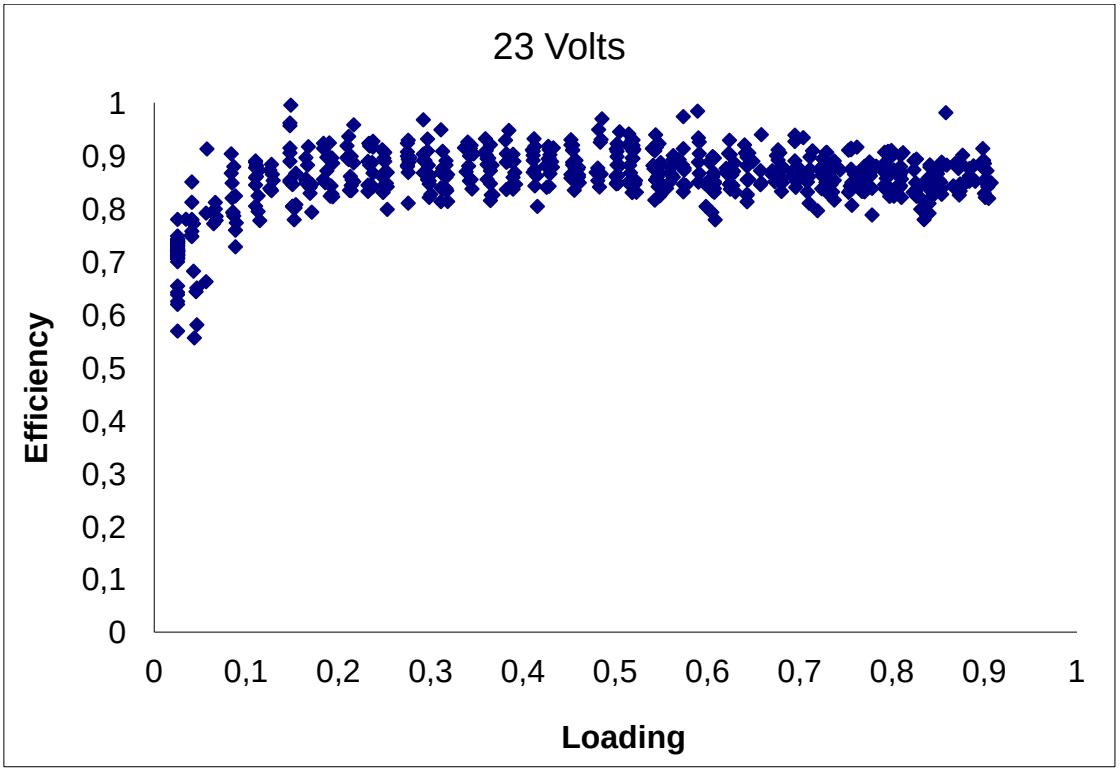

Figure 29. Inverter efficiency (at 23 Volts) function of its loading

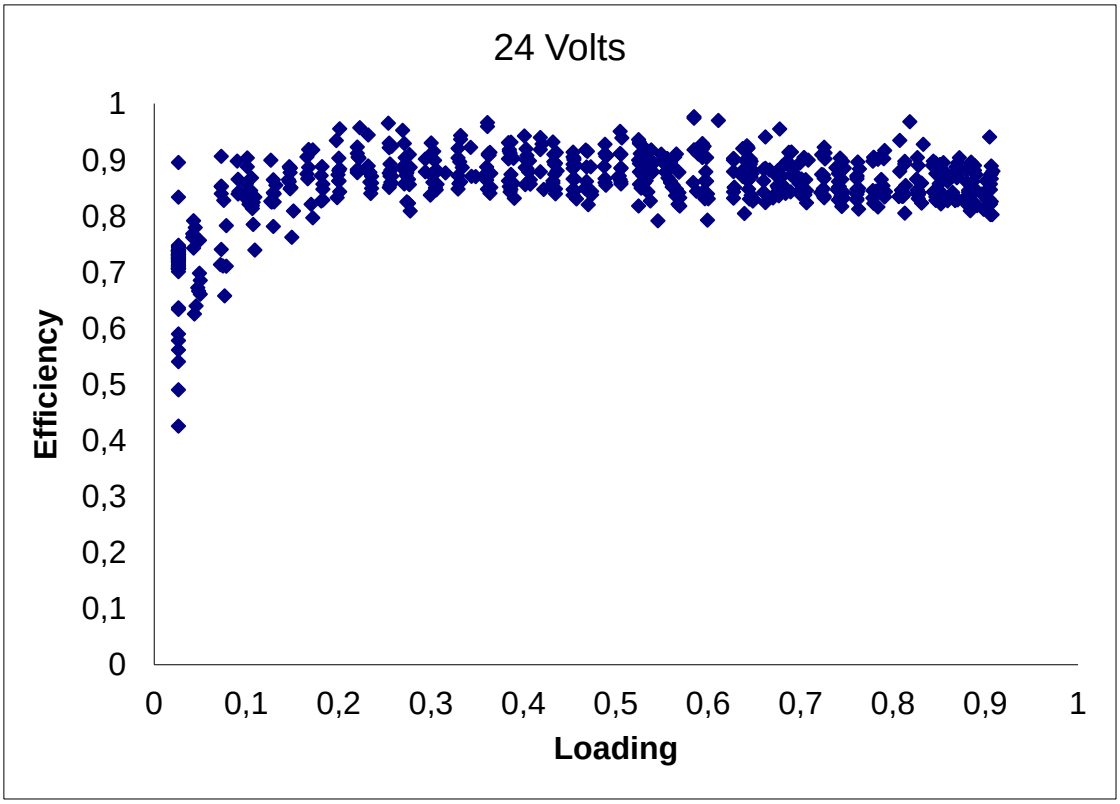

Figure 30. Inverter efficiency (at 24 Volts) function of its loading

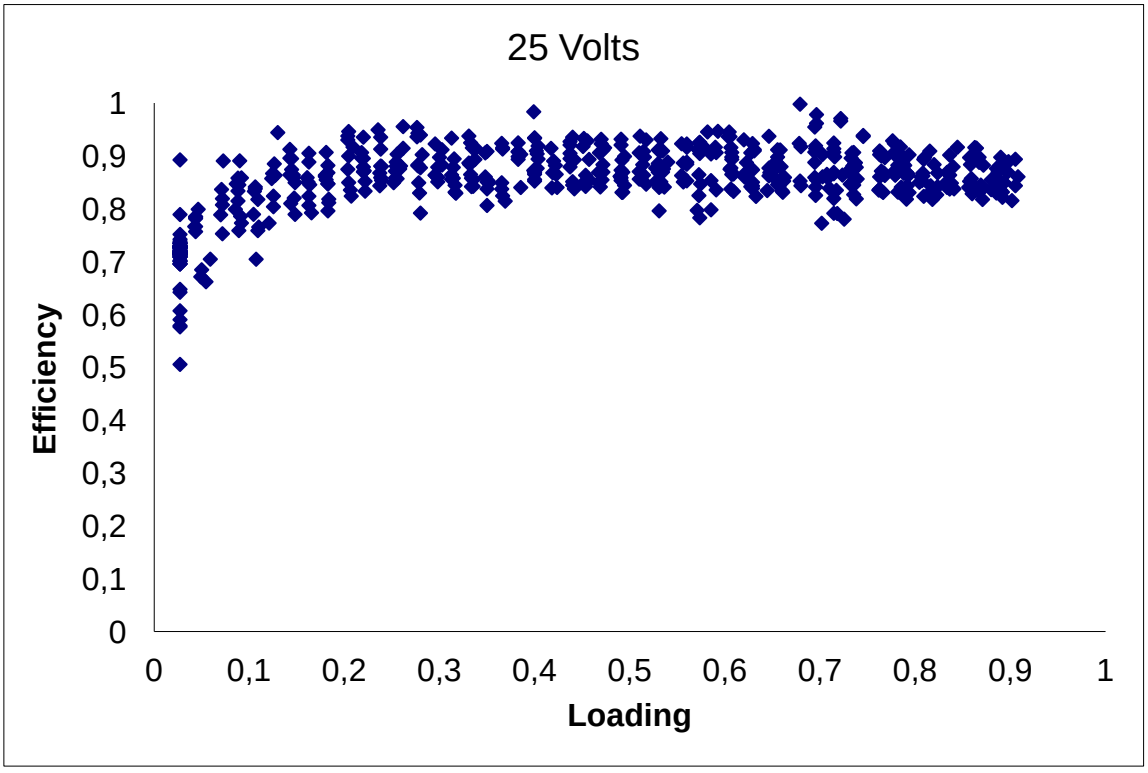

Figure 31. Inverter efficiency (at 25 Volts) function of its loading

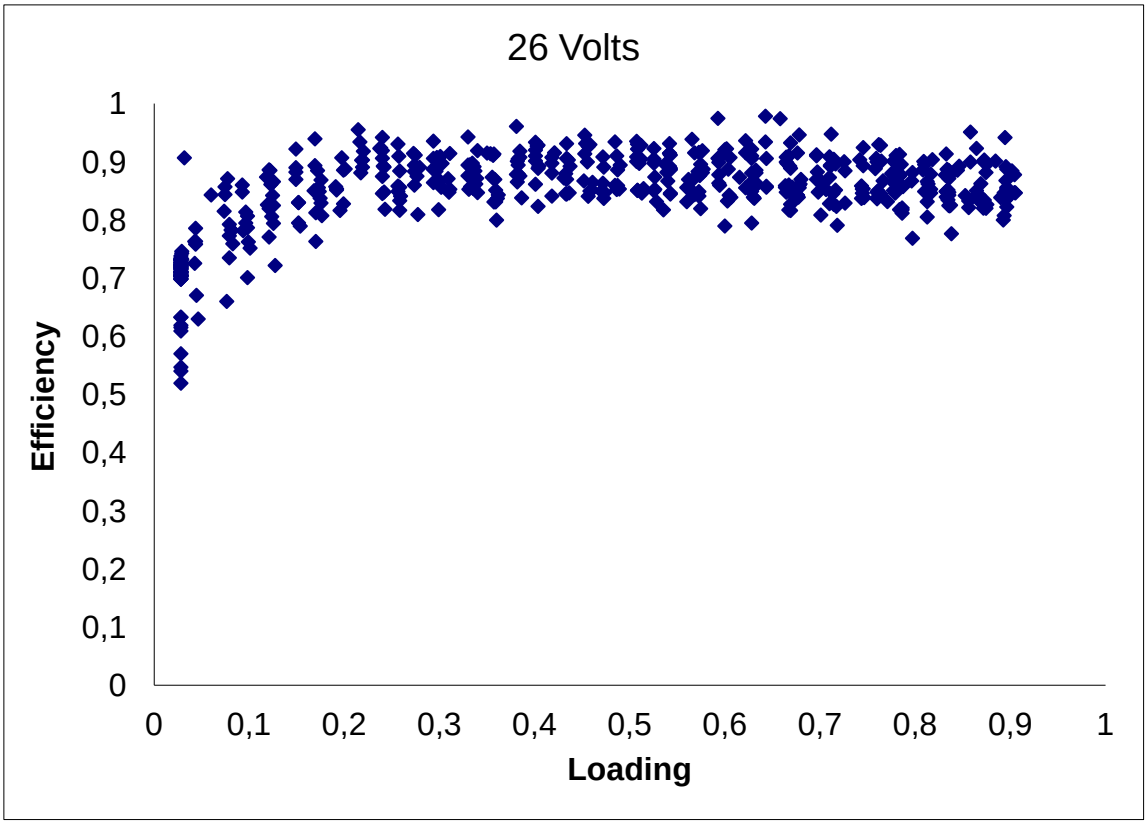

Figure 32. Inverter efficiency (at 26 Volts) function of its loading

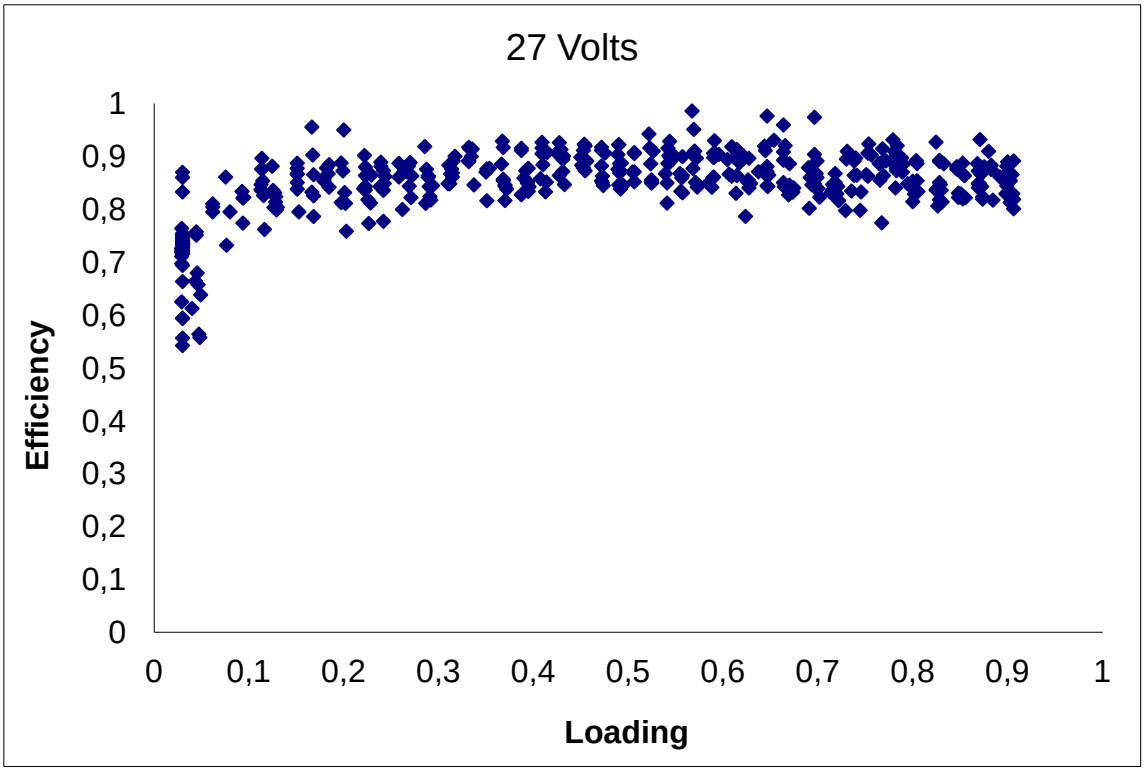

Figure 33. Inverter efficiency (at 27 Volts) function of its loading

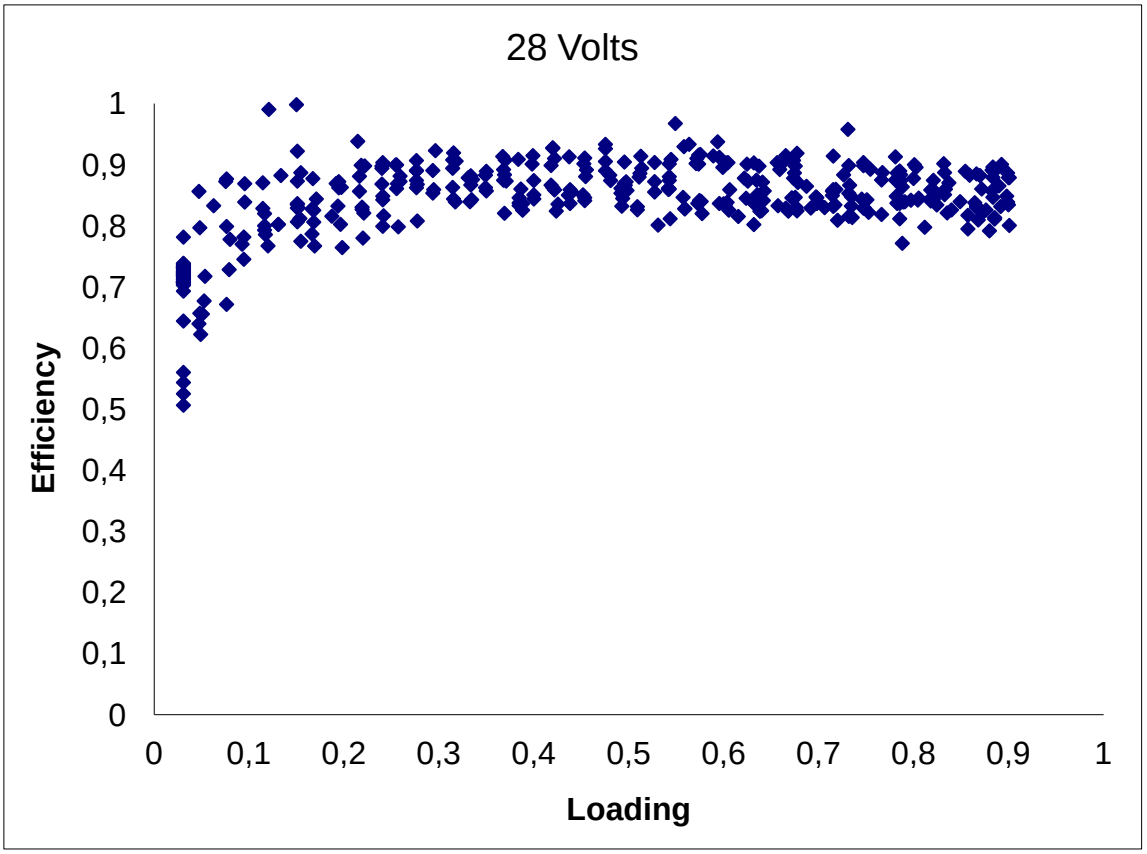

Figure 34. Inverter efficiency (at 28 Volts) function of its loading

These tests showed that the inverter had not built properly for Fuel Cell applications; in fact, as fuel cell is used to provide, in most cases, electrical energy at nominal power, larger efficiencies should be achieved for loading of, at least, 90%. From the experimental curves obtained, this does not occur and efficiency drop occurs for loading larger than 90%. Thus, for the input power of 1200W, a power up to 1000W was provided to the public grid (for an efficiency of, approximately, 83%).

Furthermore, a summary of maximum efficiency data is presented in Table 7.

Voltage	Average efficiency	Maximum Efficiency
28	0.864	0.998
27	0.869	0.986
26	0.875	0.978
25	0.876	0.998
24	0.871	0.977
23	0.872	0.996
22	0.873	0.997

Table 7. Efficiency function of voltage source

As table 7 shows, the efficiencies do not change considerably varying the input voltage of the power source (due to the small difference, only 6 Volts, of tests' voltage), while the maximum efficiencies are all larger than 91% (as SMA reports in its catalogue). However, from the point of view of the system, these high performances would be more availed if could be achieved next to maximum loading.

7.2 Economic assessment of Power generation with PEM

To conclude the analyse, power generation cost has been calculated.

Generation cost has to take in account capital cost, operation and management cost and fuel cost. Firstly, capital cost of PEM can be calculated using the following formulas:

$$\mathrm{CE_{cc}} = \frac{\mathrm{I_0} \times \mathrm{FRC}}{8760\mathrm{h} \times \mathrm{FC}} \qquad \text{Eq. 66}$$

$$FRC = \frac{i(1+i)^n}{i(1+i)^n - 1} \qquad \text{Eq. 67}$$

Where:

- CE is the cost of energy considering just capital cost (US$/MWh);
- I_0 is the investment cost (US$/kW);
- FRC is the capital-recovery factor;
- FC is the capacity factor.
- *i* is the discount rate;
- *n* is the lifespan of the fuel cell.

According to California Energy Commission[61], PEM capital cost is $ 5,000/kW, whereas inverter cost is about $ 400/kW.

To calculate FRC, discount rate is needed. In 2011, National Agency of Electrical Energy (ANEEL) has reduced *i* from 9.95% to 7.5% to indicate a less risk of energy distribution in Brazil[62]. As lifespan of PEM should be at least 5 years or more than 40,000 hours of continuous operation[63] (with a capacity factor up to 0.95), FRC is approximately 0.247. Thus, Eq. 66 becomes:

$$\mathrm{CE_{cc}} = \frac{5400 \times 0.247}{8760 \times 0.95} = 160\ \frac{\mathrm{US\$}}{\mathrm{MWh}}$$

Hydrogen cost provided by Air Liquid is, approximately, 46 US$/m^3

The heating values of hydrogen at 25 °C and constant pressure are as follows[64]:

HHV: 12,770 kJ/m^3

LHV: 10,760 kJ/m^3 .

Because the system produces water in liquid form, the HHV is used. Moreover, experimental assessments has shown that overall efficiency of 45 % can be achieved. Thus,

$$\mathrm{CE_{fuel}} = 46\frac{\mathrm{US\$}}{\mathrm{m^3}} \times \frac{1}{12770}\frac{\mathrm{m^3}}{\mathrm{kJ}} \times \frac{3600}{0.45}\frac{\mathrm{kJ}}{\mathrm{kWh}} = 28{,}818\ \frac{\mathrm{US\$}}{\mathrm{MWh}}$$

Operation and maintenance costs ranges from $ 0.005-$ 0.010/kWh (based on an annual inspection visit to the unit): therefore global power generation cost is nearly 29,000 $\frac{\text{US\$}}{\text{MWh}}$.
The above economic assessment concludes the experimental research carried out with the PEM.

Moreover, because Phosphoric acid fuel cells are the most mature fuel cell technology, in the next chapter, we will enter in the last part of this dissertation that aimed to develop an engineering-economic analysis of a PAFC potential for the co-generation of heat with electrical energy in Brazil.

8. PAFC potential for the co-generation of heat with electrical energy in Brazil

At the current state-of-art, PAFC are more suitable for co-generation applications, considering the heat availability at temperatures required by conventional processes. In fact, while polymeric electrolyte membrane fuel cells (PEMFC) and alkaline fuel cells (AFC) work at low temperature (lower than 100 °C), which makes co-generation difficult, molten carbonate fuel cells (MCFC) and solid oxide fuel cells (SOFC) still have a capital cost that is approximately 3-4 times that of PAFC, which does not permit a reasonable pay-back time [65].

A typical PAFC stationary module[32] for the supply of combined heat and power (CHP) uses natural gas and is delivered with a reforming reactor, an inverter to provide alternating current and two heat exchangers (HEXs) that recover thermal energy in two operating ranges: 173 kW at 121 °C and 281 kW at 60 °C.

8.1. Background

In São Paulo, industries that require heat and power are usually supplied with electricity and natural gas from networks operated by regulated public utility companies. Small and medium consumers pay for fully regulated services (including power, gas and distribution and transmission), whereas large consumers obtain natural gas and power directly from suppliers via free access arrangements, while paying only regulated distribution and transmission fees.

For high and medium voltages, four ranges of consumption exist (A1, A2, A3, and A4)[66]. A typical voltage for small and medium users is A4 (from 2.3-25 kV). Moreover, the industry has to support the cost of transformers to convert the electrical power acquired from the grid to low voltage (110-220V). Moreover, ANEEL, the Brazilian Electricity Regulatory Agency, recently enacted a rule that permits qualified co-generation and renewable micro generation (up to 100 kW) and minigeneration (100-1000 kW) sources to exchange power freely with the public grid, although with tariff-time compensation[67]. This new regulation has a potential to strongly incentivize the implementation of co-generation systems such as PAFC. Certain industries, such as the food and beverage, textile or laundry industries, may obtain both heat and power from a fuel cell supplied with natural gas. These industries require electricity and heat continuously; the operating temperatures of their respective factories are provided in Table 8.

Industrial sector	Process	Temperature level [°C]
• Food and beverages	Drying	30 – 90
	Heat treatment	40 – 60
	Washing	40 – 80
	Pasteurizing	80 – 110
	Boiling	95 – 105
• Textile industry	Washing	40 – 80
	Bleaching	60 – 100
	Dyeing	100 – 160
• Laundry	Water washing	65 – 90
	Vapor washing	up to 150

Table 8. Working temperature of different industrial sectors[68-70]

Thus, co-generation implies the potential opportunity to reduce an industry's dependence on an electrical utility supply, with possible lower costs for electricity, in particular during peak loads.

Furthermore, PAFC pollutant emissions are as follows[32]:

-NO_X: 0.009 kg/MWh

-CO_2: 219.15 kg/MWh with fully heat recovery

-SO_X: negligible

These are lower than typical emissions from thermal energy with NG combustion, which on average are:

-NO_X: 0.765 kg/MWh

-CO_2: 511 kg/MWh

-SO_X: 0.045 kg/MWh[71].

In countries such as the US, the federal government provides incentives for high-efficiency fuel cell power installations with the Federal Incentive Tax Credit (FITC), and fuel cell operators receive credits for excess electricity that is fed back to the utility grid; Brazil also has the possibility to begin such an energy policy.

Flexible fuel cell applications are located in buildings in San Diego and in New York City: they meet the electrical demand of a supermarket and are supplied by a fuel cell stack. Other examples include St. Helena Hospital and the World Trade Center; at the latter, a fuel cell stack of 400 kW was installed to satisfy the electrical demand[72].

8.2 The PAFC module

A typical PAFC stationary system supplies 400 kW of electrical energy with a capacity factor of up to 0.95 for an operating life of 20 years[32]. It also produces a total of 454 kW of thermal energy recoverable in the form of hot water at two different temperatures (173 kW at 121 °C and 281 kW at 60 °C)[32]. The power supply system module contains four fuel cell stacks connected in series. Each fuel cell stack contains 376 individual cells and is capable of generating over 100 kW of electricity. The system does not work with pure hydrogen, but it works with natural gas; therefore, a hydro-desulfurizer and a reforming process are required. This system device is called the fuel processing system FPS.

8.3 Material balance in the stack: hydrogen and natural gas

The amount of fuel required to supply electrical power depends on the calorific value of the fuel and on the electrical efficiency of the system. The definition of electrical efficiency is[73]:

$$\eta = \frac{electrical\ energy\ produced\ per\ mole\ of\ fuel}{-\Delta\tilde{h}_f} \qquad Eq.68$$

where $-\Delta\tilde{h}_f$ is the enthalpy of formation (the heating value of hydrogen).

As the water produced can be either a liquid or a gas, the efficiency can be calculated in one of two ways: if the product is in the liquid phase, the higher heating value (HHV) is used, while if the product is in the gas phase, the lower heating value (LHV) is used.

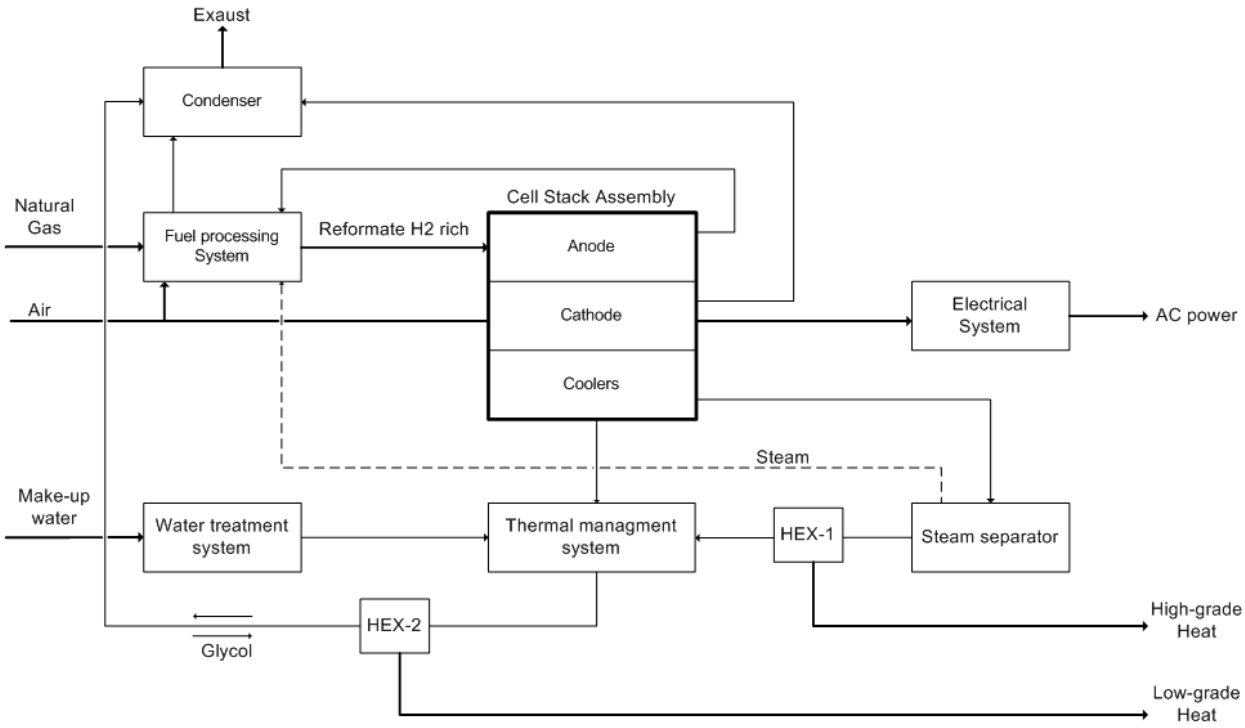

Figure 35. A drawing of PureCell® Model 400 schematic

The heating values of hydrogen at 25 °C and constant pressure are as follows[64]:

HHV: 12,770 kJ/m^3

LHV: 10,760 kJ/m^3.

Because the system produces water in gaseous form, the LHV is used. At this point in the process, the UTC PAFC stack efficiency is approximately 37.8% based on the HHV of natural gas and approximately 42% based on the LHV of natural gas. Because UTC power refers to the natural gas consumption according to the HHV, the electrical efficiency of the system is considered to be 37.8%. Therefore, the total electrical energy produced per cubic meter of hydrogen will be 4,067.28 kJ/m^3. Given this value, it is possible to determine the volume flow rate of hydrogen to be fed into the system to generate electrical power of 400kW, as given in the following equation:

$$\dot{V} = \frac{Power\ (kW)}{electrical\ energy\ produced\ by\ H_2(kJ/m^3)} \qquad Eq.69$$

The amount of hydrogen required to feed the stack is 0.098 m^3/s. To determine the mass flow rate, the hydrogen density was obtained by extrapolating its value to 25 °C[60] (0.0814g/L. Given these values, the hydrogen mass flow rate and mole flow rate are calculated to yield the following values:

$\dot{m}_{H2} = 0.008\ kg/s$

$\dot{n}_{H2} = 0.004\ \ kmol/s$ (for a molecular weight of 2.02 $kg/kmol$)

Because the fuel cell works with natural gas, it is important to establish the required natural gas and water flow rates for supply in the FPS.

		$\dot{n}$ $[kmol/s]$	$\dot{m}$ $[kg/s]$	$\dot{V}$ $[m^3/s]$	Equation reference
Natural Gas		0.001	0.018	0.0235	Section 5.4
Water	reforming process	0.004	0.072	0.000072	Section 5.4
	electrochemical reaction	0.004	0.072	0.000072	Section 6

Table 9. The feeding reagents for FPS

To calculate the mass and mole flow rate, the molecular weight and density of the natural gas must be known. According to Comgas[74], the São Paulo supplier company, the composition of NG is as displayed in Table 10.

Methane	89%
Ethane	6%
Propane	1,8%
C_4 +	1%
CO_2	1,5%
N_2	0,7%

Table 10. The composition of Brazilian natural gas

Thus, the natural gas volume flow rate is roughly 85 m^3/h. This value would be accurate if all of the natural gas were converted into hydrogen, but the reforming process has an efficiency greater than 90%[24,37,38]. Thus, the real flow rate to be fed to the stack must be 94 m^3/h. This value is in agreement with traditional system data that report a natural gas flow rate of 99 m^3/h[32]. The difference can be due to a different composition of natural gas in the US or a difference in the efficiency of the reforming process. The same model can be used with LHV from Eq. 68, yielding a supplied natural gas of 85 m^3/h; the system data yielded 89 m^3/h, corresponding to nearly 951 kW. This value allows the calculation of the overall first law PAFC efficiency if all exhausted heat is recovered, using the following equation:

$$\eta = \frac{Global\ energy\ produced\ (eletrical\ and\ thermal\ energy)}{LHV\ of\ natural\ gas}$$

$$\eta = \frac{400 + 173 + 281}{951} \cong 90\%$$

Table 9 also indicates that the water required for the reforming process is the same as the water produced through the electrochemical reaction into the stack; thus, the system operates in a water balance.

8.4 Co-generation of thermal energy

The combination of the thermal management system (TMS) and the water treatment system (WTS) maintains the thermal balance of the system by providing cooling water to the fuel cell stacks and to the balance-of-plant systems. The steam generated in the cell stack loop is transferred to the FPS for use in the natural gas reformation process. The TMS includes two heat-recovery heat exchangers and the controls and interface for rejecting heat to the cooling module. The heat recovered from the fuel cell process is provided to the customer in both low- and high-grade forms. High-grade heat is generated in the cell-stack coolant loop and is capable of heating customer-supplied fluids to 121 °C. Low-grade heat is primarily generated in the condenser and is capable of heating fluids to a maximum of 60 °C. The WTS provides process water at the proper quality for the fuel cell stacks and balance-of-plant by circulating the recovered water through a series of demineralizer bottles. Make-up water is typically not required when operating at ambient temperatures below 30 °C; at temperatures above this value, the make-up water is treated in the same demineralizer bottles. The benefits of these options were compared with those of a conventional public utility supply.

8.4.1 The design of the heat recovery system

The nominal amount of heat available is primarily a function of the efficiency of the fuel cell. When the power plant is new or when the cell stack has been overhauled, the efficiency is higher; therefore, less heat is available. The actual delivery temperature will then be a function of:

- The customer inlet water temperature and flow rate;
- The power plant power output, in kilowatts; and
- The power plant age.

8.4.2 Hot water and steam

Conforming to the PAFC performance, the co-generation process was considered. For this process, 173 kW of thermal energy was recovered by HEX-1 at 121 °C, aimed at steam generation, while HEX-2 was designed to utilize 281 kW at 60 °C, aimed at hot water generation.

Considering the thermal energy provided by the burning of NG, the results of the simulations for HEX-1 in terms of the amount of fuel saved are, as follows:

- Thermal energy: 173 kW
- Natural gas HHV: 10.932 kWh/m^3
- Natural gas flow rate saved: 15.825 m^3/h

The same simulation was performed for HEX-2.

- Thermal energy: 281 kW
- Recovered hot water: 6.04 m^3/h

8.5 Economic analysis

8.5.1 The PAFC system plus thermal energy

8.5.1.1 The PAFC cost

The California Energy Commission[61] established a PAFC capital cost of $4,000/kW, whereas the maintenance costs ranges from $0.005-$0.010/kWh (based on an annual

inspection visit to the unit). The variable cost depends on the amount of natural gas required (89 m^3/h). According to Comgas, the natural gas price for this requirement is \$0.5450/m^3.[1]

8.5.1.2 System connected to the public grid plus thermal energy

The problem of the fuel cell is the high capital cost, as most of the time, there is not a reasonable payback time. Thus, a comparison with electrical energy bought from the public grid was performed. For an A4 user, the electricity cost is divided into the capacity (\$213.48/kW/yr) and energy costs (\$91.66/MWh/yr for CF=0.95). The cost of the transformer was assumed to be \$30/kW.

To compare the two models, thermal energy at two different temperatures must be supplied. From Section 8.4.2, the Comgas natural gas price is \$78,819.11 per year.

For hot water in Brazil, electrical energy is used, and NG is seldom used.

Thus, to achieve 281 kW, a total electricity cost of \$285,916.39 is required for the variable cost, and a capital cost of \$8,439 is required for the electrical transformer.

Because the water flow rate described in Section 8.4.2 is subjected to different temperatures but used in both of the systems, the water price is not considered.

8.5.2 Cash Flow

The annual cash flow was determined to evaluate the economic feasibility of the PAFC module with respect to the public grid.

The PAFC system cost during its lifetime is composed of fixed capital and variable costs. The capital cost is represented by the fuel cell investment cost. In contrast, the operating cost depends on the amount of natural gas supplied to the PAFC and on the maintenance cost of the fuel cell. When industry acquires electric energy from the public grid, the only capital cost is the power transformer required to reduce voltage, and the variable costs are the tariffs for

[1] Using an exchange rate of \$/R\$ = 1.76 (February 2012)

electricity (in this case, a dual rate structure requiring payment for available capacity and for consumed energy). Because the amount of water and the variable cost are the same, they were not considered in comparing the two systems.

	PAFC module		Public Grid + NG for vapor + Hot water		
Capital Cost	Fuel Cell	$ 1,600,000	Power transformer		$ 20,439
Variable Cost	Natural Gas	$ 424,924.18	Electrical demand	Capacity	$ 85,390.91
	Maintenance	$ 26,280[a]	Electrical Demand	Energy	$ 305,114.78[b]
			Electricity for hot water demand	Capacity	$ 60,051.16
			Electricity for hot water Demand	Energy	$ 214,571.97 (2)
			Natural Gas		$ 78,819.11

Table 11. The capital and variable costs for the two models

---

[a] $Net\ Present\ Value = -Co \pm \sum \frac{C_n}{(1+i)^n}$

Where: C_0 is the capital cost,

C_n the net cash flow at time n,

i the discount rate,

n the time of the cash flow (years)

[b] All costs are evaluated according to CF = 0.95.

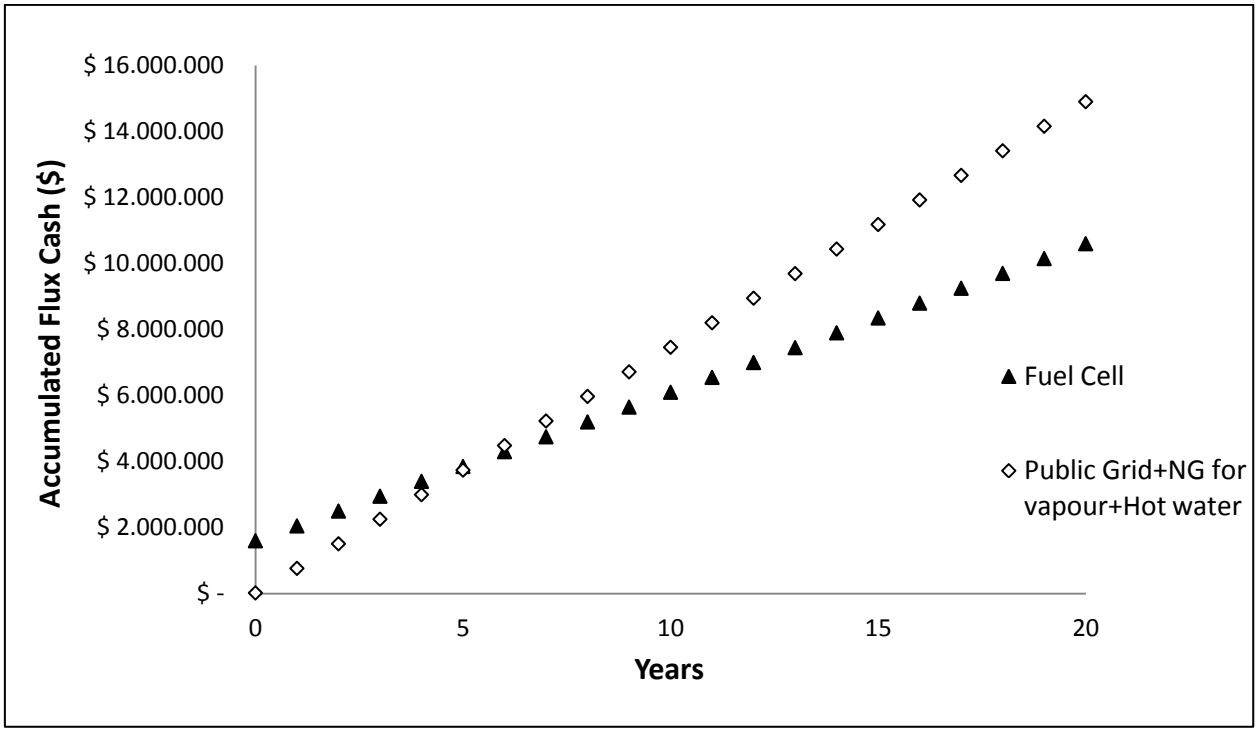

Figure 36. The flux of cash of the fuel cell system compared to the public grid

Fig. 37 suggests that the PAFC module co-generation system is competitive with the public grid supply; in fact, even if the PAFC capital cost negatively affects the cash flow, the variable costs are lower. Thus, over time, the PAFC becomes economically competitive.

8.5.3 Payback time (PBT), net present value (NPV) and internal rate of return (IRR)

Based on the positive economic balance presented in Fig. 36, the PBT, NPV and IRR were calculated for the co-generation model. The payback time is indicated in Fig. 37: from the sixth year, the PAFC module cost becomes lower than that of the public grid system. Thus, the PBT is 6 years.

To determine the NPV, the concept of "avoided cost" was used. Avoided cost is the difference between the public grid and the fuel cell costs. Thus, at year zero, the NPV corresponds to the difference between the capital cost of the two systems (it is negative due to the higher price of PAFC stack), whereas at year 20, it represents the money saved using the FC (a positive value due to the economic benefit of FC technology). All "avoided costs" needed to be evaluated at

the present value, and a discount rate DR of 10%[75] was considered, resulting in the following NPV:

NPV: $ 923,918.37[2]

The internal rate of return is strictly connected to the NPV concept: the IRR is the “annualized effective compounded return rate" or "rate of return" that makes the NPV of all cash flows equal to zero[3]:

IRR: 17.93%

8.5.2.2 Capacity factor (CF) as an assessment variable

Section 8.5.2 indicates that the PAFC system has a net economical positive balance. This result is due to a high capacity factor. In addition, this result is a crucial problem: if the user does not require this remaining energy capital cost, a traditional public grid could be less expensive. Therefore, the same calculations of the previous section were developed using CF[4] as a variable.

[2] All costs are evaluated according to CF = 0,95.

[3] IRR is the discount rate i at which NPV=0.

[4] Capacity Factor (FC) = $\frac{\text{Actual Electric generation (kWh)}}{\text{Unit Maximum Rated Capacity (kW) x period hours (h)}}$

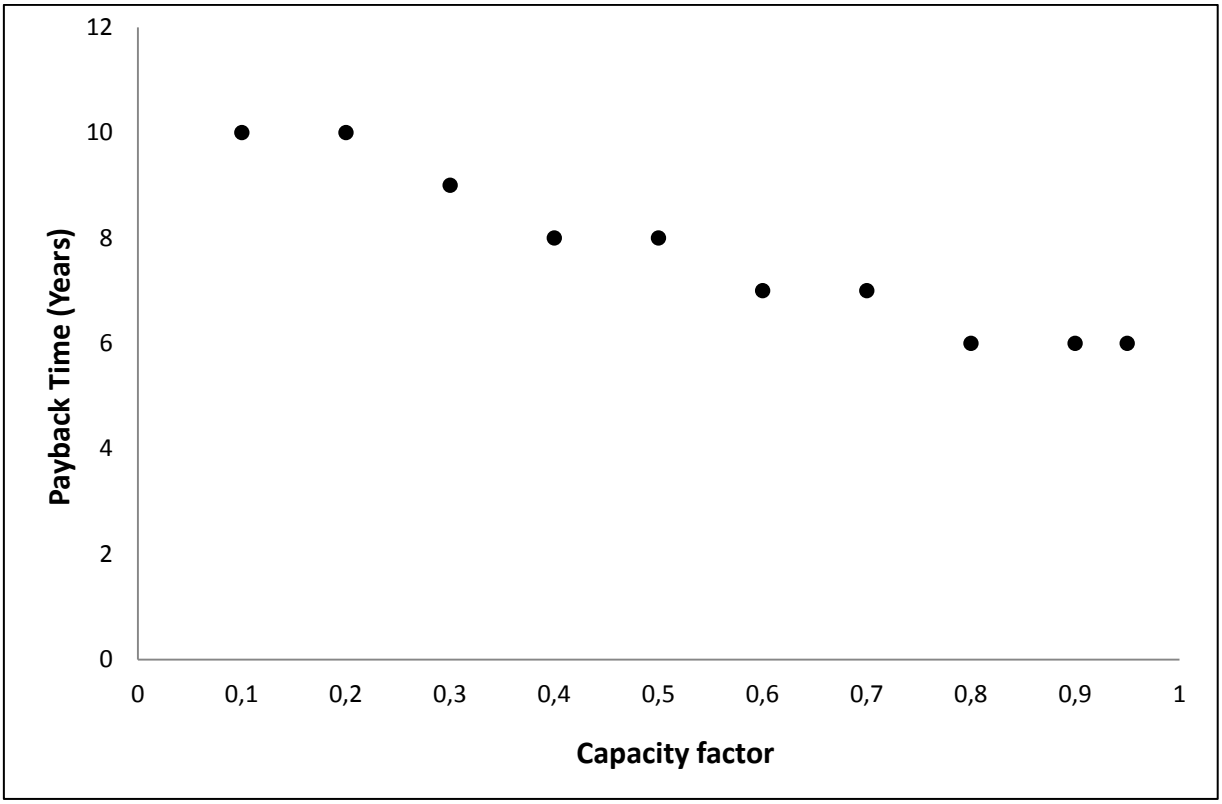

Figure 37. The payback time function for CF

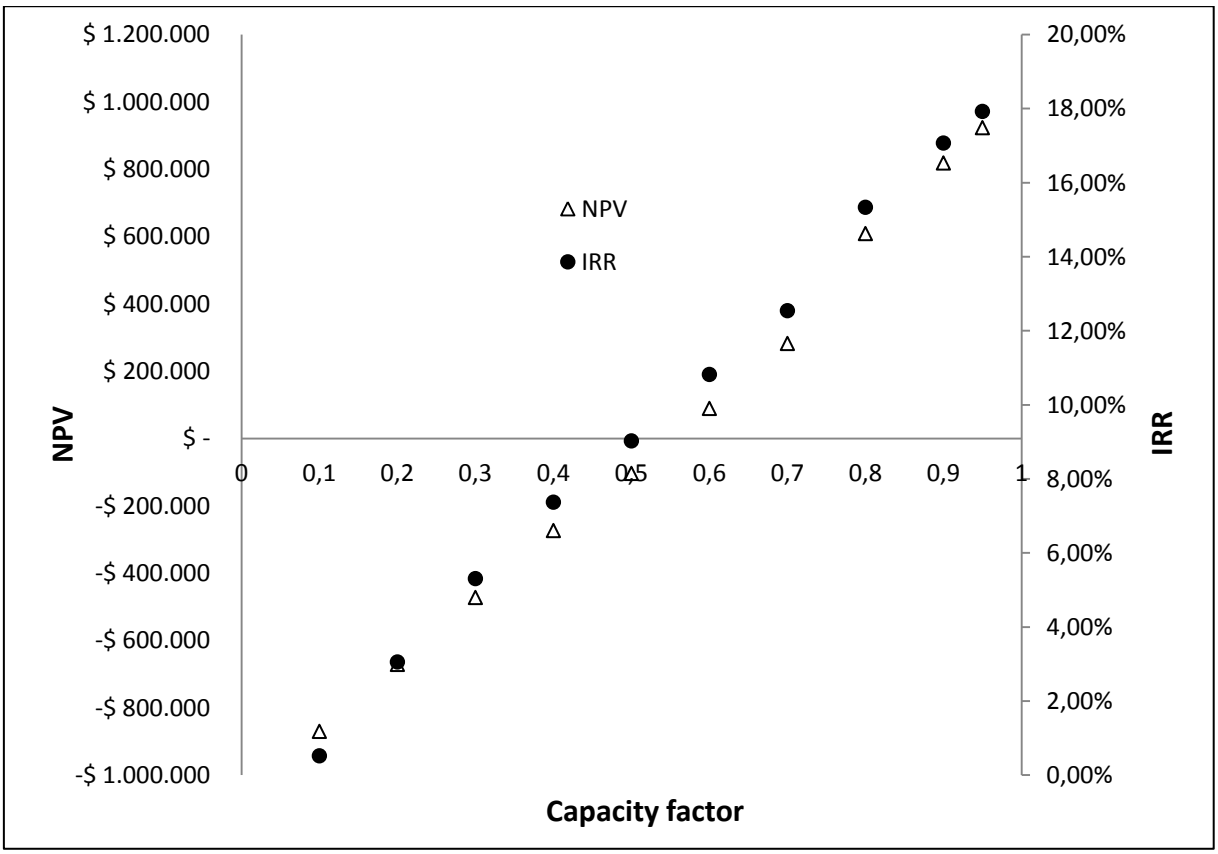

Figure 38. The net present value and internal rate of return functions of CF

Hence, for a capacity factor less than 60%, the NPV becomes negative (even if the payback time is less than the stack life). This result suggests that according to a financial point of view, the balance is positive but the gain is less profitable compared with money opportunity cost. Fig. 39 indicates that for a CF less than 0.3, the internal rate of return of the investment is lower than 10%, which is the interest rate considered.

8.6 Learning curves

Learning curves are used to describe how accumulated knowledge can reduce the cost of technologies. Typical learning curves are described by the following equation[76]:

$C_i = C_0 \times P_i^{-b}$

where the variables are defined as follows:

C_i: product cost at *i*th production

$C_{0:}$ cost of the first unit produced

P: cumulative number of products at *i*th production

b: index of experience

The meaning of "b" can be expressed by the follow equation:

$PR = 2^{-b}$

The progress ratio (PR) means that the production cost can be reduced by a factor "b" when cumulative production doubles. A typical value of "b" for PAFC technology is 0.2[77]; therefore, a PR of 87% characterizes this technology and implies that the cost is reduced to 87% each time the cumulative production is doubled. The estimation of C_0 requires at least one pair of present production cost and cumulative production quantity values to date. A learning curve for PAFC technology was developed in 1998 by Schoots et al.[78] and Whitaker[79]. In this paper, Whitaker's approach was used because of a higher correlation with the experimental data. The product cost for a cumulative production of 4 MW was \$6,000/kW. To find C_0, an extrapolation of the data for nil production was performed. Moreover, because the paper was from 1998, the costs were corrected by the inflation rate. For an IR of 38%, a C_0 of \$8,556 was found. The capital costs as a function of the total

installed capacity (TIC) are presented in Fig. 32. According to the US Department of Energy [80], the actual total installed capacity of PAFCs is more than 75 MW across 19 countries and 6 continents.

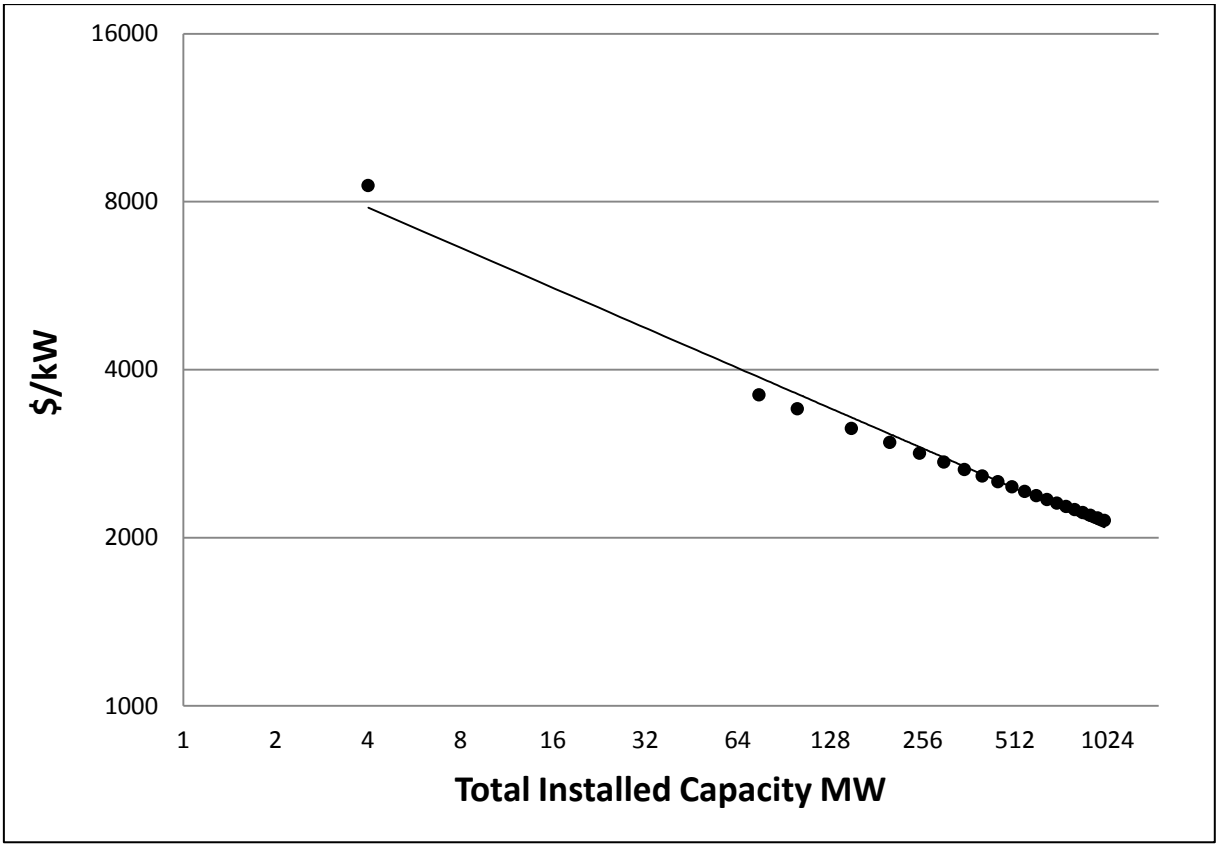

Figure 39. The capital cost reduced by the learning curve

As Fig. 40 indicates, for 75 MW, the PAFC stack cost is $3,600/kW. This number is quite close to the $4,000/kW reported in Section 8.5.1.1, so the model described by Whitaker is considered valid.

8.6.1 Payback Time function of Capacity Factor and Total Installed Capacity

Fig. 38 indicates that the payback time is function of capacity factor. Additionally, in Fig. 40, the ability of accumulated knowledge, through an increase in the PAFC installed capacity, to

reduce the cost of this technology was illustrated. Thus, a sensibility study was achieved calculating PBT varying CF and TIC.

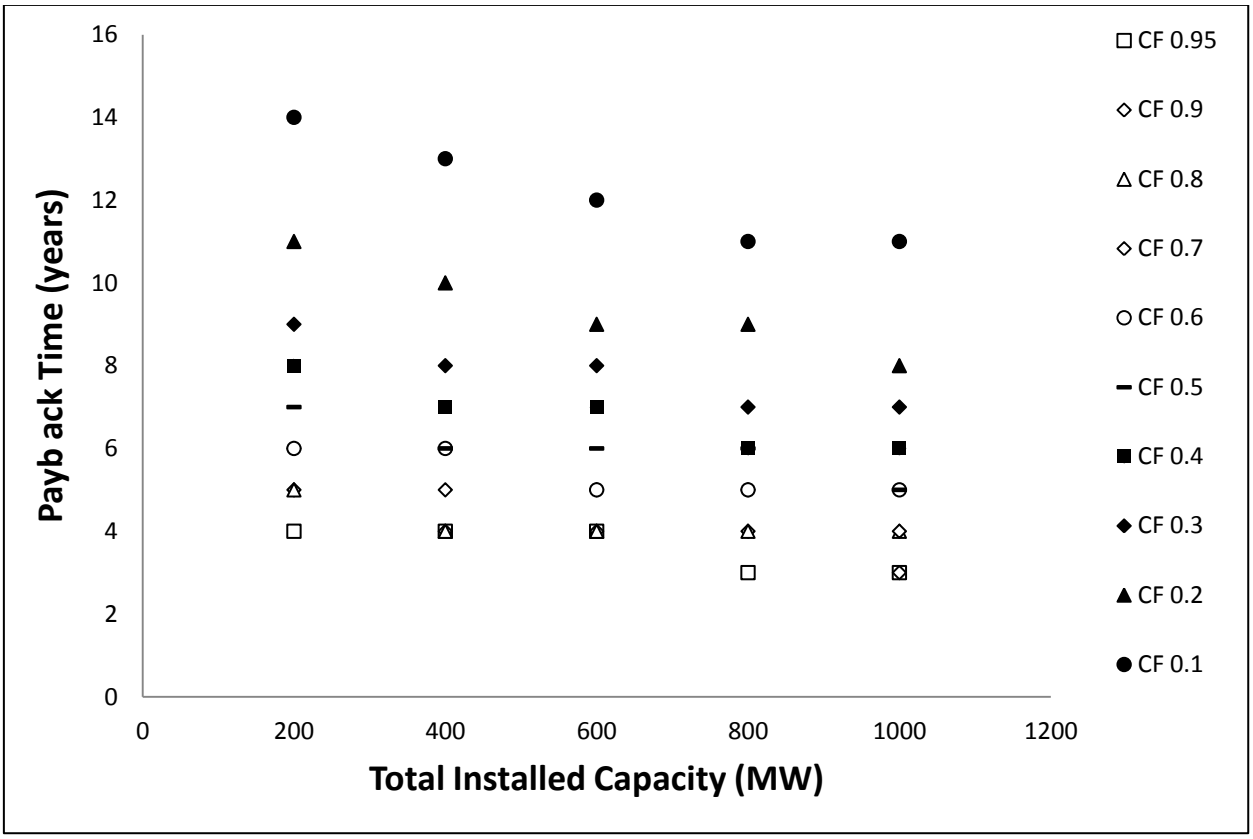

Figure 40. The payback times as a function of the CF and the total installed capacity

In addition to TIC (which influences capital cost), CF plays an important role in the assessment of PBT. In fact, with lower CF, the capital cost weighs heavily in the cash flow reducing advantages of PAFC. Thus, the assessment provided evidence concerning how economy of scale might reduce the capital cost of PAFC. Fig. 41 illustrates how PAFC can lower the PBT to 3-4 years for a high CF, rather than in 6 years, as presented in Fig. 37, for the current scale and technology stage.

8.6.2 Net Present Value function of Capacity Factor and Total Installed Capacity (TIC)

After calculating PBT, the same sensibility study was performed to calculate the NPV (using a discount rate equal to 10%[75]).

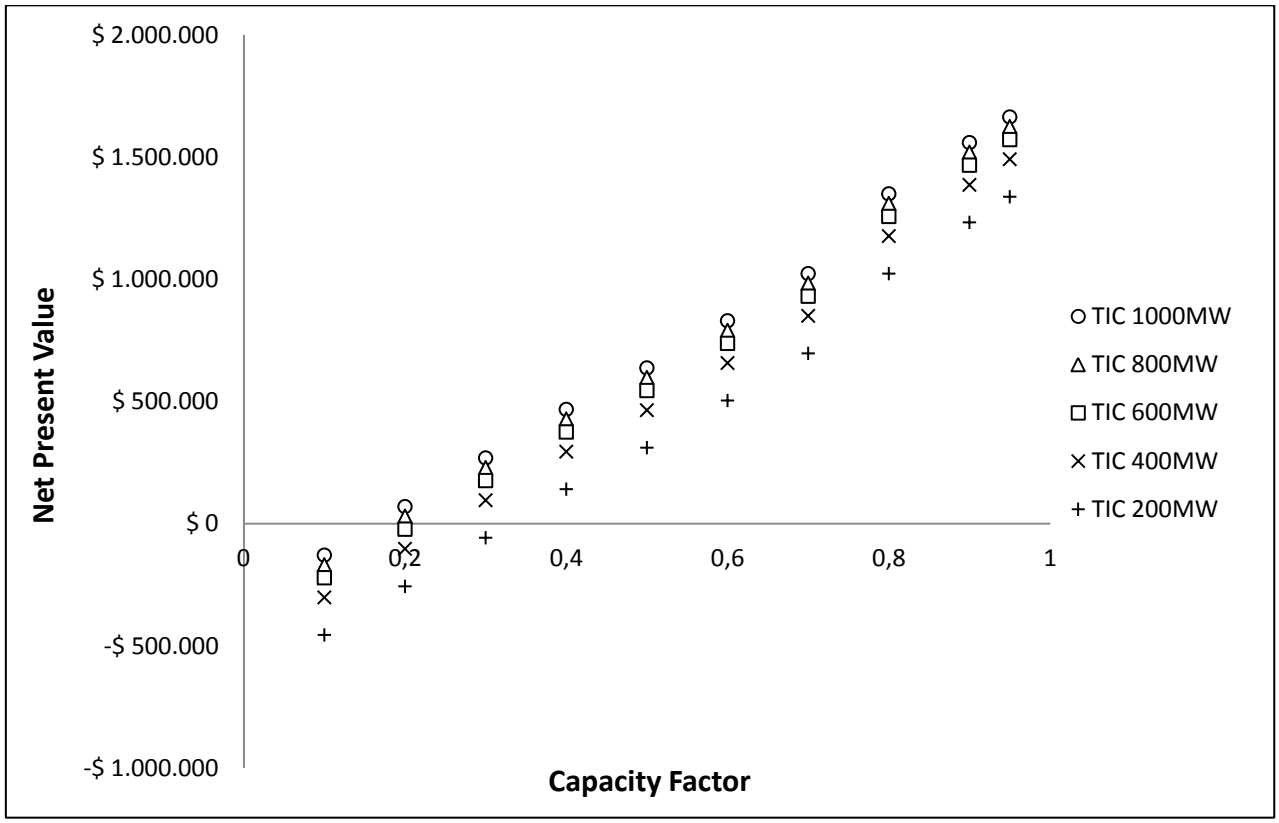

Figure 41. The net present values (using interest rate of 10%) as a function of the CF and the total installed capacity

As concluded in the previous section, Fig. 42 still suggests that increasing TIC may make PAFC profitable compared with the public grid, if a CF larger than 0.3 is adopted.

8.6.3 The interest rate effect on the NPV

The NPV depends on the discount rate (DR), which defines the profitability of a business. Thus, a sensibility study was performed for two scenarios with discount rates of 8% and 6%, respectively. The results are reported in Figs. 43 and 44.

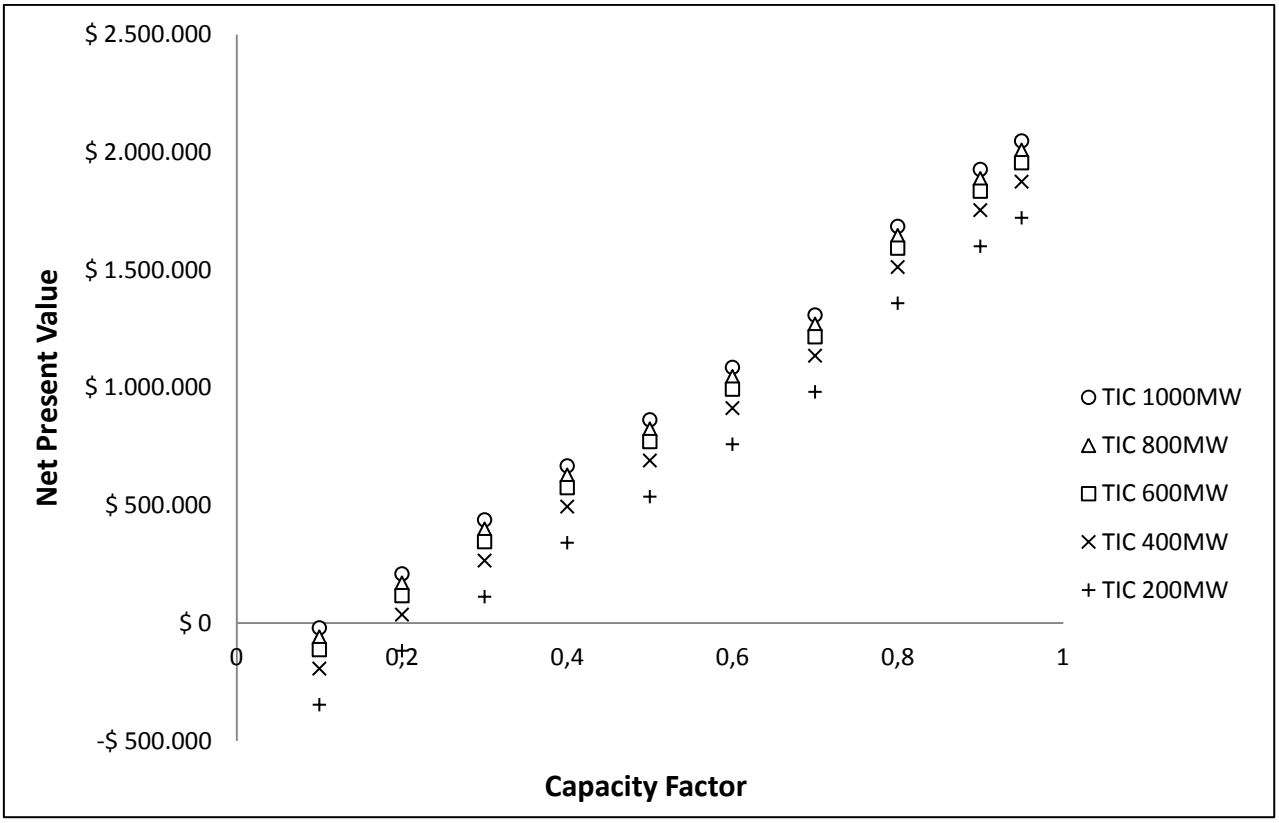

Figure 42. The net present values (using interest rate of 8%) as a function of the CF and the total installed capacity

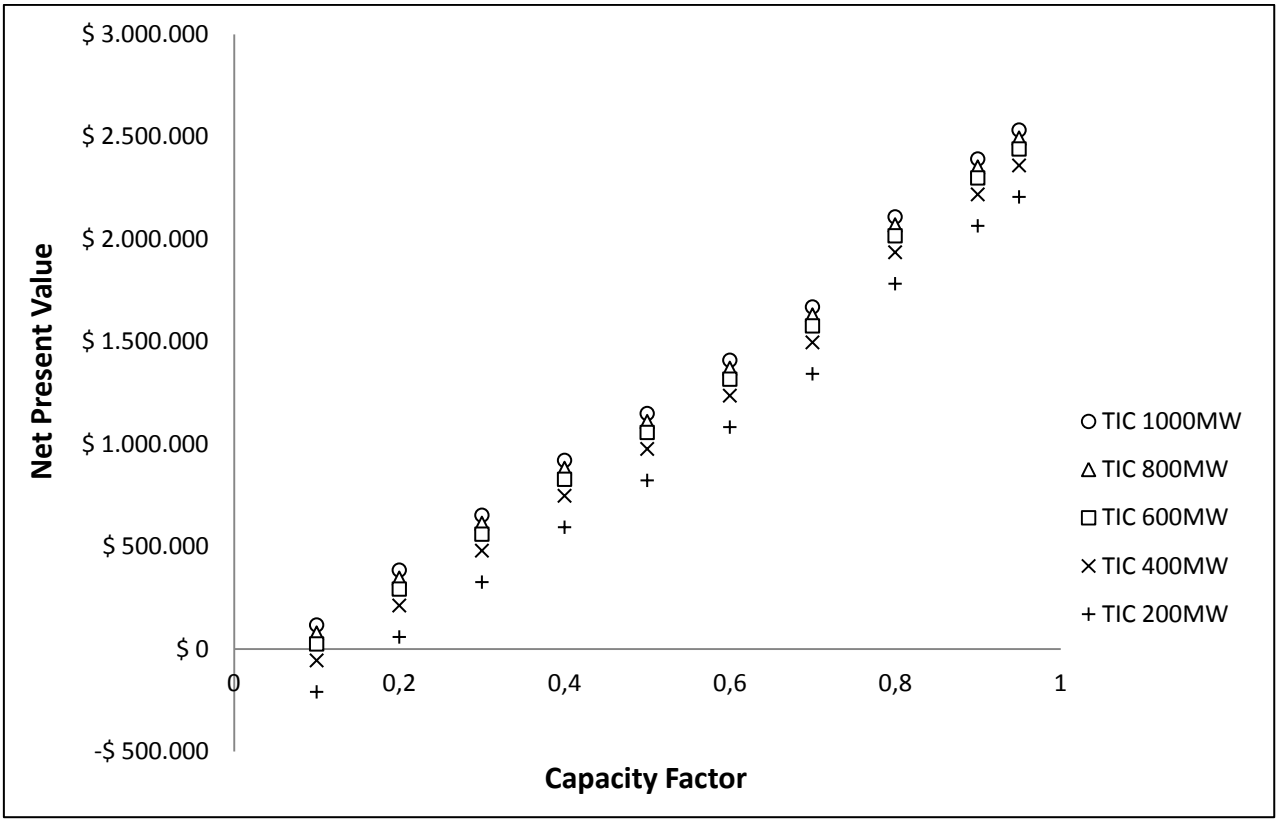

Figure 43. The net present values (using interest rate of 6%) as a function of the CF and the total installed capacity

Figs. 43 and 44 demonstrate sensitivity analysis to lower interest rates. Currently, the typical cost of capital is 10%, whereas 8% and 6% represent scenarios of foreseeable reductions being pursued by recent policies of the Brazilian Central Bank. Hence, when reducing the discount rate, the PAFC becomes cost competitive for almost any CF.

8.7 Natural gas price prospects and potential impacts on FC competition

The natural gas price in São Paulo, Brazil is composed of the city-gate cost, which the local utility pays to the supplier company (generally Petrobras) and the distribution margin. The city-gate cost is determined by the molecule (energy), as indexed to the oil international price and amended by the shipping cost, which varies with inflation and the exchange rate. Most supplies currently come from Bolivia, which is economically problematic in that Gasbol (the Bolivia-Brazil pipeline) amounts to \$0.32-0.39 per m^3 at the city gate. Currently, NG

regulation allows for free access to the distribution grid, so consumers may obtain their natural gas supply from other sources, inject it into the grid, and pay only the distribution margin to the local utility. There are two foreseeable options for an independent supply: importation of LNG (liquefied natural gas) or the development of domestic shale gas resources. We estimate that both sources could reduce the supply cost to approximately $0.13-0.15 per m^3. While the Bolivian supply is tied to the international oil price by contract, US shale gas development has resulted in the decoupling of global oil and gas prices. The international NG price reference, the Henry Hub index, is strongly influenced by shale gas development in the US; its value is nearly $0.087/$m^3$. Hence, with the addition of liquefaction and shipping (between $0.036/$m^3$) and regasification ($0.015-0.022/m^3), imported LNG could be priced at $0.14–0.15/$m^3$[81]. Another source of inexpensive NG could be domestic shale gas in Brazil, where resources are estimated to be approximately 6200 billion m^3[82]. The potential development of such resources in the southeast region of Brazil could have similar costs to those in the US (approximately $0.087/$m^3$). With an additional estimated pipeline shipping cost of approximately $0.043/$m^3$, the city-gate cost would be approximately $0.13/$m^3$. Such new scenarios for the NG supply cost could allow the economic conditions for the FC technology to penetrate into the Brazilian market. Under the assumptions of $0,13/$m^3$ for the NG supply and $0.15/$m^3$ for the distribution margin, the NPVs as a function of the CF are plotted in Figs. 45, 46 and 47 discount rates of 10%, 8%, and 6%, respectively.

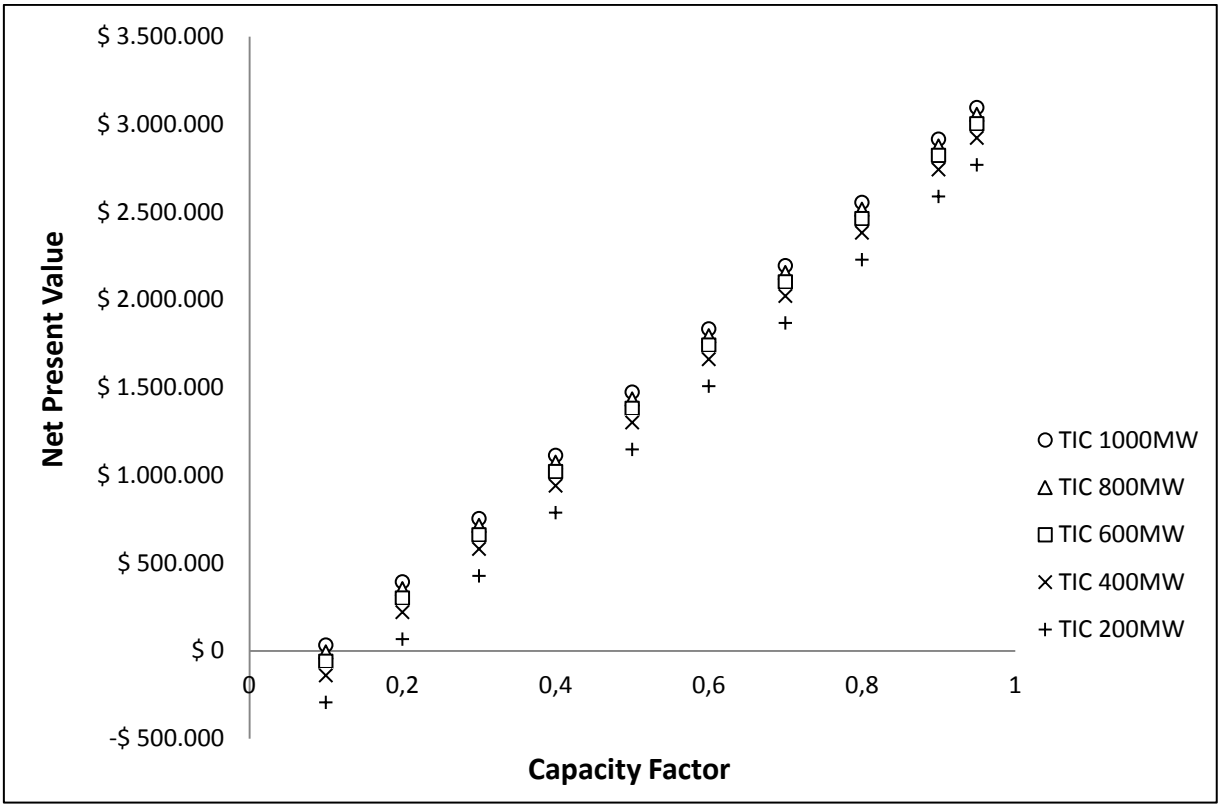

Figure 44. The NPV according to a discount rate of 10 % and reduced natural gas supply cost

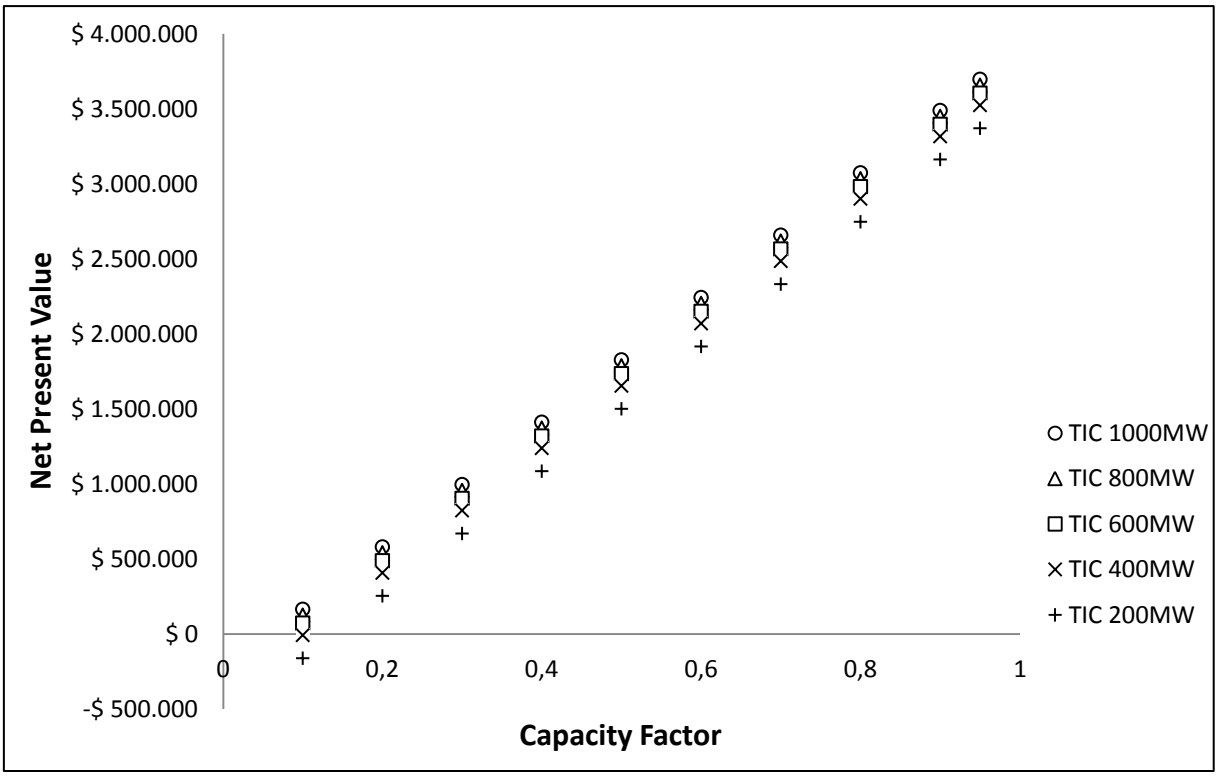

Figure 45. The NPV according to a discount rate of 8 % and reduced natural gas supply cost

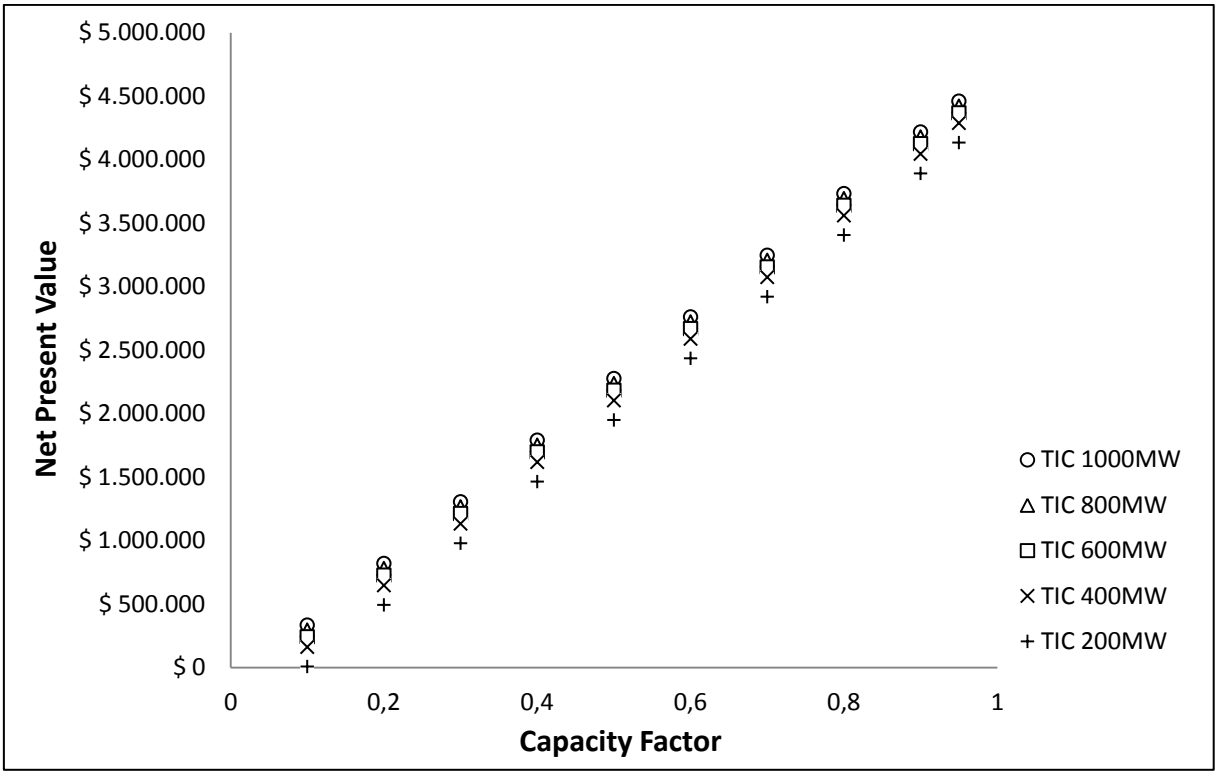

Figure 46. The NPV according to a discount rate of 6 % and reduced natural gas supply cost

Figs. 40, 41 and 42 present sensibility studies performed considering only the benefits of the economy of scale of PAFC. Furthermore, Figs. 45, 46 and 47 indicate that, in addition to the benefits derived from a reduction in capital cost, natural gas costs compatible with US and other international conditions could strongly increase the potential penetration of PAFC technology in Brazil. Again, sensibility studies of the discount rate were performed: for a CF=0,95, reduction in DR from 10% to 8% increases the profit by 15-20%, and a 6% DR could increase the NPV by 50%.

9. Conclusions and recommendations

With the present research it has been shown the assembling of a PEMFC module of 1kW (practically 720-730W for cooling problems) that could provide electrical power to the public grid using Hydrogen as primary fuel. The problem of the small voltage generated by PEM stack was overcome with the installation of a voltage source connected in series to the PEMFC. With such system, the final total installed capacity for the power plant was around 1200W (DC side, up to 1000W for the AC side). However, the cost calculated in the previous section is several order of magnitude larger than traditional power generation cost (that, in Brazil, may be approximately between 50 and 130 $\frac{\text{US\$}}{\text{MWh}}$ depending on fuel and technology used[83]). This is due to high capital cost of PEM and especially to Hydrogen cost. Regarding the former, forecast cost based on long term projections, report the value of 1,000 $\frac{\text{US\$}}{\text{kW}}$, while hydrogen production may vary between 4 and 15 $\frac{\text{US\$}}{\text{GJ}}$, depending on production technology (steam reforming is generally cheaper than hydrolyse or coal gasification)[18]. If all this prevision would be verified, power generation cost might fall between 74 and 162 $\frac{\text{US\$}}{\text{MWh}}$, giving larger possibilities to PEM technology to accede in the global market.

For what have concerned the engineering-economic analysis of commercial PAFC, based on the materials and the heat balance, the analysis have suggested that system has six years of payback time under the currently prevailing conditions. A sensitivity analysis with respect to the capacity factor was performed to estimate the payback time, the internal rate of return and the net present value as functions of the CF; these analyses indicated that the PAFC CHP module is competitive for a CF higher than 60%. Hence, even for a state-of-art technology, FC is competitive for certain niche-market applications, such as the textile and food and beverage industries. Additionally, conditions that may arise that favor the competitiveness of FC in Brazil were evaluated, including a) simulations of the potential gains due to learning and scale suggested that the capital cost can be reduced to nearly 70%; b) reduction of the discount rate from 10% to 6%, which is possible with public finance policies and economic stabilization, could allow the NPV to increase by 50%; and c) the potential reduction of the natural gas supply cost, either due to domestic shale gas resources development or due to LNG imports, would also enhance FC viability. These results warrant public policies to support and implement measures that incentivize and develop FC technology and the natural

gas supply chain to provide environmental and economic benefits to the industries that combine the heat and power markets in Brazil.

References:

[1] Larminie J, Dicks A. Fuel Cell Systems Explained. 2nd Edition. John Wiley & Sons; 2003, p.1-2

[2] Larminie J, Dicks A. Fuel Cell Systems Explained. 2nd Edition. John Wiley & Sons; 2003, p.5-7

[3] Lutz EA, Richard SL, Keller JO. Thermodynamic comparison of fuel cells to the Carnot cycle. International Journal of Hydrogen Energy 2002;27:1103-1111

[4] Appleby AJ, Foulkes FR. Fuel cell handbook. New York: Van Nostrand Reinhold 1989

[5] Xianguo Li. Fuel Cell and thermodynamic properties. 8th Annual international Conference ASME 1997

[6] Wark Jr K. Advanced Thermodynamics for Engineers. Mc-Graw-Hill. New York 1995

[7] Haynes C. Clarifying reversible efficiency misconceptions of high temperature fuel cells in relation to reversible heat engines. Journal of Power Source 2001;92:199-203

[8] Kordesch K, Simader G. Fuel Cell and Their Applications. VCH, New York 1996, p.48

[9] Larminie J, Dicks A. Fuel Cell Systems Explained. 2nd Edition. John Wiley & Sons; 2003, p. 45-48

[10] Larminie J, Dicks A. Fuel Cell Systems Explained. 2nd Edition. John Wiley & Sons; 2003, p. 6-9

[11] EG&G Technical Services. Fuel Cell Handbook. 7th Edition. U.S. Department of Energy 2004, p.9-12

[12] Larminie J, Dicks A. Fuel Cell Systems Explained. 2nd Edition. John Wiley & Sons; 2003, p. 163

[13] U.S. Department of Energy Office of Fossil Energy National Energy Technology Laboratory. Fuel Cell Handbook. 7th ed. 2004, p.111

[14] Greenspec. [July 2012]. Available from: http://www.greenspec.co.uk/energy.php

[15] J Larminie, A Dicks. Fuel Cell Systems Explained. 2nd ed. John Wiley & Sons; 2003, p.177

[16] U.S. Department of Energy Office of Fossil Energy National Energy Technology Laboratory. Fuel Cell Handbook. 7th ed. 2004, p.112

[17] Darwish MA. Building air conditioning system using fuel cell: Case study for Kuwait. Applied thermal engineering 2007;27:2869-2876

[18] Neef HJ. International overview of hydrogen and fuel cell research. Energy 2009;39:327-333

[19] U.S. Department of Energy Office of Fossil Energy National Energy Technology Laboratory. Fuel Cell Handbook. 7th ed. 2004, p.11

[20] Cao D, Sun Y, Wang G. Direct carbon fuel cell: Fundamentals and recent developments. Journal of Power Sources 2007;167:250–257

[21] Florisa Solar Center Energy. Hydrogen Basics-Production. [August 2012]. Available from: <http://www.fsec.ucf.edu/en/consumer/hydrogen/basics/production.htm>

[22] J Larminie, A Dicks. Fuel Cell Systems Explained. 2nd ed. John Wiley & Sons; 2003, p.229

[23] Lipman TE, Edwards JL, Kammen DM. Fuel cell system economics: comparing the costs of generating power with stationary andmotor vehicle PEM fuel cell systems. Energy Policy 2004; 32:101–125

[24] Ahmed S, Krumpelt M. Hydrogen from hydrocarbon fuels for fuel cells. International Journal of Hydrogen Energy 2001;26:291–301

[25] Larminie J, Dicks A. Fuel Cell Systems Explained. 2nd Edition. John Wiley & Sons; 2003, p.230

[26] Larminie J, Dicks A. Fuel Cell Systems Explained. 2nd Edition. John Wiley & Sons; 2003, p.279-281

[27] Larminie J, Dicks A. Fuel Cell Systems Explained. 2nd Edition. John Wiley & Sons; 2003, p.282-284

[28] Larminie J, Dicks A. Fuel Cell Systems Explained. 2nd Edition. John Wiley & Sons; 2003, p.284-286

[29] Larminie J, Dicks A. Fuel Cell Systems Explained. 2nd Edition. John Wiley & Sons; 2003, p.238-239

[30] Dicks AL. Hydrogen generation from natural gas for the fuel cell system of tomorrow. Journal of Power Sources 1996;61:113-124

[31] Kordesch K, Simader G. Fuel Cell and Their Applications. VCH, New York 1996, p.239-241,309

[32] UTC Power. [February 2012]. Available from: <http://www.utcpower.com>

[33] Liu JA. Kinetics, catalysis and mechanism of methane steam reforming. MSc Dissertation. Worcester Polytechnic Institute 2006

[34] Pandya JD, Ghosh KK, Rastogi SK. A phosphoric acid fuel cell coupled with biogas. Energy 1986;13:383-388

[35] Heinzel A, Vogel B, Hubner P. Reforming of natural gas - hydrogen generation from small scale stationary fuel cell systems. Journal of Power Sources 2002;105:202-207

[36] Ghenciu AF. Review of fuel processing catalysts for hydrogen production in PEM fuel cell systems. Current Opinion in Solid State and Material Science 2002;6:389-399

[37] Ayabe S, Omoto H, Utaka T, Kikuchi R, Sasaki K, Teraoka Y, Eguchi K. Catalytic autothermal reforming of methane and propane over supported metal catalysts. Applied Catalysis 2003;241:261-269

[38] Thomas A Admas II, Paul I Barton. High-Efficiency power production from natural gas with carbon capture. Journal of Power Source 2010;195:1971-1983

[39] Maillet T, Barbier Jr J, Duprez D. Applied Catalysis B 9 1996;251

[40] Kolb G, Zapf R, Hessel V, Lowe H, Applied Catalysis A 277 2004;155

[41] Resini C, Herrera Delgado MC, Arrighi L, Alemany LJ, Marazza R, Busca G. Propene versus propane steam reforming for hydrogen production over Pd-based and Ni-based catalysts. Catalysis Communications 2005;6:441–445

[42] Haryanto A, Fernando S, Murali N, Adhikari S. Energy Fuels 2005;19:2098

[43] Navarro RM, Pena MA, Fierro JLG. Chemical Reviews 2007;107:3952

[44] Ni M, Leung DYC, Leung MKH. International Journal of Hydrogen Energy 2007;32:3238

[45] Deluga GA, Salge JR, Schmidt LD, Verykios XE. Science 2004;303:933

[46] Iulianelli A, Liguori S, Longo T, Tosti S, Pinacci P, Basile A. An experimental study on bio-ethanol steam reforming in a catalytic membrane reactor. Part II: Reaction pressure, sweep factor and WHSV effects. International Journal of Hydrogen Energy 2010;35:3159-3164

[47] Calo JM. Fuel Cell & Hydrogen. Sustainable Energy Technologies 2007. Available from: <http://www.et.eng.wayne.edu/images/stories/CAAT/fuel_cells_calo.pdf>

[48] Zhao TS, Kreuer KD, Van Nguyen Trung. Advances in Fuel Cells. Oxford. Elsevier 2008, p. 426-427

[49] Meyers G. Direct Methanol Fuel Cells Are a Proven Alternative to Batteries. [March 2012]. Available from: <http://cleantechnica.com/2012/03/30/direct-methanol-fuel-cells-are-a-proven-green-alternative/>

[50] Rayment C, Sherwin S. Introduction to Fuel Cell Technology 2003, p.90-91

[51] Gunter Sand, Kordesch K. Fuel Cells and their Application. VCH, Weinheim 1996

[52] Rayment C, Sherwin S. Introduction to Fuel Cell Technology 2003, p.92

[53] Larminie J and Dicks A. Fuel Cell Systems Explained. John Wiley & Sons, Chichester 2000

[54] Larminie J, Dicks A. Fuel Cell Systems Explained. 2nd Edition. John Wiley & Sons; 2003, p. 395-400

[55] Larminie J, Dicks A. Fuel Cell Systems Explained. 2nd Edition. John Wiley & Sons; 2003, p. 90-93

[56] Larminie J, Dicks A. Fuel Cell Systems Explained. 2nd Edition. John Wiley & Sons; 2003, p. 327-328

[57] Diagrammi e Tabelle. Dipartimento di Termoenergetica e Condizionamento Ambientale. Università degli studi di Genova. [August 2012]. Available from: <http://www.ditec.unige.it/users/tgl/documents/TABELLE_FT1.pdf>

[58] Larminie J, Dicks A. Fuel Cell Systems Explained. 2nd Edition. John Wiley & Sons; 2003, p. 75-94

[59] McCabe WL, Smith JC, Harriott P. Unit Operations of Chemical Engineering. McGraw-Hill. 5th Edition, 1993

[60] RH Perry, DW Green. Perry's Chemical Engineering Handbook 8th ed. The McGraw-Hill; 2008

[61] California Energy Commission. [February 2012]. Available from: <http://www.energy.ca.gov>

[62] Agência Nacional de Energia Elétrica ANEEL. [November 2011]. Available from: <http://www.aneel.gov.br/aplicacoes/noticias/Output_Noticias.cfm?Identidade=4837&id_area=90>

[63] STAYERS Stationary PEM fuel cells with lifetimes beyond five years. [November 2012]. Available from: <http://cordis.europa.eu/search/index.cfm?fuseaction=proj.document&PJ_RCN=11823504>

[64] Gruppo Sapio. [February 2012]. Available from: <http://www.grupposapio.it>

[65] International Energy Agency IEA. [July 2012]. Available from: <http://www.iea.org/Textbase/techno/essentials.htm>

[66] Agência Nacional de Energia Elétrica ANEEL. [February 2012]. Available from: <http://www.aneel.gov.br>

[67] Agência Nacional de Energia Elétrica ANEEL. Resolução Normativa N °482. [April 2012]. Available from: <http://www.aneel.gov.br/cedoc/ren2012482.pdf>

[68] AEE-Institute for Sustainable Tecnhologies. [2010] Available from: <http://aee.intec.at>

[69] R Lombardi, A Ledda, R Curini, S Tarchiani, A Maestripieri, P Nuti, F Marrangoni, G Modi. Criteri di indirizzo per la gestione del rischio biologico in una lavanderia industriale 2010. Italian

[70] L Rubini, G Habib, M Lavra. Tecnologie solari a concentrazione-Produzione di calore a media temperatura 2011. Italian

[71] US Environmental Protection Agency EPA. [July 2012]. Availabel from: <http://www.epa.gov/cleanenergy/energy-and-you/affect/air-emissions.html#footnotes>

[72] 4th IPHE Workshop: PureCell Combined Heat & Power Fuel Cell Solutions. UTC Power 2011

[73] Van Rooijen J. A life cycle assessment of the pure cell stationary fuel cell system: Providing a guide for environmental improvement. Center for Sustainable Systems, University of Michigan; 2006

[74] Comgas. [February 2012] Available from: <http://www.comgas.com.br>

[75] Banco do Brasil. [February 2012]. Available from: <http://www.bb.gov.br>

[76] Tsuchiya H, Kobayashi O. Mass production cost of PEM fuel cell by learning curve. Int JHydrogen Energy 2004;29:985-990

[77] Rogner HH. Hydrogen Technologies and the technology learning curve. Int JHydrogen Energy 1998;23:833-840

[78] Schoots K, Kramer GJ, van der Zwaan BCC. Technology learning for fuel cells: an assessment of past and potential cost reductions. Energy Policy 2010;38:2887-2897

[79] Whitaker R. Investment in volume building: the 'virtuous cycle' in PAFC. JPower Sources 1998;71:71-74

[80] US Deparment of Energy DOE. [February 2012]. Available from: <http://www.fossil.energy.gov>

[81] Kurmanaev A. Brazil plans fourth LNG terminal. [February 2012]. Available from: <http://interfaxenergy.com/natural-gas-news-analysis/latin-america/brazil-plans-fourth-lng-terminal/>

[82] International Energy Agency IEA. [April 2012]. Available from: <http://www.eia.gov/analysis/studies/worldshalegas>

[83] JF de Carvalho, IL Sauer. Does Brazil need new nuclear power plants?. Energy Policy 2009;37:1580–1584